

**Morphology and Physiology of Motor Neurons
Innervating Labral Muscles of *Locusta migratoria***

Von der Fakultät für Mathematik, Informatik und Naturwissenschaften
der RWTH Aachen zur Erlangung des akademischen Grades
eines Doktors der Naturwissenschaften genehmigte
Dissertation

vorgelegt von

M.Sc. Agri. Entomology
Abid Mahmood Alvi
aus
Layyah, Pakistan

Berichter:

Herr Universitätprofessor Dr. Peter Bräunig
Herr Privatdozent Dr. Rudolf Loesel

Tag der mündlichen Prüfung: 08.06.2011

Diese Dissertation ist auf den Internetseiten der Hochschulbibliothek online
verfügbar

Table of Contents:

1. Introduction:	1
1.1. Insect head segmentation:	1
1.2. Nature of labrum:	6
1.3. Segmental affiliation of the labrum:	7
1.4. Aims of Thesis:	8
2. Materials and Methods:	11
2.1. Animals:	11
2.2. Locust ringer solution:.....	11
2.3. Retrograde labelling of neurons:	11
2.3.1. Dissection:.....	12
2.3.2. Neurobiotin staining:.....	12
2.3.3. Nickel chloride staining:	13
2.3.4. Photography and Microscopy:	13
2.4. Electrophysiology:.....	13
2.4.1. Dissection:.....	14
2.4.2. Intracellular recording:.....	14
2.4.2.1. Enzyme treatment:	14
2.4.2.2. Glass microelectrode:	15
2.4.2.3. Glass micro electrode mounting:.....	15
2.4.2.4. Indifferent electrode:.....	15
2.4.2.5. Amplifier:.....	15
2.4.2.6. Probing of neurons:.....	15
2.4.2.7. Data acquisition:	16
2.4.2.8. Identification of neurons:.....	16
2.4.2.9. Orthodromic stimulation:.....	16
2.4.2.10. Antidromic stimulation:	16
2.4.3. Intracellular staining:	17
2.4.4. Data analysis:	17
3. Results	19
3.1. Morphology of insect labrum:	19
3.2. Musculature of labrum:	19
3.2.1. Compressor muscles of labrum (M1):	20
3.2.2. Anterior retractor muscles of labrum (M2):.....	21
3.2.3. Posterior retractor muscles of labrum (M3):.....	21
3.2.4. Anterior dilator muscles of foregut (M38):.....	21
3.3. Innervation of labral muscles:	21
3.3.1. Insect nervous system:	21
3.3.2. Branching pattern of frontal connective.....	22
3.3.3. Innervation of compressor muscles of labrum (M1):.....	23
3.3.4. Innervation of anterior retractor muscles of labrum (M2):.....	24
3.3.5. Innervation of posterior retractor muscles of labrum (M3) and anterior dilator muscles of foregut (M38):	25
3.3.6. Peripheral neurosecretory cells:	26
3.3.7. General motor innervation pattern of labral muscles:.....	26
3.4. Retrograde labelling of motor neurons innervating labral musculature:.....	27

3.4.1.	Neurons innervating compressor muscles of labrum (M1):	27
3.4.2.	Neurons innervating anterior retractor muscles of labrum (M2):	27
3.4.2.1.	Backfilling of M2-commissure:.....	27
3.4.2.2.	Backfilling of motor nerve branch to M2:.....	31
3.4.2.3.	Backfilling of M2-commissure or motor nerve branch to M2 and suboesophageal ganglion neurons:	41
3.4.3.	Neurons innervating posterior retractor muscles of labrum M3:.....	41
3.4.3.1.	Backfilling of motor nerve branch to M3:.....	41
3.4.3.2.	Direct backfilling of M3:.....	46
3.4.4.	Neurons innervating anterior dilator muscles of foregut (M38):.....	47
3.4.5.	Backfilling of M3 and M38 motor nerves together:	51
3.4.6.	Contralateral targets of suboesophageal neurons:.....	57
3.5.	Action of motor neurons innervating labral muscles:	59
3.5.1.	Intracellular recording from anterior retractor muscles of labrum (M2):	59
3.5.2.	Intracellular recording from posterior retractor muscles of labrum (M3): ...	60
3.5.3.	Intracellular recording from ipsilateral M2 and M3:	61
3.5.4.	Intracellular recording from ipsilateral M3 and M38:	62
3.6.	Physiological properties of suboesophageal ganglion motor neurons:	63
3.6.1.	Simultaneous intracellular recording from fibers of M2, M3 and suboesophageal ganglion motor neurons:.....	63
3.6.2.	Simultaneous intracellular recording from fibers of M38 and SOG neuron:.....	70
4.	Discussion:	73
4.1.	Innervation pattern of labral muscles:	73
4.2.	Organization of motor neurons:	74
4.3.	Neurosecretory and neuromodulatory innervation:.....	77
4.4.	Physiology of labral musculature:.....	78
4.5.	Absence of inhibitory innervation:.....	80
5.	Conclusion:	83
5.1.	Sequence of labral muscles:	83
5.2.	Innervation pattern:	83
5.3.	Appendage of intercalary segment:.....	84
6.	Summary:	87
7.	References:	89
	Acknowledgements	105
	Curriculum Vitae	107

1. Introduction:

Multicellular life appeared in the Precambrian period and no lineage of animals is known until the Cambrian (Morris, 1979, 1989, 1993, 2000). The lineages of animals are recognized as phyla (singular, phylum) and each phylum represents a basic ground plan or bauplan. Among the diversity of ground plans for building an animal, the phylum Arthropoda is more dominating on earth relative to all others. Arthropods are characterized by various features (Brusca and Brusca, 2002; Grimaldi and Engel, 2005; Moore, J. 2006) such as external and internal body segmentation bearing paired articulated appendages, hardened exoskeleton composed of cuticle, paired compound eyes and median simple eyes, open circulatory system, a complete digestive tract, a ventral nerve cord, growth via molting, striated muscles arranged in isolated segmental bands and appendages equipped with extrinsic and intrinsic muscles which connect them with body segments and move the various parts of an appendage. Most important feature of arthropods is the grouping of their segments into specialized functional unit, the tagmata by a process known as tagmosis. Among arthropods, the most successful lineage is the Insecta. Insects are the largest group and make up a significant proportion of the world's biota by representing 85 % of all the known animal species (Matthews and Matthews, 2010). The class Insecta is divided into a number of orders reflecting the present understanding of the evolutionary history of the class. In insects, the phenomenon of tagmosis has given rise to three main body regions; head, thorax and abdomen. Head comprises of 5 or 6 segments, thorax has 3 segments and abdomen consists of 11 segments. However, in insects, fusion of head segments had left no boundaries between the segments and involvement of actual number of segments in head formation is still a matter of dispute among today's evolutionary biologists.

1.1. Insect head segmentation:

Insect's head functions as sensory and feeding apparatus of the animal. It bears brain, compound eyes, simple eyes; ocelli, antennae and mouthparts appendages. Insect morphologists believe that the head of modern insects represents the fusion of several segments that were present in an ancestral condition. Head region is divided into anterior and posterior parts. Posterior part of the head is termed as gnathocephalon and is composed of three gnathal segments (mandible, maxillae, and labium) carrying gnathal appendages arranged around the mouth opening. Anterior of the head is termed as procephalon and is composed of acron/ocular region, antennal and intercalary segment (Brusca and Brusca, 2002; Snodgrass, 1935). However, total number of segments involved in the composition of insect's head has been remained a dispute for more than a century and numerous articles and reviews were published (Goodrich, 1897; Folsom, 1899; Holmgren, 1916; Hanström, 1928; Weber, 1952; Siewing, 1963; Scholtz, 1995; DuPorte, 1957; Matsuda, 1965; Scholtz and Edgecombe, 2005, 2006, Posnien, et al. 2010; Bitsch and Bitsch, 2010; Liu, *et al.* 2010). Rempel, 1975 has stated it as an "endless dispute". Snodgrass, 1960 stated, "it would be too bad if the question of head segmentation ever should be finally settled; it has been for so long such fertile ground for theorizing that arthropodists would miss it as a field for mental exercise". Scholtz and Edgecombe 2006 said, "Model, theories and hypothesis building have become an intellectual challenge unmatched by other problems of arthropod morphology".

Reason for this long standing dispute was the lack of unequivocal morphological indication of segmental boundaries and underlying problem of their homology with thoracic appendages. The only indication of segmental limitation in adult insect head comes from cuticle invaginations called sutures that are externally visible as grooves or lines on the head. Following sorts of suture (Fig.1) are recognised;

1. Post occipital suture is thought to be the remnants of original segmental boundary between maxillary and labial segments (Snodgrass, 1935).

2. Coronal suture separates the dorsal head (vertex) into right and left parts and anteriorly splits into frontal sutures. These three sutures together make a "Y" and are named epicranial suture. Along these sutures the head capsule of the immature insect splits at molting.
3. Subgenal suture separates the lateral part of head called gena from the ventrally located gnathal appendages.
4. Frontoclypeal or epistomal suture separates frons from clypeus.

Aside from these sutures, head exoskeleton consists of several invaginated ridges and arms, most prominent of which are anterior and posterior tentorial arms. The invagination of the tentorial arms externally makes pits on head. These pits and sutures provide prominent landmarks on the head but have no association with the segments.

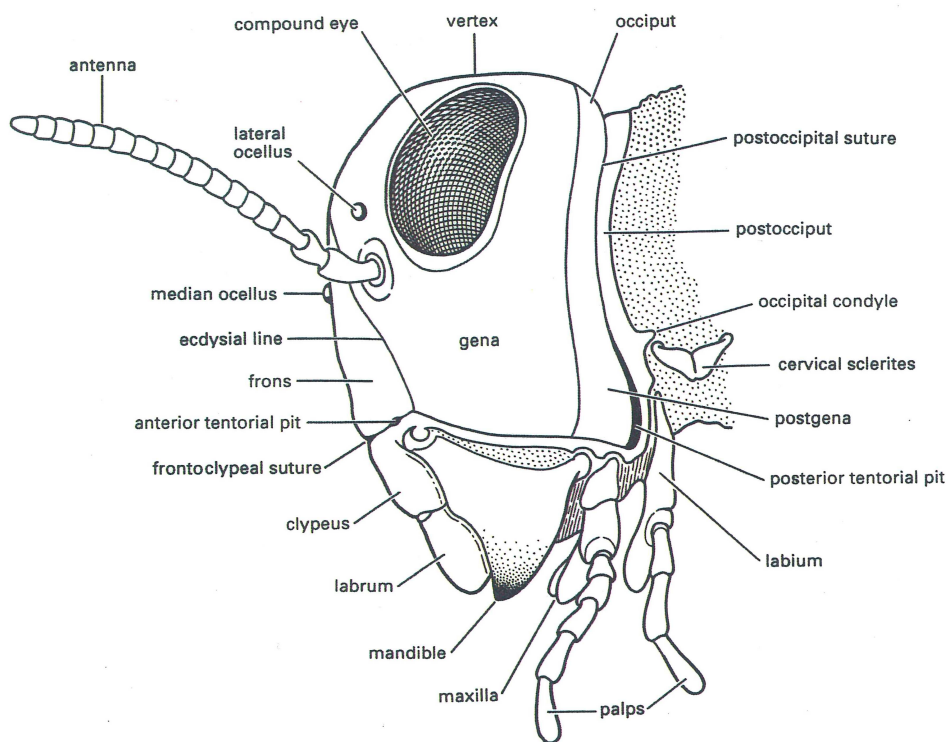


Figure: 1 Lateral view of generalized insect head (Snodgrass, 1935).

From the beginning of dispute, people were completely convinced with the involvement of segments into the composition of the arthropod head and there was a general agreement that during development three gnathal segments (mandibular, maxillary and labial segments) took part in the composition of gnathocephalon (DuPorte, 1957; Rempel, 1975). Their ganglia fused to form suboesophageal ganglion. Their segmental identity and serial homology to the thoracic ganglia during embryonic development was clearly followable by their distinct appendages. But the problem that remained controversial was the number and nature of segments involved anterior to the mandibular segments that make procephalon. Major disputes related to this issue were;

1. Pre-oral region of the head derived from the embryonic head lobes and bearing eyes and antennae, belongs to an unsegmented acron or it represents post oral segments (Snodgrass, 1935; Rempel, 1975; Cohen and Jürgen, 1991; Posnien, *et al.* 2010).

2. Presence of intercalary segment and its associated neuromere, tritocerebrum (Ferris, 1942, DuPorte, 1957; Singh, 1981; Budd, 2002; Page, 2004; Dewel and Dewel, 1996).
3. Nature of labrum; whether it is part of acron or it represents highly modified pair of limbs. If yes, then from which segment was it derived?

Different disciplines of biology exploited embryological, morphological, molecular and neuroanatomical characters to resolve these problems and tried to define the homologies of arthropod head segments and drew conclusions concerning the relationship among heads of major arthropod lineages as Chelicerata, Crustacea, Myriapoda and Hexapoda.

Early embryologists made their interpretations about the insect head segmentation chiefly based on the presence of serial repetition of coelomic sacs along anterior-posterior axis of early embryo and their association with neuromeres. The coelom is a secondary body cavity of mesodermal origin and is filled with fluid. Its ancestral function has been thought of as hydrostatic skeleton (Tautz, 2004). According to these authors, true segmentation can be defined by embryologically visible repetition of coelomic sacs. However, they did not agree on a single pattern of insect head segmentation and different views were presented by various workers. According to Heymons, 1901 (cited by many authors), Tiegs, 1940, 1947 and Weber, 1952 (Both authors cited by Rempel, 1975) insect head is composed of non-segmental anterior cap, the acron, followed by six segments; preantennal, antennal, intercalary and three gnathal segments i.e. mandibular, maxillary and labial. They described acron was bearing head lobes and labral rudiments and archicerebrum as its neuromere, while prosocerebrum, deutocerebrum and tritocerebrum were the neuromeres of preantennal, antennal and intercalary segments respectively. According to these authors, prosocerebrum and archicerebrum together make the protocerebrum. Siewing, 1963 and Rempel and Church, 1971 were in agreement with the above mentioned authors as insect head composed of acron and six segments. But, they associated the labrum with preantennal segment and considered its innervation from the labral nerve as a secondary feature. Manton, 1960 also accepted the presence of acron followed by six segments but considered the protocerebrum as neuromere of preantennal segments and labrum as a mere unpaired sclerite overhanging the mouth. Matsuda, 1965 regarded the presence of acron bearing eyes and labrum and protocerebrum as its neuromere but differ from the foregoing authors in denying the presence of a preantennal segment and considered the antennal segment as first definitive head segment. Leuzinger, *et al.*, 1926 and Roonwal 1937, 1938 denied the presence of an acron and its neuromere; the archicerebrum, and described that the anterior of insect head represents a segment, composed of head and labral lobes with protocerebrum as its neuromere. The labral segment was followed by preantennal, antennal, intercalary and three gnathal segments. Roonwal, 1938 further stated labrum is not innervated by its neuromere but it is secondarily innervated by tritocerebrum. Eastham, 1930 studied the embryology of *Pieris rape* and observed six pair of appendages in head tagma. The first pair fuses early during development and make the labrum. He denied the presence of both acron and preantennal segment and described that the insect head is composed of six segments. According to him, the most anterior segment was protocerebral segment bearing head lobes and labrum as its appendage and protocerebrum was its neuromere.

DuPorte, 1957 reviewed the literature and described that coelomic sacs could not be the real criterion for the identification of a segment. He argued that mesoderm appears as a solid mass of cells, and first expression of segmentation comes by the division of these solid strands. However, the coelomic sacs appear later in the development and might represent the differentiation of mesodermal derivatives. Therefore, embryological evidences could not alone prove that the labral, preantennal and antennal segments are the real segments incorporated in the constitution of the procephalon. According to this author, insect head is composed of a large acron followed by three gnathal segments.

There is no intercalary segment and acron bears animal eyes, antennae and labrum. Moreover, some of the embryologist also contradicted their own ideas in accepting the labrum as a segment despite having a pair of coelomic sacs. Snodgrass, 1960, contradicted the embryologists views by rejecting the Haeckel biogenetic law, "ontogeny recapitulate phylogeny" and stated that the embryo in closed egg shell could not develop in the same way as its free living ancestor has evolved.

By studying the morphology of adult animal's brain, many renowned researchers provided the interpretation for insect head segmentation. Pioneers of this field were two Swedish scientists named Holmgren, 1916 and Hanström, 1928. Their work was later followed by many later workers and modern neuroanatomical studies implied for phylogenetics studies are based on the idea that brain structures could be potential sources to draw evolutionary relation among various animal taxa. Both studied the neuroarchitectural features of annelids, and proved the homology of segments and their appendages among different groups of arthropods. They described that the dorsal portion of the brain in polychaeta is developed by the concentration of nerve cells associated with the sense organs of the prostomium, and it is not a part of segmental ganglia. They furthered stated that in insects, eyes and antennae are derived from prostomium of annelids, and insect protocerebrum and deutocerebrum is equivalent to dorsal portion of the brain of polychaeta. Later, a world^s leading insect morphologist and anatomist, Snodgrass, 1935, 1960 adopted Holmgren and Hanström theory by stating that anterior of insect head; procephalon, is composed of non segmental acron bearing archicerebrum as its neuromere. According to this author, acron is equivalent to the annelid prostomium. Insect antennae arise from the lateroventral angles of the acron, and no antennal segment exists. Archicerebrum is secondarily divided into the protocerebrum and the deutocerebrum. Mouth is located between acron and second antennal segment, with the latter having the tritocerebrum as its neuromere which join the archicerebrum after migrating around the stomodeum. He regarded labrum and clypeus have no segmental importance but as an outgrowth of acron, and considered the labral innervation as a secondary feature.

Ferris, 1942, 1943 and Henry, 1947a, b stated that the principle transverse sutures of the adult animal are intersegmental lines marking the limits of the labral, clypeal, oculo-antennal, mandibular, maxillary and labial segments, and each segment is innervated by its own ganglion. They presented the evidences for their theory in a series of papers on comparative study of nervous system of annulates. Both authors accepted the Hanström idea of prostomial origin of eyes and antennae. However, they recognised the prostomium of polychaeta as not to be a preoral structure but a dorsal lobe of the third metamere; oculo-antennal. According to them, the proboscis of polychaeta was composed of three anterior body segments, and mouth was situated at the anterior end of the first segment. Their conclusion was mainly based on the observation of the innervation pattern of nerves of polychaeta proboscis. In polychates, proboscis nerves, arising from cerebral mass and circumoesophageal nerve cord, were assumed to represents three pairs of segmental nerves. By comparing the innervation pattern of polychaeta prostomium with those of the insect head, they concluded that three segments of polychaeta prostomium are represented as insect's labral, clypeo-hypopharyngeal and oculo-antennal segments. They denied the presence of intercalary segment and regarded the tritocerebrum as a ganglion of labral segment, and assumed that the tritocerebrum has phylogenetically shifted posteriorly.

Butt, 1957, 1960 presented a novel interpretation of insect head by modifying Ferris and Henry's theory. With Snodgrass, he identified the acron as bearing eyes and antennae, and archicerebrum as its neuromere but excluded the labrum. According to this author, labral lobes are the highly modified appendages of intercalary segments formed from the material that moves around the stomodaeum and fuses to form the upper lip.

These appendages are primarily innervated from the tritocerebrum that moves forward to join posteriorly the archicerebrum.

However, existence of acron has never been directly shown among the different arthropod taxa (Scholtz, 2002, Scholtz and Edgecombe, 2006). But the acron concept was based on the assumption of close relationship between annelids and arthropods; the Articulata hypothesis (Brusca and Brusca, 2002; Snodgrass, 1935; Scholtz, 2005; Wägele and Misof, 2001). Based on this relation, it was hypothesized that insect procephalon which has eyes, antennae and brain anterior to the mouth is homologous to adult annelid's unsegmented preoral piece; the prostomium. The latter one is located anterior to the mouth and bears animal brain, eyes and sensory organs; tentacles. This homologous part in insect head was termed as acron. But recent molecular studies (Aguinaldo et al. 1997; Giribet, 2003) has challenged the monopoly of the Articulata hypothesis and proposed a new cladogram, "the Ecdysozoa". According to this hypothesis, arthropods are closely related to the cycloneuralians, which includes the Nematoida (nematodes and nematomorphs) and Scalidophora.

Similarly, the applications of modern molecular and genetic approaches, new neuroatomical methods and latest palaeontological studies have also provided new interpretations to the "endless dispute" (Rempel, 1975) of insect head segmentation and has outdated many old views (Diederich *et al.* 1991; Schmidt-Ott and Technau, 1992; Schmidt-Ott *et al.* 1994a; Rogers and Kaufman, 1996; Damen *et al.* 1998; Telford and Thomas, 1998; Abzhanov and Kaufman, 1999; Boyan *et al.* 2002, 2003; Haas *et al.* 2001a, b; Rogers *et al.* 2002; Budd, 2002; Chen, *et al.* 2004; Waloszek, *et al.* 2005; Kukulova-Peck, 1987; Budd and Telford, 2009; Maxmen, *et al.* 2005; Mittmann and Scholtz, 2003; Page, 2004; Eriksson, *et al.* 2010). The advantage of gene expression studies was their early appearance in embryonic anlagen before the morphological differentiation, and thus developing units were identifiable before major morphogenetic movements occur to give final shape to heads (Posnien, *et al.*, 2010). Among the vast array of genes, genetic patterning mechanism of segment polarity genes; *wingless (wg)* and *engrailed (en)*, is well described. Both genes mark the anterior and posterior segmental boundary at embryonic stages (Kornberg et al, 1985; DiNardo et al, 1985; Baker, 1987; Arias, et al. 1988; Van den Heuvel, 1989). Expression of these genes have revealed homology of ocular, antennal and intercalary segments across major arthropod taxa; Chelicerata, Crustacea, Myriapoda and Hexapoda (Fleig, 1994; Scholtz, 1995; Rogers and Kaufman, 1997; Telford and Thomas, 1998; Damen, 2002; Hughes and Kaufman, 2002; Chipman *et al.* 2004; Janssen *et al.* 2004). Serial homology of antennae to the thoracic legs was also corroborated by ectopic expression of genes. In such studies, a leg developed at antennal place rather than the antennae and vice versa (Rieckhof, *et al.* 1997; Abbot and Kaufman, 1986; Schnewly, *et al.* 1987; Struhl, 1981, 1982; Ronco, *et al.* 2008). In contrast to the findings of many classical embryologists (Siewing, 1963; Rempel and Church, 1971; Manton, 1960; Leuzinger, *et al.*, 1926; Roonwal, 1937), molecular studies have never revealed any additional preantennal segment, bearing the labrum as its appendage, between ocular and antennal segments. The genetic patterning mechanism involved in head segmentation was consistent in all types of arthropods investigated so far. These findings were also supported by *Drosophila* embryo mutant for head gap gene (*ems*); in which ocular, antennal and intercalary regions were reduced (Schmidt-Ott, et al. 1994b) without affecting the labrum because if there was any preantennal segment then labrum should also be deleted.

In parallel to the molecular studies, investigations of neuroatomical features have not only provided the additional support to resolve the hotly debated issue of the arthropod head segmentation (Maxmen, *et al.* 2005; Mittmann and Scholtz, 2003; Page, 2004; Eriksson, *et al.* 2003; Eriksson and Budd, 2000) but has also equally affected the phylogenetics relationship among various arthropod taxa (Strausfeld, 1998, 2009; Strausfeld, *et al.* 2006; Harzsch and Waloszek, 2000; Harzsch, 2006; Farris, 2003; Dove

and Stollewerk, 2003; Kadner and Stollewerk, 2004; Muller, 2008; Heuer, 2010). For example, the traditional view of reduction of the deutocerebrum in chelicerates, and correspondence of their cheliceral segment to the intercalary segment of hexapods and myriapods was challenged by molecular studies, and suggested that the cheliceral segment in chelicerates is homologous to the deutocerebral segment of hexapods (Telford and Thomas, 1998; Damen *et al.* 1998; Damen, 2002; Hughes and Kaufman, 2002). But the morphological evidence for this homology was provided with neuroanatomical studies conducted by Mittmann and Scholtz, 2003. They studied the development of nervous system of Horseshoe crab; *Limulus polyphemus*, by using antibodies against α -tubulin and synapsin, and showed that there was no additional segment in front of the chelicerae. Instead, developing brain structures (neuropile ring) of *Limulus* shows remarkable similarities with that of crustaceans and insects. Similarly, existence of intercalary segment was supported by embryological character such as segmental neuroblasts (Urbach and Technau, 2003). Maxmen, *et al.* 2005 studied the developmental neuroanatomy of the pycnogonid sea spider, a basal arthropod, with immunohistochemical techniques and concluded that three anterior pairs of ganglia in early protonymph central nervous system are homologous to the tripartite anterior brain (protocerebrum, deutocerebrum and tritocerebrum) of other arthropods (Scholtz and Edgecombe, 2006). Their finding of innervation of first pair of appendages of pycnogonid called chelifores by protocerebrum also corroborated other evidences against the acron concept, drawn from onychophoran neuroanatomy and nephridiogenesis (Eriksson, *et al.* 2003, 2010; Eriksson and Budd, 2000; Mayer and Koch, 2005) and palaeontological studies (Budd, 2002).

1.2. Nature of labrum:

The foregoing review shows that conflicting views were held by various workers with respect to the segmental elements involved in the formation of the procephalon and nature of labrum. But wide distribution of labrum among Hexapoda, Myriapoda and Crustacea leaves no doubt that morphologically the labrum is not an unimportant structure. Additionally, many of its developmental similarities are shared among the Euarthropoda. In embryo, labrum appears in front of the stomodeal invagination and anterior to the central nervous system (Eastham, 1930; Butt, 1957; Anderson, 1973; Scholtz and Edgecombe, 2006, Posnien, *et al.* 2009). It is formed by two anlagen which later fuse to form a single lobe. The genetic expression pattern mechanism is also similar throughout the Euarthropod representatives studied so far (Scholtz and Edgecombe, 2006). However, several studies suggested that labrum is an appendicular structure. First evidence for the appendicular nature of the labrum is inferred from embryological studies that contrasted the concept of acron, and provided support for the limb nature of the labrum. These studies implies that during embryonic development, labrum arises as a pair of limb buds close to the midline at the anterior of germband and is equipped with mesoderm which resembles the formation of appendages in trunk. Later in development, these lobes become fused and form a lobe like structure anterior to the mouth opening (Eastham, 1930; Butt, 1957, 1960; Siewing, 1969; Ullmann, 1964; Rempel and Church, 1969, Rempel, 1975; Posnien, *et al.* 2009, 2010). Second evidence for appendicular nature of labrum arrives from modern paleontological studies. Kukalova-Peck, 1991, 1992, 1998 studied Palaeozoic palaeodictyopteran insects and compared with recent pterygote insects. She concluded that clypeolabrum of insect was derived from the fusion of basal parts (coxopodites) of a pair of appendages associated with first head segments. She assumed that clypeolabrum, like those of thoracic legs, consisted of subcoxa, coxa and trochanter. According to her interpretation, coxal endites have formed the epipharyngeal lobes while the fusion of trochanteral endites has given rise to apical part of labrum. Budd, 2002 studied the Palaeozoic stem group arthropods and recognized two preoral appendages. He concluded that anterior most appendage is associated with ocular segment which has been reduced in crown group Euarthropods and is most likely a component of labrum while second appendage is the homolog of first antenna of

crustaceans. Appendage marker genes; *Distal-less* (*Dll*), *dachshund* (*dac*) and *extradenticle* (*exd*), have also provided the strongest support for the appendicular nature of the labrum. The most conspicuously studied gene is *Distal-less*. This gene is required for development of distal portion of limb, that is, the portion farthest from the body. It directs cells to create organs such as legs and antennae that bud off from a main body axis. The overall expression pattern of (*Dll*) in labrum is similar to that of arthropods limbs (Scholtz and Edgecombe, 2006). Labral expression of (*Dll*) is found in chelicerates (Popadic *et al.* 1998; Thomas and Telford, 1999, Schoppmeier and Damen, 2001), myriapods (Scholtz, *et al.* 1998; Prpic and Tautz, 2003), crustaceans (Panginiban, *et al.* 1995; Abzhanov and Kaufman, 2004; Scholtz, *et al.* 1998) and hexapods (Panginiban, *et al.* 1995; Rogers and Kaufman, 1997; Scholtz, *et al.* 1998; Prpic *et al.* 2001). The expression pattern of second appendage marker gene, *dachshund* (*dac*), was found as a half circle in anterior portion of embryonic labral buds of myriapods, chelicerate and hexapods (Prpic *et al.* 2001, 2003; Prpic and Tautz, 2003; Urbach and Technau, 2003). The expression pattern of third appendage marker gene, *extradenticle* (*exd*), was studied in grasshopper, *Schistocera americana*, where it expressed in labrum in a similar way as legs and antennae (Dong and Friedrich, 2005). Further, Kimm and Prpic, 2006 studied the expression patterns of the genes *wingless* (*wg*) and *decapentaplegic* (*dpp*) in the developing labrum of the red flour beetle, *Tribolium castaneum* and the spider *Cupiennius salei*. Both genes are responsible for dorsal-ventral patterning of the developing appendages (Jiang and Struhl 1996; Brook and Cohen 1996). Additionally, *wg* and *dpp* act co-operatively to set up the proximal–distal axis of the appendages (Diaz-Benjumea *et al.* 1994; Jiang and Struhl 1996; Lecuit and Cohen 1997, Jockusch and Williams, 2004). Kimm and Prpic found that both genes were expressed in the labrum of *T. castaneum* and *C. salei*, but their expression pattern was reversed compared to the other appendages. They concluded that labrum derives from paired appendage like primordia, which first undergo rotation and then fusion. Haas *et al.* 2001a provided a novel interpretation to the appendicular nature of labrum by showing that in *Antennagalea-5* (*Ag⁵*) mutant *Tribolium castaneum*; labrum was transformed into a mandibular like structure. They suggested that labrum is a fused structure composed of two pair of appendage endites which represents the coxal portion of a limb, and is serially homologous to gnathal appendages. Similar conclusions were also put forwarded by Boyan *et al.* 2002 examined the expression patterns of segment polarity gene, *engrailed* (*en*) and glial homeobox gene, *reversed polarity* (*repo*) in embryonic appendages of locust. They observed that the expression of *en* in posterior epithelium of labrum was typical of all appendages in early embryo, and *repo* positive glial cells were arrayed on stereotypical positions in the path taken by labral nerve in each half of this appendage. From their observation, they concluded that labrum is not only the appendicular but also articulated, composed of two jointed elements homologous to the coxa and trochanter of the leg. Later, Boyan *et al.* 2003 studied the embryonic developmental pattern of sensory innervation of labrum in a locust embryo and found organizational similarity with that of mouthparts and legs (Meier and Reichert, 1991), and proposed labrum as a serial homolog to gnathal and thoracic appendages.

1.3. Segmental affiliation of the labrum:

If labrum is an appendicular structure, then the question arises about its actual segmental origin. But a bias was laid for the identification of a segment. A segment was initially defined by Snodgrass, 1935 as, “a subdivision of body between areas of flexibility associated with muscle attachments.” Later, Butt, 1960 introduced the term of primary body segment covering from embryonic germ band to full grown adult and defined it as, “a primary body segment is a ring like portion of the body separated from similar rings by areas of flexibility and bearing, at some time during the development of the animal, a pair of appendages which may consist of simple transitory lobes in the embryo, a pair of coelomic sacs and a ganglion forming a part of the central nervous system with nerves running to the appendages”. Rempel, 1975 extended the criterion and described a

segment generally encompassing the following: A pair of mesodermal somites and coelomic sacs, a pair of appendages and their accompanying musculature, a pair of apodemes and a neuromere with its associated innervation pattern. More recently, appendage marker gene *distal less (Dll)* (Panganiban, *et al.* 1994; Popadic *et al.* 1998) or the segment polarity gene *engrailed (en)*, which have expression in the posterior epithelium of embryonic segment, have provided an additional criterion of a segment and its appendage.

Depending on the definition of a segment, conflicting views were put forward by many workers about insect head segmentation and segmental origin of the labrum. Embryologists have emphasized on the presence of coelomic sacs while others have stressed on innervation and muscle arrangement. Holmgren, 1916; Hanström, 1928, Snodgrass, 1960; DuPorte, 1957; Matsuda, 1965; Manton, 1960 have described labrum as a mere outgrowth of the body or an unpaired sclerite anteriorly overhanging the mouth. Eastham, 1930 and Roonwal, 1939 considered the labrum as appendage of first head segment innervated secondarily from tritocerebrum. Ferris, 1942 and Henry, 1947 regarded the labrum itself as a first head segment, innervated by its own neuromere; the tritocerebrum, and assumed that the tritocerebrum has phylogenetically shifted posteriorly. Rempel and Church, 1971; Rempel, 1975; Scholtz, 2001 interpreted the labrum as an appendage of the preantennal segment, innervated secondarily by the tritocerebrum which shifts from posterior to preoral position both in ontogeny and phylogeny. Butt, 1960 concluded that labrum is composed of highly modified appendages of premandibular/intercalary segment and is innervated by tritocerebrum. Snodgrass, 1960 and Matsuda, 1965 contested the view of labrum being a fused pair of intercalary appendages by stating that in crustacean both labrum and well developed intercalary appendages; second antennae, are present, and one could not expect same appendage at two places at once. But more recent studies describing the absence of expression of appendage marker gene *Distal-less (dll)* in insect intercalary segment (Cohen, 1990) and its expression in labrum and second antennae of crustacea (Panganiban *et al.* 1995; Popadic *et al.* 1998) has resurrected the idea of Butt for the labrum being a fused appendages of intercalary segment. A second support for this idea also came from the study of Haas, *et al.*, 2001a, b. On the basis of genetic mutant analysis in *Tribolium castaneum*, they assumed labro-intercalary as a composite structure, and proposed a new model of insect head segmentation called “L-/Bent-Y model”. This model envisioned ocular, antennal and labro-intercalary as the more anterior segments and the stomodeum develop completely between labro-intercalary segments. By considering the neuraxes and using molecular, immunocytochemical and retrograde axonal staining methods, Boyan, *et al.* 2002 also showed in locust embryo that the labrum is non-apical and topologically fused appendicular pair of intercalary segment. And all but one of the adult and embryonic motor neurons innervating the muscles of labrum have their cell bodies and dendrites within the tritocerebrum and are derived from the *engrailed* expressing tritocerebral neuroblast.

1.4. Aims of Thesis:

By definition, every appendage must be innervated by its own segmental ganglion and innervation pattern should include the sensory and motor elements (Rempel, 1975). Although it has been already described that sensory structures formation and their innervation patterns in embryonic labrum share similarity with that of head and thoracic appendages (Boyan *et al.* 2002, 2003), it lacks information about its motor innervation patterns. But, given in the similar way that the ganglia in all segments are formed embryologically, there seems good reason to believe that the principles underlying the design and operation will be broadly applicable to the rest of the central nervous system. Based on this principle, it seems sound to investigate the motor innervation patterns of labrum in adult animal and to compare these patterns with other well studied body appendages both at anatomical and physiological level. Such comparable studies might

reveal the changes in morphology and physiology of a given set of neurons innervating the underlying structure that went on to adopt different function during the course of evolution. The aim of the present work, therefore, is to expand the knowledge of anatomy, physiology and innervation of neurons of musculature of labrum in adult locust by combining the both electrophysiological and neuronal tract tracing methods, and to reveal the evolutionary changes underlying neuronal circuitry, which might help to solve the controversy related to this apical structure. Specifically, the present work aims to answer the following questions.

1. How many muscles are controlling the shape and movements of labrum in adult locust?
2. What is the innervation pattern of this musculature?
3. How many neurons innervate these muscles and where are their somata located?
4. What are the size of somata and which courses are taken by their primary neurites and axons inside the ganglion?
5. What are the branching pattern of primary neurites and in which neuropile do their ramification project?
6. What are the physiological properties of these neurons?

By knowing the answers of these questions, a conclusion will be made about the hypothesis: The labrum represents a structure that developed during the evolution by fusion of paired appendages associated with head third metamere; the intercalary segment.

2. Materials and Methods:

2.1. Animals:

Adult male and female of African migratory locusts, *Locusta migratoria migratorioides* (R. & F.) were taken from institute laboratory culture, fed on wheat seedlings and bran supplement and maintained for 12h: 12h of light and dark photoperiods. Before dissection, insects were collected in small boxes and kept in refrigerator for 30 minutes to anaesthetise by cooling at 4°C.

2.2. Locust ringer solution:

Locust ringer solution was made by following the recipe of Clements and May (1974). Two stock solutions, A and B were prepared, and working solution was prepared by diluting stock solutions. All salts used for stock solution were obtained from Merck KGaA, Germany. For solution A, 82g NaCl, 7.5g KCl, 5.52g NaH₂PO₄ and 10.68g Na₂HPO₄ were dissolved in distilled water to make a total volume of one litre. For solution B, 2.9g CaCl₂ was mixed with distilled water to get similar volume of 1000 ml. Thereafter working solution was prepared by diluting 100 ml of stock solution A in 600 ml of distilled water and later 100 ml of stock solution B was added by stirring slowly to avoid the precipitation of calcium phosphate. A final volume of 1000 ml was made by adding more distilled water and its pH was maintained at 6.89 with 1 M NaOH or 1 M KCl. All solutions were stored at 4°C in a refrigerator.

2.3. Retrograde labelling of neurons:

To know the total number and position of motor neurons innervating labral muscles and anterior dilator muscle of foregut (M1, M2, M3 and M38, Snodgrass, 1928), motor nerve branches of individual muscle were backfilled with retrograde neuronal tracer Neurobiotin® (Fig. 2.1 a, b).

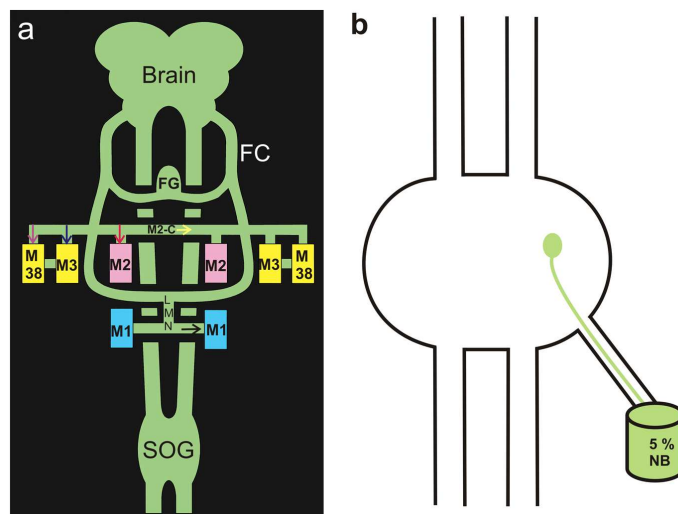


Figure: 2.1: (a) Schematic motor innervation pattern of labral muscles, reconstructed from present study of anterograde filling of frontal connective (FC) with 2% NiCl₂ and previous studies (Schachtner and Bräunig, 1993; Boyan *et al.* 2002; Ayali *et al.* 2002). Muscle numbering is used by following Snodgrass (1928). Different coloured arrows indicate motor nerve branches being backfilled. Muscle (M), Frontal ganglion (FG), Suboesophageal ganglion (SOG), Labral median nerve (LMN), M2-commissure (M2-C). (b) Schematic drawing demonstrating backfilling method. Peripheral nerve of a ganglion is cut at suitable length and kept in Vaseline container, filled with solution of retrograde tracer (5% Neurobiotin™). Motor neuron projecting its axon into the peripheral nerve was stained in retrograde fashion.

For staining the motor neurons of M1, branches of labral medial nerve (LMN) were backfilled. Both M2 are connected with each other by a peripheral commissure; M2-commissure (M2-C, Fig. 3.6), and are innervated by branches of FCM2 (Fig. 3.6). For staining the motor neurons, experiments were carried in two different fashions. In first case, a cut was given at the middle of M2-commissure and backfilled either in right or left direction. In second case, motor neurons were stained by backfilling specific motor nerve branches to each of M2. Motor neurons innervating M3 and M38 were stained either by their direct backfilling or by their specific motor nerve branches.

2.3.1. Dissection:

For the exposure of motor nerve branches of compressor muscles of labrum (M1) and anterior retractor muscles of labrum (M2), insect's heads were decapitated and mounted in Sylgard® Petri dishes (Dow corning, Midland, MI, USA) viewing frontal side up (Fig. 3.1a). Locust ringer solution was poured into the dishes and changed frequently during the dissection. Dissections were carried at room temperature under Zeiss stereomicroscope, and tissues were illuminated by infrared-free light source, KL 1500 LCD (Carl Zeiss Microscopy, Göttingen, Germany). Motor nerve branches of M1 (Fig. 3.5) were exposed by cutting the cuticle of median quadrate area of anterior wall of labrum (Fig. 3.1) and clearing the underlying fatty tissues. While M2- commissure (Boyan *et al.* 2002) and motor nerve branches of M2 (Fig. 3.6) were made visible by removing frons and clypeus and subsequently clearing the underlying tracheae, air sacs and fat bodies.

Posterior retractor muscles of labrum and anterior dilator muscles of foregut (M3 and M38 respectively, Fig. 3.7) lie parallel to each other and have common innervation. For the exposure of their motor nerve branches, and in the case where frontal connective was filled in anterograde fashion, decapitated insect heads were pinned laterally in Sylgard® Petri dishes. Mandible of underlying side was removed by cutting genal and post-genal cuticles. Thereafter, mandibular and antennal muscles (M8, M9, M4 and M5 Snodgrass, 1928) were removed and subsequently tracheae and fatty tissues were cleared. In case of direct backfilling of M3 or M38, muscles were exposed in same way as was for their motor nerve branches, and taken into filling chamber by cutting near to the insertion of their fibers on a tendon (dotted line, Fig.3.2b). In experiments, where longer incubation periods were required, oxygen supply was also maintained to keep the tissues alive. For that a big tracheae entering posteriorly into head was kept intact and stumps of it were opened at the surface of saline.

2.3.2. Neurobiotin staining:

The staining procedure was followed by a slight modification of a protocol described by Bräunig, (2008). Exposed motor nerve branches of each muscle were cut at suitable lengths. A Vaseline® chamber was build near the cut ends of muscles or nerve branches using a Vaseline® filled syringe (Fig.2.1 1b). The tip of syringe was equipped with a polythene tube of 0.86 mm internal diameter. The stumps of nerves or cut ends of muscles were isolated in chamber, and exposed to distilled water for 1-2 minutes to open the cut ends of nerves. Thereafter, the chamber was filled with retrograde neuronal tracer, Neurobiotin™ (5% (w/v) in distilled water, vector laboratories) and finally sealed with Vaseline®. Small amount of ringer solution was poured into the Petri dishes and covered them by glass lids. Tissues were incubated for 1-2 nights at 4°C in refrigerator. After incubation, Vaseline® chamber was removed. But to avoid leakage from Vaseline® chamber during its removal, first a hole was made into chamber and Neurobiotin™ was sucked by using fine tip glass pipette and finally Vaseline® chamber was removed. After rinsing the preparations 2-3 times with ringer solution; brain and suboesophageal ganglion along with frontal ganglion were dissected out of the head. The ganglia were fixed in formaldehyde (4% in distilled water) for 2 hours at 4°C in refrigerator. After fixation, tissues were washed for 6 hours with phosphate buffered saline containing 0.1% Triton x100 (PBS-TX) to increase membrane permeability. PBS-TX was changed after

every half an hour. To make visible the Neurobiotin™ staining, ganglia were incubated in CY³-conjugated streptavidine (Jackson Immuno Research) at a dilution of 1:2000 in PBS-TX for 24-36 hours. After incubation, preparations were washed with PBS-TX for 3 hours to remove dye on outer surface of the tissues. Again PBS-TX was changed after every half an hour. Now tissues were dehydrated for 5 minutes in each ascending series of 30%, 50%, 70%, 80%, 90% and 100% of Isopropanol. Finally tissues were mounted on glass slides using methyl salicylate as mounting medium and covered with glass cover slips.

2.3.3. Nickel chloride staining:

Investigation of the branching pattern of frontal connective was made by filling it in anterograde fashion with 2% NiCl₂ solution. For that, frontal connective was exposed as described in section 2.3.1 and a cut was given near the tritocerebrum. A Vaseline® chamber was made near the cut end of frontal connective and exposed to distilled water for 1-2 minutes. After that, chamber was filled with few drops of 2 % NiCl₂ solution and sealed with Vaseline®. Small amount of ringer solution was poured into the Petri dish and covered it with glass lid, and incubated the tissues over nightly at 4°C in refrigerator. After incubation, to remove Vaseline® chamber, a hole was drilled into the chamber and NiCl₂ solution was sucked by using fine tip glass pipette, and finally Vaseline® chamber was removed. Thereafter rinsing the preparations for 2-3 times with ringer solution, few drops (1 drop pro ml of ringer solution) of rubeanic acid were poured into Petri dishes. A bluish colour precipitation was developed after 10-15 minutes (Sakai and Yamaguchi, 1983). Again by rinsing for 2-3 times with ringer solution, heads were fixed in formaldehyde (4% in distilled water) for 2 hours at 4°C in refrigerator. After fixation; brain, frontal ganglion and labrum along with its musculature were carefully removed out of the head capsule. Finally tissues were dehydrated for 5 minutes in each ascending series of 30%, 50%, 70%, 80%, 90% and 100% of isopropanol and cleared in methyl salicylate.

2.3.4. Photography and Microscopy:

Photographs of freshly dissected preparations and Nickel chloride stained preparations were taken by a high resolution digital camera; Axiocam (Carl Zeiss vision, Germany), connected to a personal computer and attached to a stereomicroscope viewing the preparations directly from above. Preparations stained by using Neurobiotin® as retrograde tracer or iontophoretic injection were made visible under fluorescence microscope (Axiophot 2, Zeiss) at filter set 15. Digital images of Neurobiotin™ stained wholemount ganglia were taken by confocal laser scanning microscope (TCS SP2 from Leica Micro system, Germany). A x10 air objective was used to generate serial sections of 1-2 µm thickness, and a green line of 543 nm of Helium/Neon laser was used to excite CY³. For high resolution images, x20 multi-immersion objective was used. Images were taken at 1024 x 1024 resolutions and stored at a scanning speed of 200 Hz. 3D reconstructions and stereo images were made by merging stacks of digitized images using software provided by the leica microscope. Further, graphics editing software (Adobe Photoshop CS3, Adobe system, San Jose, California, USA) was used to adjust brightness and contrast, and to convert the false colours of images in red and green scale. Line drawings were made by using drawing tube attached to a Leica M3Z stereo microscope or by using graphics design software (Coral Draw® Graphics Suite X4, Coral corporation, Ottawa, Ontario, Canada).

2.4. Electrophysiology:

Suboesophageal ganglion neurons have common innervation to M1, M2, M3 and M38. To investigate the electrophysiological properties of these neurons, semi-intact preparations were used, and intracellular recordings from neuronal somata and muscle fibers were made. After recording, neurons were identified by iontophoretic injection of Neurobiotin™.

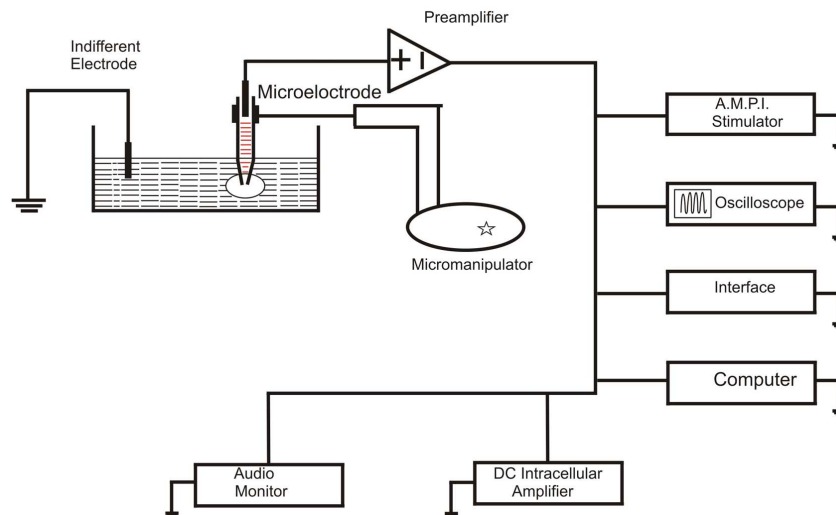


Figure 2.2: Flow chart diagram showing the intracellular recordings set up.

2.4.1. Dissection:

Electrophysiological experiments were conducted in two different modes. In some experiments, only post synaptic potentials (PSPs) from muscle fibers were recorded. While in others, simultaneous intracellular recordings from muscle fibers and neuronal somata were made. For the recordings of PSPs from muscle fibers, decapitated insect heads were pinned into Sylgard® Petri dishes viewing frontal side up and superfused with locust ringer solution. M2, M3 and M38 were exposed by removing frons and underlying fat bodies and tracheae. To maintain the oxygen supply to the ganglia, heads were pinned laterally into the Sylgard® Petri dishes and mandibular muscles (M8, M9. Snodgrass, 1928) were removed, and a big trachea entering posteriorly into the head was opened above the surface of saline.

In case of simultaneous intracellular recordings from muscle fibers and neuronal somata, decapitated heads were pinned in Sylgard® Petri dishes viewing their frontal side up and super fused with ringer solution. M2, M3 and M38 of only one half of the labrum were exposed. Thereafter, position of heads was inverted and pinned viewing their back side up. Suboesophageal ganglion was excised out of head capsule by removing labium, maxillae, mandibles and tentorium. Main tracheal supply to the suboesophageal ganglion was kept intact and its peripheral nerves were cut at suitable length. Now labrum was tilted laterally and pinned into the Sylgard® Petri dishes viewing the dissected half of its muscles up. Finally suboesophageal ganglion was fixed in Sylgard® Petri dishes. For that, suboesophageal ganglion was also tilted laterally without twisting the circumoesophageal connective and pinned in Sylgard® dishes with small insect pins using its peripheral nerves as “guy-ropes” (Schachtner and Bräunig, 1995, Bräunig, 1991, 1997). Finally tissues were superfused with locust ringer solution and stump of tracheae supplying to the SOG was opened at saline surface (Rast and Bräunig, 1997, 2001a).

2.4.2. Intracellular recording:

Preparations were kept in recording chamber and all recordings were made at room temperature. Following equipments and procedures were used for recordings from the dissected tissues. Figure 2.2 explains the actual experimental setup.

2.4.2.1. Enzyme treatment:

To facilitate the penetration of glass microelectrodes (Wilson, 1979a, Rast and Bräunig, 2001a), nerve sheath of the ganglia was digested by an enzyme, Pronase (Sigma-Aldrich, Germany). A direct enzyme application method was used. A filter paper of

ganglion size was cut and soaked in saline solution. Few crystals of enzyme were placed on it and mounted on ganglion for 30-60 seconds. After that, preparations were rinsed for 2- 3 times with locust ringer solution. Later it was also frequently changed during the experiment.

2.4.2.2. Glass microelectrode:

Intracellular recordings from neuronal somata and muscle fibers were carried with glass microelectrodes, made from borosilicate glass (GB 120F-8P, Science Products GmbH, Germany) using a vertical pipette puller (David Kopf instruments, Tujunga, California, U.S.A.). Electrodes used to record from neuronal somata were filled with two different solutions. Their tips were filled with Neurobiotin™ (5% (w/v) in distilled water) to stain the neurons after recordings, and shafts were filled with 2 M electrolyte solution of CH₃COOK. While electrode used to record the PSPs from muscle fibers were filled only with electrolyte solution of 2 M CH₃COOK. Before recordings, resistance of filled electrode was measured in bath solution using the option of electrode resistance testing on main intracellular amplifier. In former case resistance of electrodes was measured 40-80 M Ω while of those filled only with electrolyte solution was measured 40-60 M Ω.

2.4.2.3. Glass micro electrode mounting:

Filled electrodes were mounted in our own lab made electrode holders. Further to aid the impalement of neurons, electrode holders were connected with mechanical micromanipulator (Leitz, Germany).

2.4.2.4. Indifferent electrode:

Potential difference between two points can be measured by using two electrical leads. For intracellular recordings, microelectrode forms one lead and indifferent electrode the second one. To make indifferent electrode, a silver wire was connected to the grounding wire and dipped into the ringer solution and used as an indifferent electrode.

2.4.2.5. Amplifier:

Two amplifier, head stage and main D.C. intracellular amplifiers, were used for recording from neuronal somata and muscle fibers. The electrolyte solution of the microelectrode shaft was connected via a silver wire inside the electrode holder to the input cable of head stage amplifier. Output cable of the head stage amplifier was connected to the main D.C. intracellular amplifier. Main intracellular amplifier was also equipped with active bridge circuit, making it possible to simultaneously stimulate and record by using a single electrode. It also had the facilities for input capacity compensation, current injection, electrode resistance compensation, and electrode resistance testing.

2.4.2.6. Probing of neurons:

The procedure used to impale the neurons was a slight modification of the technique described by Pearson and Fourtner, 1975 and Wilson, 1979a. Following steps were carried to make successful impalement of microelectrode.

1. Tips of electrodes were dipped into Indian blue ink™ to make them visible under high intensity light.
2. A loud speaker was connected to the output wire of storage oscilloscope (Tektronix 5111A) to hear the sound produced by the recorded signal.
3. Positions of somata inside the ganglion were estimated by the reference of tracheal branches entering into the ganglion.
4. The electrodes were lowered slowly onto the ganglionic sheath with the aid of micromanipulator under visual guidance of high magnification stereomicroscope (M5A, Wild Heerbrugg, Switzerland). As the electrode crossed the ganglionic sheath, a sound was produced due to the increase in electrode noise.

-
5. Further slow and gentle penetration led the electrodes to impale the somata. As the neuronal somata were impaled, a negative potential was observed on storage oscilloscope (Tektronix 5111A).
 6. For the confirmation of impalement of somata, antidromic or orthodromic stimuli were applied and a spike was elicited.

After successful impalement of the somata, rise time of the output signal was improved by adjusting the amount of capacitive feedback, applied to the input cable to cancel the effect of stray input capacitance. Shift in the output potential, caused by the application of depolarising current to the cell, was cancelled by adjusting the active bridge circuit with stimulus balance knob of main intracellular amplifier.

2.4.2.7. Data acquisition:

Neuronal signals were monitored on a storage oscilloscope (Tektronix 5111A), and digitized with CED, power1401 interface (Cambridge electronic design, U.K.) by running spike2 software (version 6.04) and stored on a laptop.

2.4.2.8. Identification of neurons:

Neuronal somata were identified by adapting the standards set by many electrophysiologists (Hoyle and Burrows, 1973, Wilson, 1979a, Bowerman and Burrows, 1980, Bräunig, 1990, 1991, 1997). According to these authors one can identify a neuron by applying the following procedure:

1. Stimulate an axon of a neuron antidromically and record the responses from soma. Correlate latencies between soma responses and stimulus artifacts. If there is a constant relation between them, then a neuron can be tentatively described as right one.
2. Correlate the spontaneously activated soma spike with the muscle PSPs. If there is 1:1 correlation between them, then it could be the probed neuron.
3. Depolarise a neuron. Record responses simultaneously from neuronal soma and muscle fibers. If there is 1:1 correlation between passive soma spikes and PSPs of muscle fibers, then a neuron is identified as a motor neuron innervating a certain muscle.

2.4.2.9. Orthodromic stimulation:

For orthodromic stimulation, neuronal cell bodies and fibres of ipsilateral M2, M3 and M38 were impaled by glass microelectrodes. A constant depolarising current of maximally 10 nA was injected through the same recording electrodes to cause the spikes in cells, and simultaneously soma spikes and PSPs of muscle fibers was recorded. A 1:1 correlation was found by measuring the latencies between the responses recorded from soma and muscle fibers.

2.4.2.10. Antidromic stimulation:

For antidromic stimulation of motor axons of neurons innervating labral muscles, small holes in the cuticle at the site of muscles attachment were made. Pair of 30 μm steel wires, insulated except for their tips, was inserted through the holes into the fibers of M2, M3 and M38 under the visual aid of high magnification stereomicroscope (M5A, Wild Heerbrugg, Switzerland). Pair of these wires was connected to the constant voltage stimulus isolator (DS2A, Digitimer limited) to control the magnitude and duration of stimuli. Stimulus isolator was triggered by multi channel constant pulse generator (A.M.P.I. Master-8, Science Products GmbH, Germany). Voltage pulses of magnitude 3-5 volts and 1ms duration were applied after every 2 seconds to propagate an action potential inside the motor axons. Propagated action potential travelled towards the soma (a direction opposite to the normal), where it was recorded by a glass microelectrode

along with stimulus artefacts. A 1:1 correlation was made by measuring latencies between soma spikes and stimulus artefacts.

2.4.3. Intracellular staining:

After physiological identification of the neurons, intracellular staining was made by adapting the technique of Stretton and Kravitz, (1968), described in their pioneer work of electrophoretic injection of Procion Yellow to study the neuronal connection in lobster abdominal ganglia. In present work, neurons were stained by iontophoretic injection of Neurobiotin™. For that, multi channel constant pulse generator (A.M.P.I.) was connected to the stimulus input socket of main D.C. intracellular amplifier. Positive pulses of constant current of magnitude 5-10 nA and duration of 500 ms at 1.0 Hz were applied for 20-45 minutes. After filling, microelectrode was carefully pulled out, and insect heads were fixed in formaldehyde (4% in distilled water) for 2 hours at 4°C in refrigerator. After fixation, ganglia were removed out of the head and same histological protocol was carried out as described in section 2.3.2 for Neurobiotin staining. Results regarding these stainings were compared with the anatomical data investigated during retrograde fillings.

2.4.4. Data analysis:

Intracellular recording made from neuronal somata and muscle fibers showed noise signals in their traces. Before analysis, noise signals were removed by using the option of digital filters in spike2 software (version 6.04). Low pass second order IIR filters (infinite impulse response filter) were used for each trace and cut off frequency was adjusted at 100 Hz.

In case of simultaneous intracellular recordings from fibers of two different muscles, latencies between rising phases of PSPs of both muscles were measured. Amplitude and duration at half amplitude of PSPs of each muscle were also calculated.

In case of antidromic stimulation of axonal terminals, latencies between the stimulus artifacts and soma responses were measured. Latencies were calculated by taking time difference between stimulus onset and rising phase of passively invading soma spikes.

In case of orthodromic stimulation, latencies between passively invading soma spikes and PSPs of muscles were calculated. In this case, time differences between rising phases of passive soma spikes and PSPs of muscles were measured. Amplitude and duration at half amplitude were also calculated for both passive soma spikes and their evoked PSPs in muscles.

3. Results

3.1. Morphology of insect labrum:

The labrum is a feature of the arthropod head and active during feeding. The shape of labrum is variable in different insect groups. In orthopteroid insects, the labrum is a broad oval plate, freely suspended from the lower edge of clypeus in front of mouth and forms the upper lip (Fig. 3.1). Labrum is made of two cuticular flaps and is notched at the middle of its ventral margin (Fig. 3.1a). These cuticular flaps make anterior and posterior walls of the labrum (Snodgrass, 1928). On the outer basal half of anterior wall of labrum is a median quadrate area; below this area is a curved transverse sulcus that makes a low ridge on the inner surface of the anterior wall called transverse ridge. On the lateral basal margins of inner surface of anterior wall of the labrum are two small chitinous bars, the tormae that separate posteriorly the clypeus from labrum (Fig.3.2 a-f). A median Y-shaped thickening of cuticle of posterior wall of labrum makes a ridge on its inner surface (Fig.3.2 e, f). Inner surface of posterior wall is membranous and makes anterior wall of preoral cavity; epipharynx, and presents a number of features of special interest. Lateral parts of this surface are concave and fit closely over the anterior surface of the mandibles and bands of hairs are present on it that guards the exits from between the mandibles (Snodgrass, 1928). Minute sense organs are scattered over this surface, especially at each side of the notch in the ventral border of the labrum.

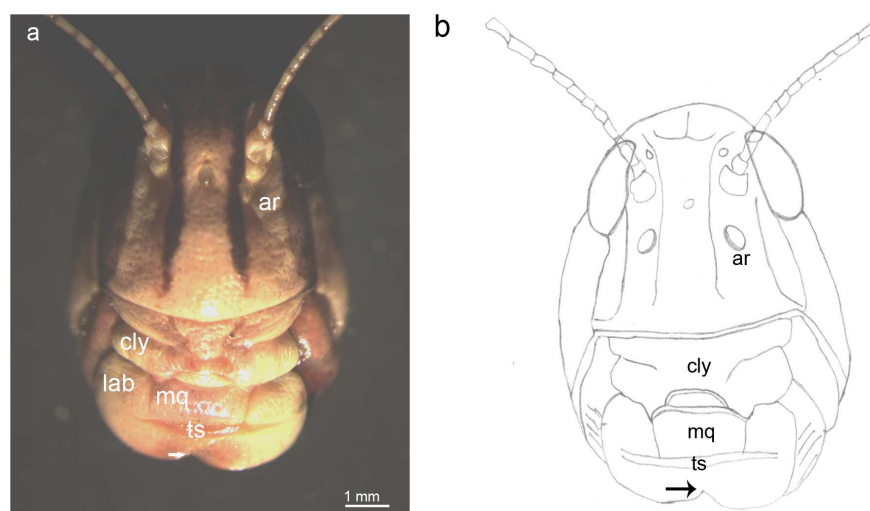


Figure 3.1(a) Frontal view of the head of *Locusta migratoria*. (b) Schematic view showing different parts of labrum. Antennal ridge (**ar**), Clypeus (**cly**), Labrum (**lab**), Median quadrate area (**mq**), Transverse sulcus (**ts**).

3.2. Musculature of labrum:

The shape and movements of the labrum in locust are controlled by three pairs of muscles; compressors of labrum (M1), anterior (M2) and posterior retractor of labrum (M3). Originally, these muscles were described and named by Snodgrass, 1928 in Carolina locust (*Dissostertia carolina*). A similar set of all three muscles is also found in *Locusta migratoria*. Usually skeletal muscles are fixed at either end to the integument and span a joint in the skeleton in such a way that the contraction of muscles moves one part of the skeleton relative to other. Such types of muscles have an origin in a fixed or more proximal part of the skeleton and an insertion into a distal movable part. In some other cases, muscles are attached to the invaginations of cuticle called apodemes. We have reinvestigated morphology and innervation of labral musculature in *Locusta migratoria*

and described their origin, insertion, size and shape of muscles related to the labrum of *Locusta migratoria*.

3.2.1. Compressor muscles of labrum (M1):

Compressors of labrum are short, cylindrical shaped muscles, present medially between the anterior and posterior cuticle walls of labrum (Fig.3.2 a, b, d, e). These muscles have their origin on the transverse ridge of the anterior wall of the labrum and run obliquely posteriorly to insert on arms of Y-shaped ridge in the posterior wall of labrum (Fig.3.2 c, f). These muscles do not take part in labral movements. Contraction of these muscles might help to pump out the haemolymph from the anterior part of the head and perhaps may help to sustain a flow of haemolymph within the labrum.

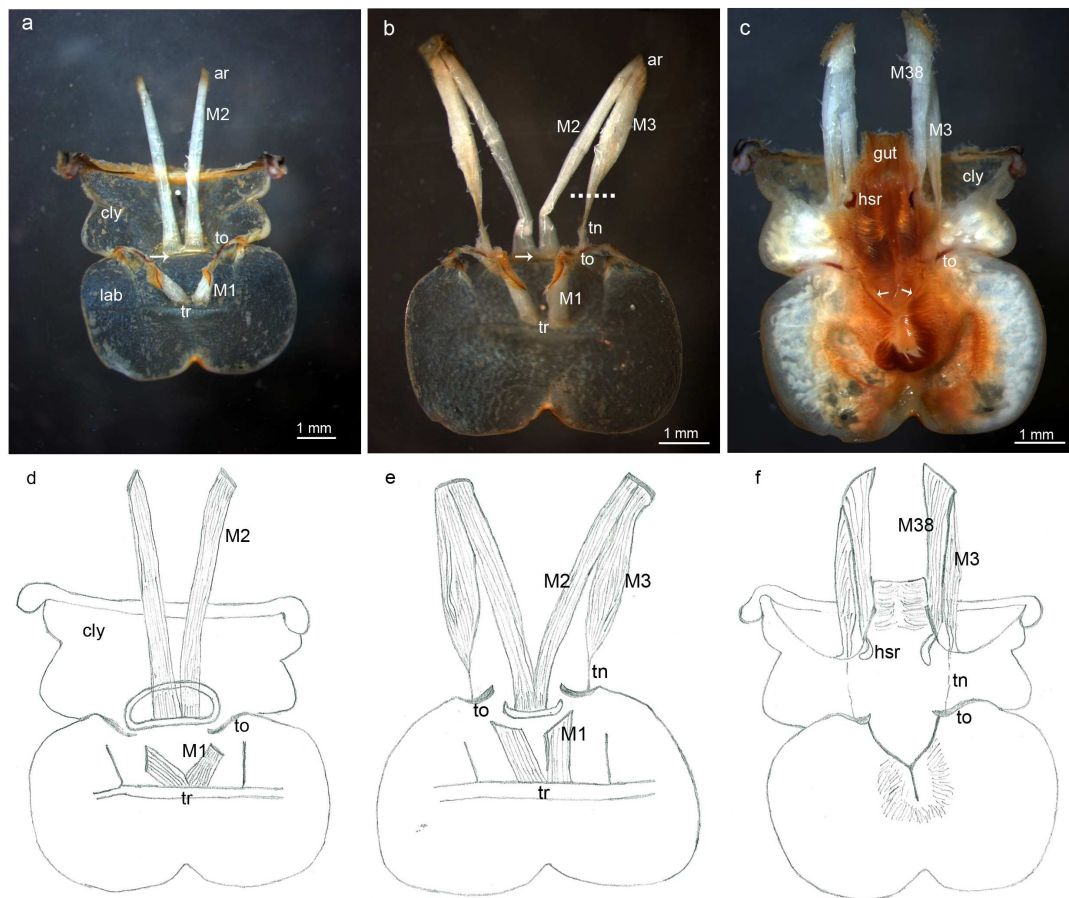


Figure 3.2. Photographs of musculature of labrum.

(a,b) shows inner surface of anterior wall of labrum along with muscle origins and insertions. M1 is originated at the transverse ridge (**tr**). M2, M3 have origin at antennal ridge (**ar**). **Arrows** indicate the insertion of M2 at the base of anterior wall of labrum while M3 is inserted at cylindrical tendon (**tn**), attached to the tormae (**to**). Dashed line on M3 marks the cut made for its direct backfilling. (d,e) schematic view of inner surface of anterior wall of labrum showing the transverse ridge, base of anterior wall of labrum and the tormae. In (e) thin cylindrical shaped tendon of M3 is attached to the tormae. (c) Inner surface of the posterior wall of labrum (epipharynx). **Arrows** show a median Y shaped thickening of cuticle that makes a ridge inside it, on which M1 are inserted. M38 have origin at antennal ridge (**ar**) and inserted at oral arms of the hypopharyngeal suspensorial rods (**hsr**). (f) Schematic view of epipharyngeal surface. Dotted line shows part of M3 tendon on the inner surface of clypeus.

3.2.2. Anterior retractor muscles of labrum (M2):

Anterior retractors of labrum are long cylindrical shaped muscles and have their origin on sub antennal ridge of frons (Fig.3.1 a, b). From their origin, muscles run ventrally under the cuticle of frons and pass through the clypeus to insert medially on the base of anterior wall of labrum (Fig.3.2 a, b, d, e). Their contraction raises the labrum from mandibles.

3.2.3. Posterior retractor muscles of labrum (M3):

Posterior retractors muscles of labrum are large cone shaped muscles and also have their origin on sub antennal ridge of frons (Fig. 3.1 a, b). They run ventrally on side lateral to M2 under the cuticle of frons. Fibers of these muscles are inserted on a thin, cylindrical shaped tendon which is short and sclerotized and attached to the tormae at the base of inner surface of anterior wall of labrum (Fig. 3.2 c-f). Contraction of posterior retractors muscles closes the labrum against mandibles and differential use of M2 and M3 can produce a lateral rocking movement of the labrum (Chapman, 1998).

3.2.4. Anterior dilator muscles of foregut (M38):

Beside the muscles of labrum, innervation of anterior dilator muscle of foregut was also studied. These muscles are closely associated with posterior retractors of labrum (M3) and both types of muscles have common innervation. Anterior dilators of foregut are long cylindrical shaped muscles of foregut. These muscles have same origin on antennal ridge of frons (Fig. 3.1 a, b), located medio-lateral to the M3 and run posteriorly to their insertion on oral arms of the hypopharyngeal suspensorial rods (Fig. 3.2 c-f).

3.3. Innervation of labral muscles:

3.3.1. Insect nervous system:

Insect nervous system consists of three elements; central, peripheral and stomatogastric nervous system. Central nervous system has brain and ventral nerve cord. In locust, brain is moved in dorsal direction viewing the ventral side of brain as frontal one (Fig.3.3). It is the principle association centre of body and receives the sensory input from the sense organs of head and from more posterior ganglia via ascending interneurons. It has three neuromeres; protocerebrum, deutocerebrum and tritocerebrum. Protocerebrum is bilobed and continuous with the optic lobe, process the visual and olfactory stimuli and is involved in insect learning. Deutocerebrum contains the antennal lobes and the antennal mechanosensory and motor centre and process sensory information collected by the antennae. Tritocerebrum consists of a pair of lobes beneath the deutocerebrum and connect the brain with ventral nerve cord and stomatogastric nervous system (Fig. 3.3 a).

Ventral nerve cord consists of chain of segmental ganglia. First ganglion of this chain is suboesophageal ganglion. It is a fused ganglion of three neuromeres and innervates the mouthparts. Suboesophageal ganglion is anteriorly connected to tritocerebral lobe of brain by circumoesophageal connectives. Both, brain and suboesophageal ganglion are located in the head capsule.

Stomatogastric nervous system in locust consists of unpaired frontal and hypocerebral ganglia and paired ingluvial ganglia (Fig3.3c). Frontal ganglion lies dorsal to the foregut and is anteriorly connected to the tritocerebrum by paired frontal connectives.

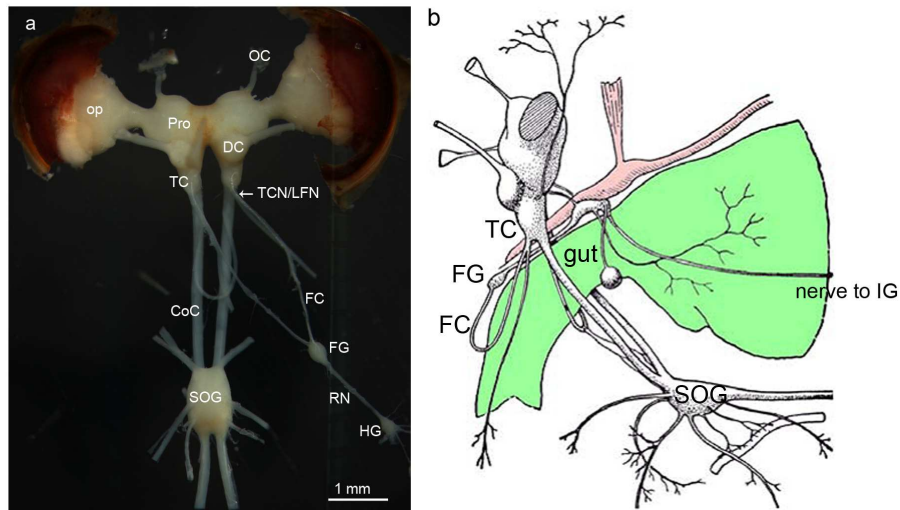


Figure 3.3 (a) Photograph showing the ventral view of the ganglia of central nervous system located in the head of *Locusta migratoria* and dorsal view of frontal ganglion and hypocerebral ganglion. For clarity the latter two ganglia are displaced on lateral side of the image. (b) Diagram showing the lateral view of the ganglia of central nervous system and stomatogastric nervous system (Modified from Snodgrass, 1928). Frontal ganglion (**FG**) is located dorsal to foregut and connected anteriorly to the brain by paired frontal connective. Optic lobe (**OP**), Ocellus (**OC**), Protocerebrum (**PRO**), Deutocerebrum (**DC**), Tritocerebrum (**TC**), Frontal connective (**FC**), Circumoesophageal connective (**CoC**), Suboesophageal ganglion (**SOG**). Tritocerebral nerve/ labro-frontal nerve (**TCN/LFC**, Auble and Klemm, 1977, Boyan *et al.* 2002). Ingluvial ganglion (**IG**). In (a) anterior is towards top of image.

3.3.2. Branching pattern of frontal connective

The musculature of labrum is innervated by nerve branches of frontal connective. Each frontal connective originates ventro-anteriorly from the tritocerebrum as a composite nerve called labro-frontal nerve or tritocerebral nerve (Aubele and Klemm, 1977, Boyan *et al.* 2002 respectively). After a short distance, both nerves become separated, and each frontal connective continues lateral to the foregut and passes between M3 and M38 to join the frontal ganglion anteriorly (Fig. 3.7). At level between M3 and M38, each frontal connective gives off 2 to 3 branches that innervate foregut dilators and labral muscles (Auble and Klemm, 1977, Ayali *et al.* 2002). Labral nerve of either side proceeds ventrally and gives off branches in each half of clypeo-labral complex to innervate sensory structures endowed by this complex (Boyan, *et al.* 2003). We have reinvestigated the branching pattern of frontal connective using nickel chloride staining (Section, 2.3.3). Staining revealed large variation in its branching pattern (Fig. 3.4 a-e). Variation was not only found in branch numbers but also in innervation of labral musculature. Each frontal connective was giving off anteriorly or posteriorly 2 to 3 branches and labral and gut musculature was innervated either directly by these branches or indirectly by their sub-branches.

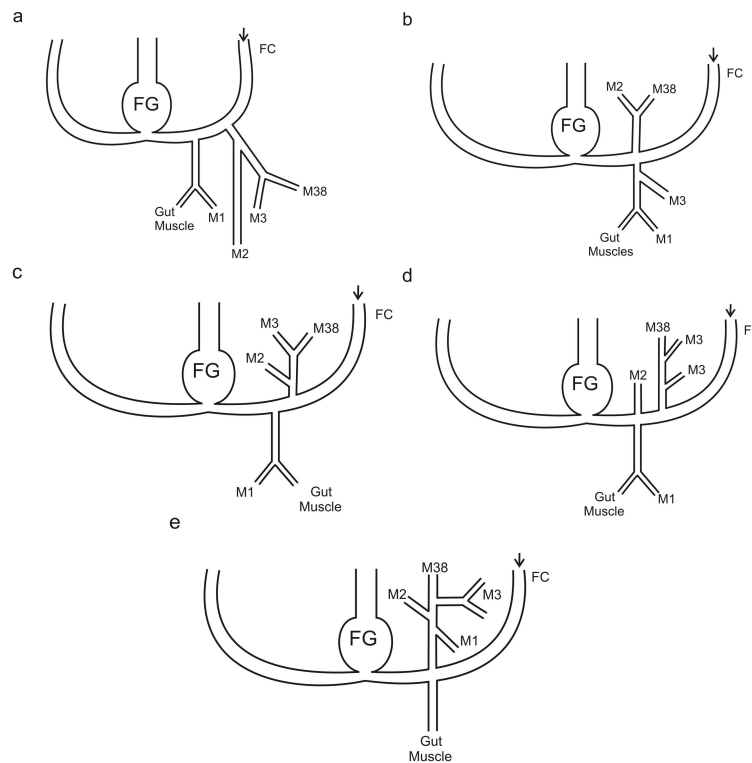


Figure 3.4 (a-e) Line drawings showing variation in branching pattern of frontal connective (FC), revealed after its anterograde filling with 2 % NiCl₂ (arrows indicate the direction of filling). Muscles and their innervation have not been drawn.

3.3.3. Innervation of compressor muscles of labrum (M1):

Musculature of labrum and gut is innervated either by directly arising branches of frontal connective or indirectly by their sub-branches (Fig. 3.4). However, in this and the following two sections, innervation pattern of labro-frontal nerve, revealed by nickel chloride staining of labro-frontal nerve, is described without considering direct or indirect branches and are taken as general branches. Compressors of labrum (M1) have their motor innervation on dorsal and ventral surfaces. Single branches of either frontal connective innervating the M1 (FCM1) first runs ventrally but lateral to foregut and then turns medially into the clypeus and make a loop. In clypeus, these branches fuse with one another and form a single nerve named as labral median nerve (LMN, Schachtner, 1993). The labral median nerve runs ventrally at mid line between both M2 and continues into labrum. When it reaches at the level of labral compressor muscles (M1), it divides again into two branches, named nerve root M1N by Boyan *et al.* (2002) to innervate the left and right M1 (Fig. 3.5). Close to the muscles, each M1N bifurcates and makes a dorsal branch to innervate the muscle fibers from dorsal side and a ventral branch to innervate the M1 fibers from its ventral side. Besides the motor nerve branches of M1, very thin nerves of satellite nervous system (Bräunig, 1987) were also seen that form anastomoses with labral median nerve and then give off branches to innervate both M1.

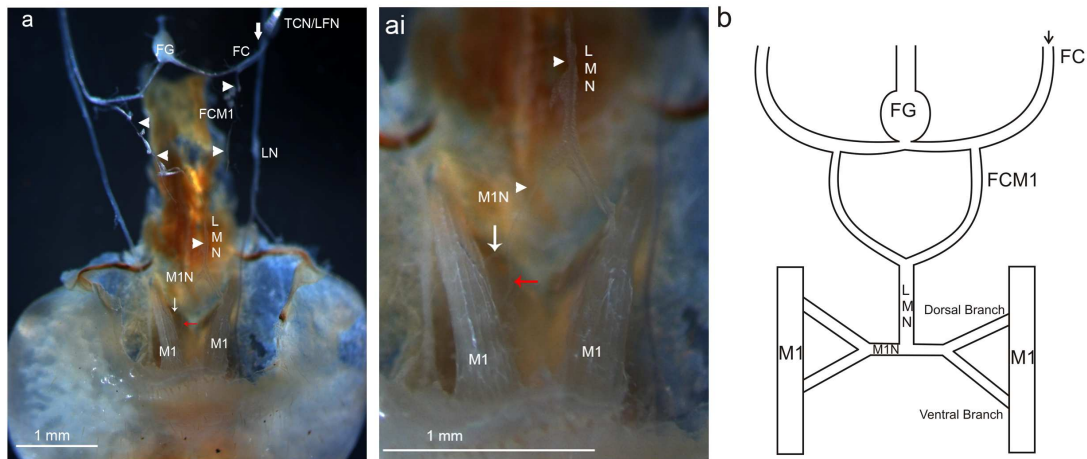


Figure 3.5 (a, ai) Photographs showing the innervation of **M1**, made after anterograde filling of tritocerebral/ labro-frontal nerve (**TCN/LFN**) with 2% NiCl₂. Thick **arrow** in this and following figure marks the direction of backfilling). (a) Ventral view of **M1**. Clypeus and cuticle of median quadrate area of anterior wall of labrum are removed. **FCM1** from either side (**white arrowheads**) run ventro-lateral to foregut and make labral medial nerve (**LMN**) in clypeus. (ai) Photograph of (a) at higher magnification. **LMN** bifurcate into right and left Nerve root **M1N** (Boyan *et al.* 2002). Each **M1N** again divides into dorsal and ventral branches (**white** and **red arrows** respectively). (b) Schematic figure showing innervation of **M1** reconstructed from the nickel chloride staining as shown in (a).

3.3.4. Innervation of anterior retractor muscles of labrum (**M2**):

Anterior retractors muscles of labrum (**M2**) have motor nerve innervation on their dorsal surfaces. Single branch of either frontal connective innervating the **M2** (**FCM2**) runs towards the **M2**, divides on its dorsal side and proceeds towards the midline. At mid line, the opposing branches fuse with each other and make a commissure in periphery (Fig. 3.6). This commissure was named as **M2-commissure** by Boyan *et al.* (2002). On its dorsal side of **M2**, each **FCM2** is divided into proximal and distal branches. Proximal branch innervates anterior part of muscle and distal branch innervates posterior part of muscle.

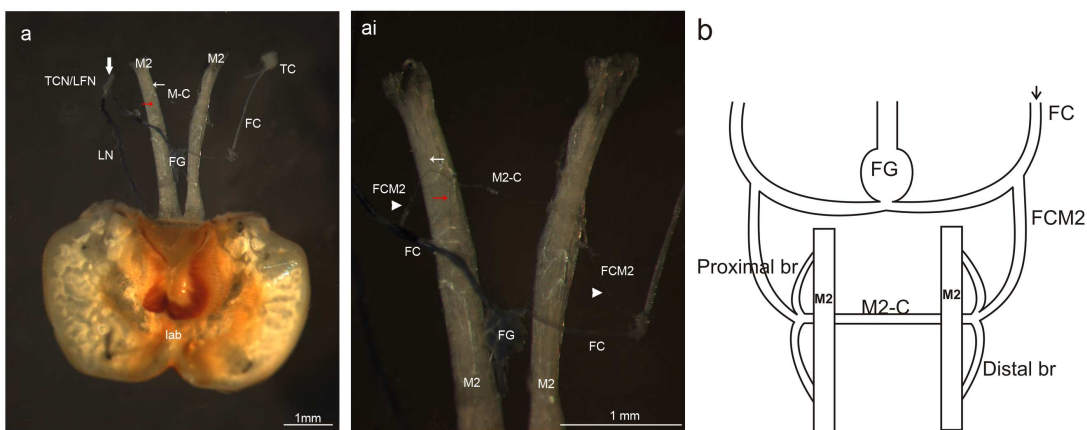


Figure 3.6 (a, ai) Photographs showing the innervation of anterior retractors of labrum (**M2**), made after anterograde filling of tritocerebral nerve/ labro-frontal nerve (**TCN/LFN**) with 2% NiCl₂. (a) Dorsal view of **M2** along with inner surface of the posterior wall of labrum (epipharynx). Clypeus and foregut are removed. Frontal ganglion is ventrally viewed, and for clarity is placed between **M2**. Both **M2** are connected with each other by **M2-commissure (M2-C)** and are innervated by proximal (**white arrow**) and distal (**red arrow**) branches of **FCM2**. (ai) Photograph of **M2**, as shown in (a), is taken at higher magnification. Each **FCM2** (**white arrowheads**) runs towards the **M2** and gives off proximal and distal (**white** and **red arrows** respectively) branches and proceeds towards the midline to make **M2-commissure** (Boyan *et al.* (2002). (b) Schematic figure showing innervation of **M2** reconstructed from the nickel chloride staining as shown in (a).

3.3.5. Innervation of posterior retractor muscles of labrum (M3) and anterior dilator muscles of foregut (M38):

Filling of labro-frontal nerve with nickel chloride revealed that M3 and M38 are innervated by a common branch of frontal connective (FCM3&M38). This branch bifurcates into ventral and dorsal branches to innervate M3 and M38 respectively (Fig.3.7). Innervation pattern of both branches was variable. Two patterns of innervations were found. In first pattern, ventral branch was innervating distal part of M3 and dorsal branch was giving off branches over the whole dorsal surface of M38. At antero-dorsal surface of M38, one of its branches runs towards the M3 and innervates proximal part of M3 while in second case, dorsal branch was innervating distal part of M38 and ventral branch was giving off braches over whole ventral surface of M3. At antero-ventral surface of M3, one branch runs towards M38 and innervate proximal part of M38 (Fig. 3.7 ai, aii).

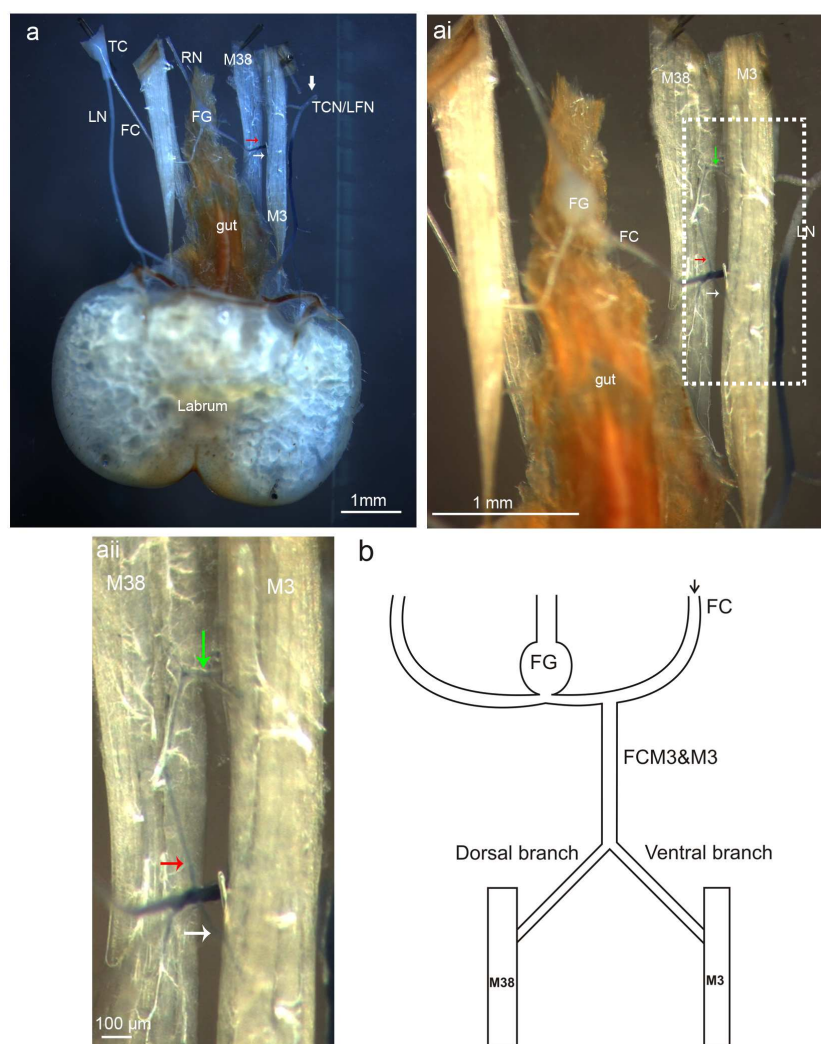


Figure 3.7 (a, ai) Photographs showing the innervation of posterior retractor of labrum (**M3**) and anterior dilator of foregut (**M38**), made after anterograde filling of tritocerebral nerve/ labro-frontal nerve (**TNC/LFN**) with 2% NiCl₂. (a) Dorsal view of M3 and M38 showing their innervation by common branch of frontal connective (FCM3 & 38). This branch bifurcates into dorsal and ventral branches (**red** and **white arrows** respectively). Dorsal branch innervates M38 while ventral branch innervates M3. (ai) Photograph of dorsal view of M3 and M38 as shown in (a) is taken at higher magnification using different light intensity. Image shows that at the antero-dorsal surface of M38, dorsal branch (**red arrow**) bifurcates and one branch (**green arrow**) runs ventrally to innervate proximal part of M3. (aai) Stippled area in (ai) is shown at higher zoom. (b) Schematic figure showing innervation of M3 and M38 by common branch of frontal connective (FCM3&M38) reconstructed from the nickel chloride staining as shown in (a).

3.3.6. Peripheral neurosecretory cells:

During course of investigation of innervation patterns, in some preparations, we found a small group of cells in periphery, located anterior to the frontal ganglion (Fig. 3.8). Many small thin nerves were emerging from these cells. Anteriorly, cells were connected by one of thin nerves to frontal ganglion and posteriorly, these cells were connected by a thin nerve to the M-2 commissure. Thin nerves were anastomosing with branches of motor nerves innervating the labral and gut muscles.

3.3.7. General motor innervation pattern of labral muscles:

Filling of frontal connective in the direction of frontal ganglion with 2% NiCl₂ revealed variation in its branching and innervation patterns. But, for the ease of subsequent work explanation, a general motor innervation pattern was derived (Fig. 3.8) on the basis of line drawings shown in figures 3.4e and 3.5. In this scheme, innervation of gut muscles has not included. According to this pattern, one branch of each frontal connective was immediately divided into three branches to innervate labral musculature. We named them as; frontal connective branch to M1 (FCM1), frontal connective branch to M2 (FCM2) and frontal connective branch to M3 and M38 (FCM3&M38).

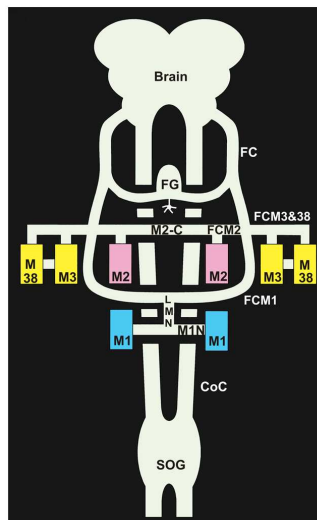


Figure 3.8 Schematic general motor innervation pattern of labral muscles, reconstructed from present and previous studies (Schachtner and Bräunig, 1993; Boyan *et al.* 2002; Ayali *et al.* 2002). Star shaped structure attached to the anterior of frontal is the mass of peripheral neurosecretory cells. Muscle (**M**), Frontal ganglion (**FG**). M2-commissure (**M2-C**), Frontal branch to M1 (**FCM1**), Frontal branch to M2 (**FCM2**), Frontal branch to M3 and M38 (**FCM3&38**), Labral median nerve (**LMN**), Nerve root M1 (**M1N**), Circumoesophageal connective (**CoC**).

3.4. Retrograde labelling of motor neurons innervating labral musculature:

3.4.1. Neurons innervating compressor muscles of labrum (M1):

In a total of 23 preparations, dorsal and ventral motor nerve branches of nerve root M1N innervating to M1 (Fig. 3.5) were exposed and backfilled with retrograde neuronal tracer Neurobiotin™. Motor nerve branches were stained either from left or right M1. In both cases results were similar (Fig. 3.9). Two motor neurons were consistently stained. Each lobe of tritocerebrum was containing one soma (Fig.3.8a). Staining revealed that axon of each neuron bifurcates in periphery to innervate ipsilateral and contralateral M1. Each neuron projects its axon into ipsilateral frontal connective and innervates via FCM1, labrum median nerve and nerve root M1N (Fig.3.9b). Cell bodies were oval in shape and located at ventro-lateral side of the tritocerebrum close to the deutocerebrum. Morphology of both neurons was similar and their ramification was not stained consistently in each experiment. Diameter of somata measured along their longest axis was ranging from 25-30 µm. In each lobe of the tritocerebrum, primary neurites after their emergence from the cell bodies run approximately 90-150 µm posteriorly close to the ventral surface and then turn towards the midline of the lobe and again run posteriorly deep into the ganglion. In the middle of the neuropile, near the exit into the frontal connective, the primary neurites give rise branches and turn ventrally to enter into the frontal connective as an axon. Individual axon was traced in each frontal connective. Branches of primary neurites project dorso-anteriorly, ventro-anteriorly and latero-anteriorly. These branches profuse and make very thin and fine cup shaped ramification in dorsal half of the tritocerebrum. Most of the arborisation was limited to the posterior half of the tritocerebrum while a few fibers project dorsally and ventrally into the anterior half of the tritocerebrum. In many stainings, an asymmetry was observed for one of the axons of the neurons. It makes a curve before entering into the frontal connective (Fig. 3.9 d). It could be an affect of fixative or might be due to a trachea that lies only along one of the frontal connectives.

Besides the stainings of motor neurons in lobes of the tritocerebrum, somata of satellite nervous system (Bräunig, 1987) were also faintly stained in mandibular neuromere of suboesophageal ganglion (results not shown). In some preparations, their faintly stained axons were visible in the mandibular nerve (N1, Altman and Kien, 1979).

3.4.2. Neurons innervating anterior retractor muscles of labrum (M2):

3.4.2.1. Backfilling of M2-commissure:

Both M2 are connected by M2-commissure (Fig. 3.6). Total number of motor neurons crossing this commissure was found by severing the middle of M2-C and backfilling either in right or left direction.

Motor neurons in the tritocerebrum:

In a total of 18 backfilling of M2-commissure either in right or left direction consistently stained three neurons in ipsilateral lobe of the tritocerebrum (Fig.3.10). Somata of two neurons were large while of the third was small. Backfilling revealed that their axons project into ipsilateral frontal connective and first innervate ipsilateral M2 via FCM2, proximal and distal branches to M2 (Nerve root M2N, Boyan *et al.* 2002) and then projects via M2-commissure to innervate the contralateral M2 (Fig.3.9 D). Diameter of smaller cell bodies was 17-30 µm while of larger cell bodies was 25-42 µm. Somata were round and oval in shape and their position was variable among individuals. They were lying separately or grouped together but were located in frontal and lateral cell body layer of the tritocerebrum, close to the deutocerebrum, as described by Aubele and Klemm, (1977). Primary neurites of separately located somata run latero-posteriorly close to the ventral surface and turn toward the middle of lobe to enter into the neuropile from latero-posterior of the tritocerebrum. At the turning point, the primary neurites group together and run posteriorly deep into the neuropile (Fig.3.10 b, c). The primary neurites of closely-

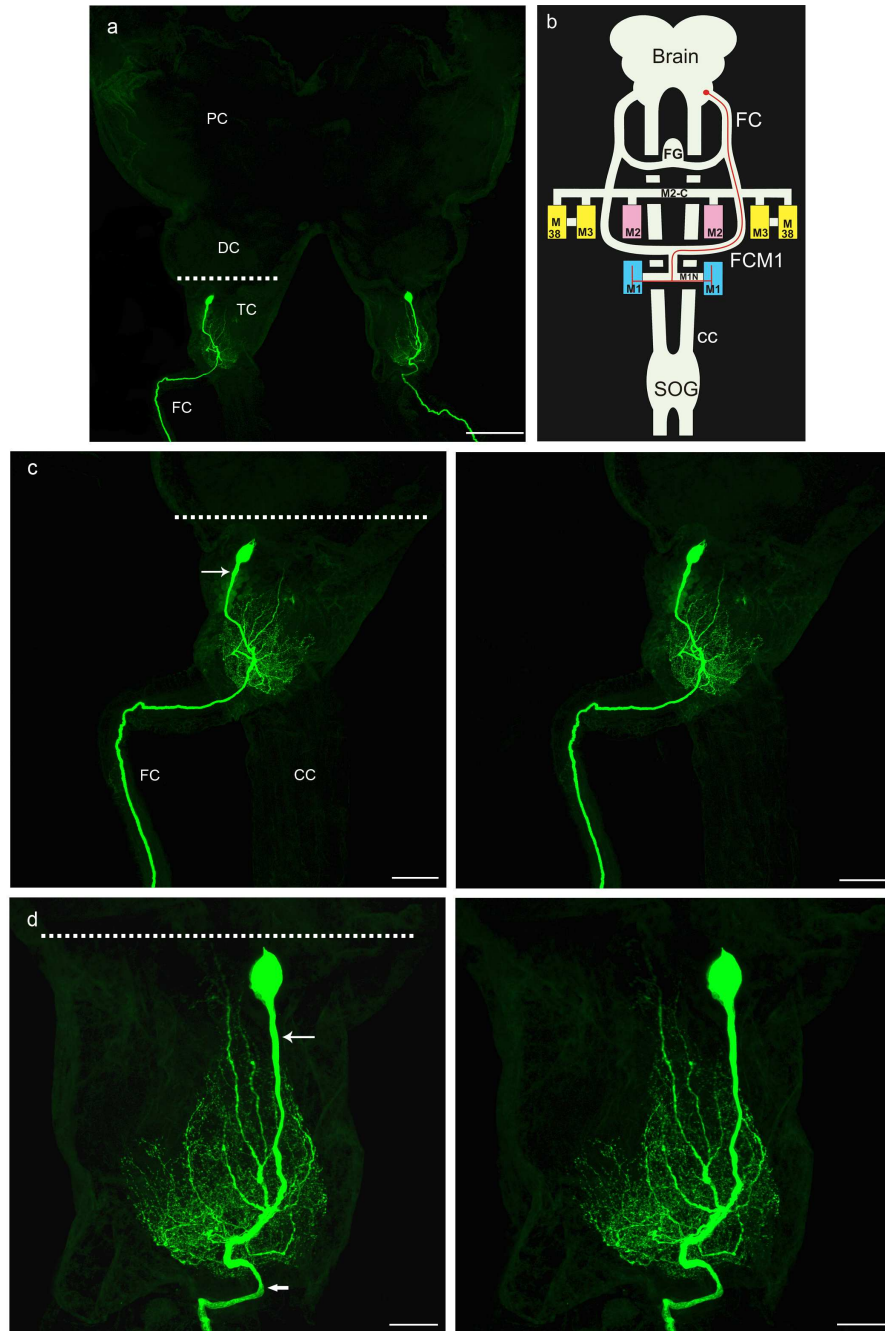


Figure 3.9 (a) Confocal image of a whole mount of brain of adult *Locusta migratoria* viewed ventrally, shows motor neurons in both lobes of the tritocerebrum (TC), stained with Neurobiotin through retrograde filling of motor nerves to M1 (Snodgrass, 1928). Somata are located at ventro-lateral side of the tritocerebrum close to the border of deutocerebrum (DC). Dashed line mark the border between two ganglia. (b) Schematic drawing showing the projection of motor neuron to M1. Only the projection of left side motor neuron is shown. Axon of the motor neuron (red) projects through the branch of frontal connective (FC) into labral medial nerve and bifurcates in periphery to innervate the ipsilateral and contralateral M1 via nerve root M1N. (c, d) Stereo pair of confocal images of motor neurons, shown in the right and left half of the tritocerebrum in (a), are taken using high magnification objective. Primary neurites (thin arrows in c, d) run ventro-posteriorly and turns medially to enter into the neuropile. Near exit into the frontal connective as an axon, each primary neurite gives off branches to make cup shaped ramification in the dorsal half of the tritocerebral lobe. Thick arrow in (d) marks the curve made by axon before entering into the ipsilateral frontal connective. In (a, c, d) anterior is towards the top of image. Scale bars: 200 μ m (a), 80 μ m (c), 40 μ m (d).

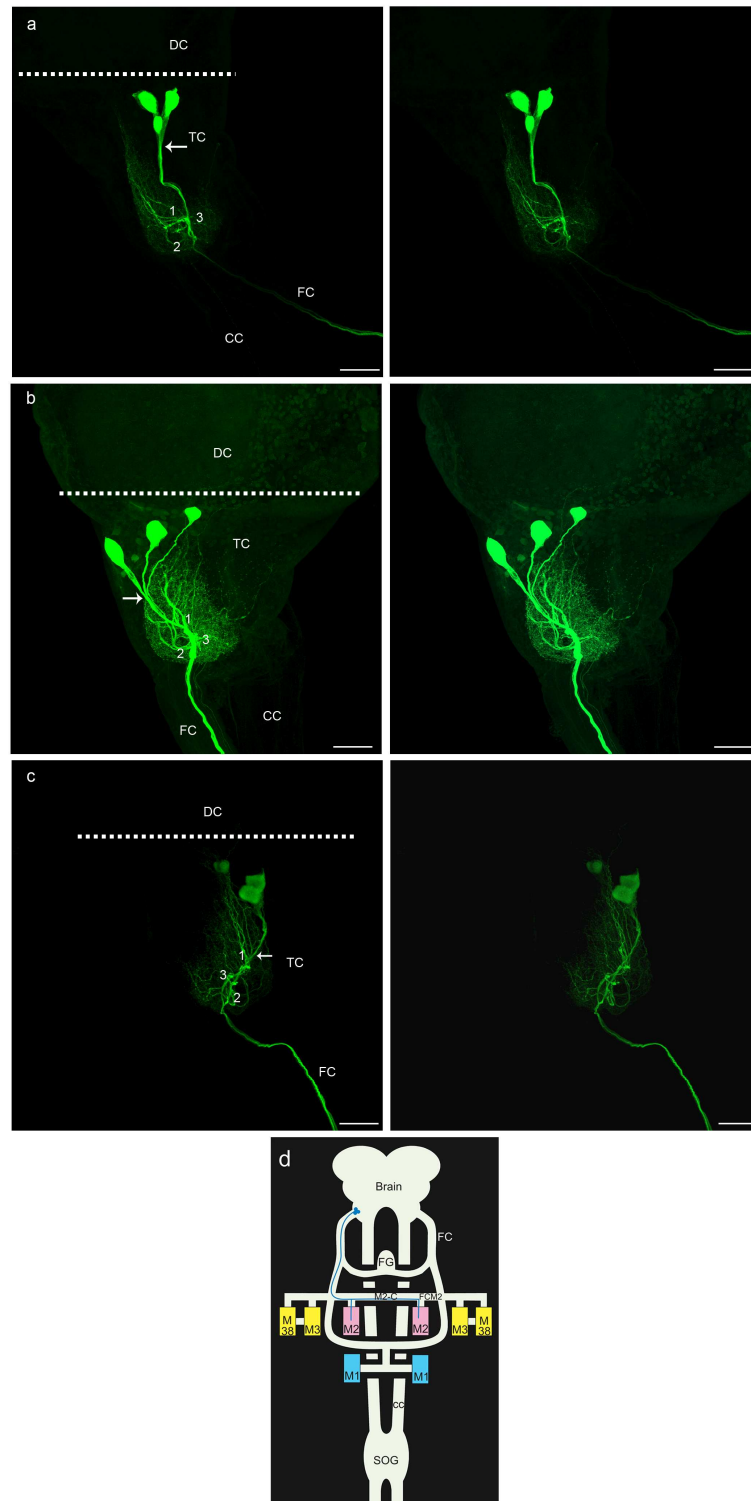


Figure 3.10 Backfilling of M2-Commissure. Stereo pair of confocal images of a whole mount of the tritocerebrum (TC) of adult *Locusta migratoria* viewed ventrally, show three motor neurons in the ipsilateral lobes of the tritocerebrum, stained after retrograde filling of M2- commissure (Boyan *et al.* 2002) with Neurobiotin™. Somata are present at ventral surface of the tritocerebrum close to the border of deutocerebrum (DC). **Dashed line** mark the border between two ganglia. **White arrows** mark the primary neurite. Inside the neuropile, (1, 2, 3) show three sets of overlapping branches at different region of integrating segments. (a, b) Stereo pair of confocal images showing motor neurons in right lobe of the tritocerebrum when M2-C was backfilled in right direction. (a) Cell bodies lie antero-ventrally at middle of the tritocerebrum. Larger somata are anterior to the smaller one. Primary neurites are packed together, run postero-medially to enter into the tritocerebral neuropile. (b) Small sized soma is antero-ventrally at middle of the tritocerebrum while larger somata are towards outer lateral border of the tritocerebrum. Primary neurites run latero-posteriorly and come close together to

enter into the tritocerebral neuropile. (c) Stereo pair of confocal images show motor neurons in left lobe of the tritocerebrum when M2-C was backfilled in left direction. Small sized soma is antero-ventrally at middle of the tritocerebrum while the larger somata lie close to each other at outer lateral border of the tritocerebrum. Their primary neurites run together latero-posteriorly and join the primary neurite of small sized soma before entering into the tritocerebral neuropile. (d) Schematic drawing showing the innervation of motor neuron to anterior retractor of labrum, M2. Only the innervation of left side motor neuron is shown. Axons of the motor neurons (**blue**) projects into frontal connective (**FC**) and innervate ipsilateral M2 via FCM2, proximal and distal branches to M2 (Nerve root M2N, Boyan *et al.* 2002). Anterior is towards the top of images. Scale bars: 80 μ m (a, b, c).

-located somata after their emergence get packed together and run posteriorly close to the ventral surface. After short distance, they turn toward the middle of lobe to enter into the neuropile and again run posteriorly deep inside the neuropile (Fig.3.10 a). Primary neurites give off three sets of overlapping branches at different region inside the neuropile before entering into the frontal connective as axons. Individual branch of each primary neurite and its ramification could be not distinguished separately. We have labelled these three sets of branches as 1, 2 and 3 (Fig. 3.10). Axons inside the frontal connective were closely packed and were not individually followable. Branches of primary neurites project dorso-anteriorly and latero-anteriorly. These branches bifurcate intensively and make fine triangular shaped ramification in dorso-lateral area of the tritocerebral neuropile. Whole ramification was limited to the tritocerebrum and no fiber was projecting into the deutocerebrum.

Motor neurons in suboesophageal ganglion:

Backfilling of M2-commissure also stained some motor neurons in mandibular neuromere of suboesophageal ganglion. Maximum two somata were stained. With respect to M2-C backfilling direction, one soma was located in the ipsilateral half of the mandibular neuromere and second was in the contralateral half of mandibular neuromere of the suboesophageal ganglion. Neurons were not stained in all experiments, and preparations showing SOG neurons were also not describing the complete picture of the neurons. In some, only somata were visible and their ramification and complete path of axons could not be traced while in others, only axons in circumoesophageal connectives were visible and their somata were not stained. However, the overall map of suboesophageal neurons was obtained from two preparations that revealed both somata and axons in single preparation. The incomplete stainings of neurons may be due to the following reasons;

1. Backfilling of a nerve may not stain completely because an axon may get damaged during dissection or blocked when stump of a nerve is placed in Vaseline™ container. In both cases an axon will fail to take up the tracer being used to stain the neurons. Such problems were described by Bräunig (1991) during his course of investigation of dorsal unpaired neurons of suboesophageal ganglion. He backfilled circumoesophageal or cervical connective differentially with NiCl_2 and CoCl_2 to labels the DUM neurons in the suboesophageal ganglion, and described then neurons with axons in connectives might fail to take up one or the other dye, or might entirely fail to stain.
2. Second possibility for the incomplete staining of suboesophageal ganglion neurons could be accounted for long distance between labral motor nerves and suboesophageal ganglion. Incomplete stainings of the suboesophageal ganglion neurons due to long distance between brain and suboesophageal ganglion were described by Bräunig (1990) during the study of the suboesophageal neurons projecting their axons into the nervus corporis cardiaci III (NCC III). Backfilling of the NCC III with CoCl_2 solution revealed faint and incomplete stainings in suboesophageal ganglion. In another study, Bräunig (1991) made intracellular fills of DUM neurons of suboesophageal ganglion innervating the principal neuropile areas of brain and described the circumoesophageal connectives in locusts are very long, and

it is difficult to get complete intracellular fills of neurons showing all ramifications within the brain.

The axons of suboesophageal ganglion motor neurons ascend through circumoesophageal connectives into the tritocerebral lobe of brain and proceed into the respective side frontal connectives without making ramification in the tritocerebral lobes. The axon of ipsilateral neuron runs in close association with the axons of the tritocerebral neurons and could not be traced individually. Neurons innervate the ipsilateral M2 via FCM2, proximal and distal branches to M2 (Nerve root M2N, Boyan *et al.* 2002). But axons of both ipsilateral and contralateral suboesophageal neurons, give rise to branches into the respective frontal connective that cross the midline in periphery using the frontal ganglion as a commissure and innervate the contralateral side muscles. The type of muscle which is specifically innervated on contralateral side is described in section 3.4.6. Only two fibers were found to cross the frontal ganglion. Detailed morphology of suboesophageal ganglion motor neurons is described in next section (3.4.2.2).

Serotonergic and dorsal unpaired median neurons:

Like the M1, Backfilling of M2-commissure in right or left direction also stained somata of satellite nervous system (Bräunig, 1987) and their axons were visible in mandibular nerve, N1 (Altman and Kien, 1979). In one preparation, a single soma and axon of dorsal unpaired median neurons was also faintly stained in suboesophageal ganglion.

3.4.2.2. Backfilling of motor nerve branch to M2:

Backfilling of M2-commissure showed that motor neurons in the ipsilateral lobe of the tritocerebrum cross the mid line in periphery using M2-commissure to innervate the contralateral muscles. To find the contralateral targets of these neurons and to know the detailed morphology of the suboesophageal ganglion neurons, proximal or distal motor nerve branches to M2 (Fig.3.6) were backfilled with or without severing the M2-commissure.

Neurons in the tritocerebrum:

In total, 9 backfilling of specific motor nerve branch to M2 were made either from right or left M2 without severing the M2-commissure. Each case showed consistently three motor neurons in ipsilateral lobe of the tritocerebrum and three motor neurons in the contralateral lobe of the tritocerebrum. In 3 backfilling of specific motor nerve branch to M2 with severing the M2-commissure stained three motor neurons only in the ipsilateral lobe of the tritocerebrum (Fig.3.11). Staining confirmed that motor neurons in the either lobe of the tritocerebrum not only innervate ipsilateral M2 but their axons cross the M2-commissure in periphery and also innervate the contralateral M2. Morphology of neurons found in both lobes of the tritocerebrum was similar to the neurons found by backfilling M2-commissure (compare figure 3.10, 3.11 and 3.12). Neuronal morphology was not completely stained in all backfills. Two large somata and one small soma were stained in each lobe of the tritocerebrum. Diameter of smaller somata stained by severing M2-commissure was 17-24 μm and of larger somata was 21-35 μm and in case of staining without severing M2-commissure, smaller somata were 21-25 μm and larger somata were 25-42 μm . Shape of somata was round or oval and their position varied among individual. Smaller soma was located at the ventral middle surface of the tritocerebral lobe. Larger somata were also located at ventral surface of the tritocerebral lobe but one of the two large somata was 1-2 cell layers deep while second was 3-4 cell layers deep. Positions of larger somata were more variable than the position of smaller one. Three main types of variation were found with respect to the position of small soma.

In first case, one larger soma was present lateral to the small soma in the direction of outer lateral border of the tritocerebral lobe while second larger soma was in the direction of inner medial border of tritocerebral lobe (Fig.3.11 a, ai). In second case, both larger somata were present lateral to the small soma in the direction of outer lateral borer of the

tritocerebral lobe (Fig.3.11 b, bi.). Either both were present at more lateral position to smaller soma close to the outer lateral border of the tritocerebrum (Fig.3.12 b, c and 3.10c) or one larger soma was close to the outer lateral border of the tritocerebrum while second was close to the small soma (Fig.3.11bii and 3.10b). In third case, larger somata were present on the same middle location of the small soma in lobe of the tritocerebrum but these were either lying anterior or posterior to the small soma (Fig.3.10a, Fig.3.11aii and 3.12a).

Like the morphology of motor neurons innervating leg muscles, primary neurites of the motor neurons stained either by backfilling of M2-commissure or specific motor nerve to M2 can be divided into two segments; an “initial segment” and an “integrating segment” (Burrows and Hoyle, 1973; Wilson 1979a). Initial segment run latero-posteriorly close to the ventral surface and later take turn medially to enter into tritocerebral neuropile. Part of primary neurite inside the neuropile forms an integrating segment. In integrating segment, the primary neurites first run posteriorly deep into the neuropile and then turn again ventrally to enter into the frontal connective as axons. When somata were lying close to each other at ventral middle surface of the tritocerebral lobe, the initial segments of their primary neurites immediately after their emergence come close together and form a tract that runs posteriorly for short distance and then take turn medially to enter into the neuropile (Fig.3.10a and 3.12aii). When somata of larger neurons were lying close to each other but lateral to the small soma, initial segments of their primary neurites run together latero-posteriorly and join the primary neurite of the small soma at entrance into the neuropile (Fig.3.10C and 3.12c). Initial segments of primary neurites have no branches while integrating segments give rise branches into the neuropile. Branches project dorso-anteriorly and latero-anteriorly. At integrating segments, three sets of overlapping branches arise in dorso-medial and medial regions of neuropile (Fig.3.10 and 3.12c). In preceding section, we named them as set 1, 2, and 3. Branches in set 1 emerge at start of the integrating segments while of 2 and 3 emerge opposing each other on the part of integrating segments close to the their exit into frontal connective as axons. Branches in set 1 proceed dorso-anteriorly and their bifurcations run latero-anteriorly and dorso-anteriorly. Branches in set 2 make a characteristic loop inside the neuropile. First, branches proceed posteriorly within the neuropile and then turn to outer lateral border of the neuropile and finally run dorso-anteriorly to join the branches of set 1. Beside the main branches of set 2, many thin branches emerge from the integrating segments and run in the same postero-lateral fashion outer to the loop made by branches of 2, and join latero-anteriorly projecting ramification of branches of 2. These small thin branches cover the most posterior and lateral area on dorsal side of the neuropile. Branches in set 3 proceed dorsally towards the inner medial border of the neuropile. At border of the neuropile branches bifurcates; one part projects anteriorly close to the most dorsal surface of the neuropile while second part run at ventral surface of the neuropile.

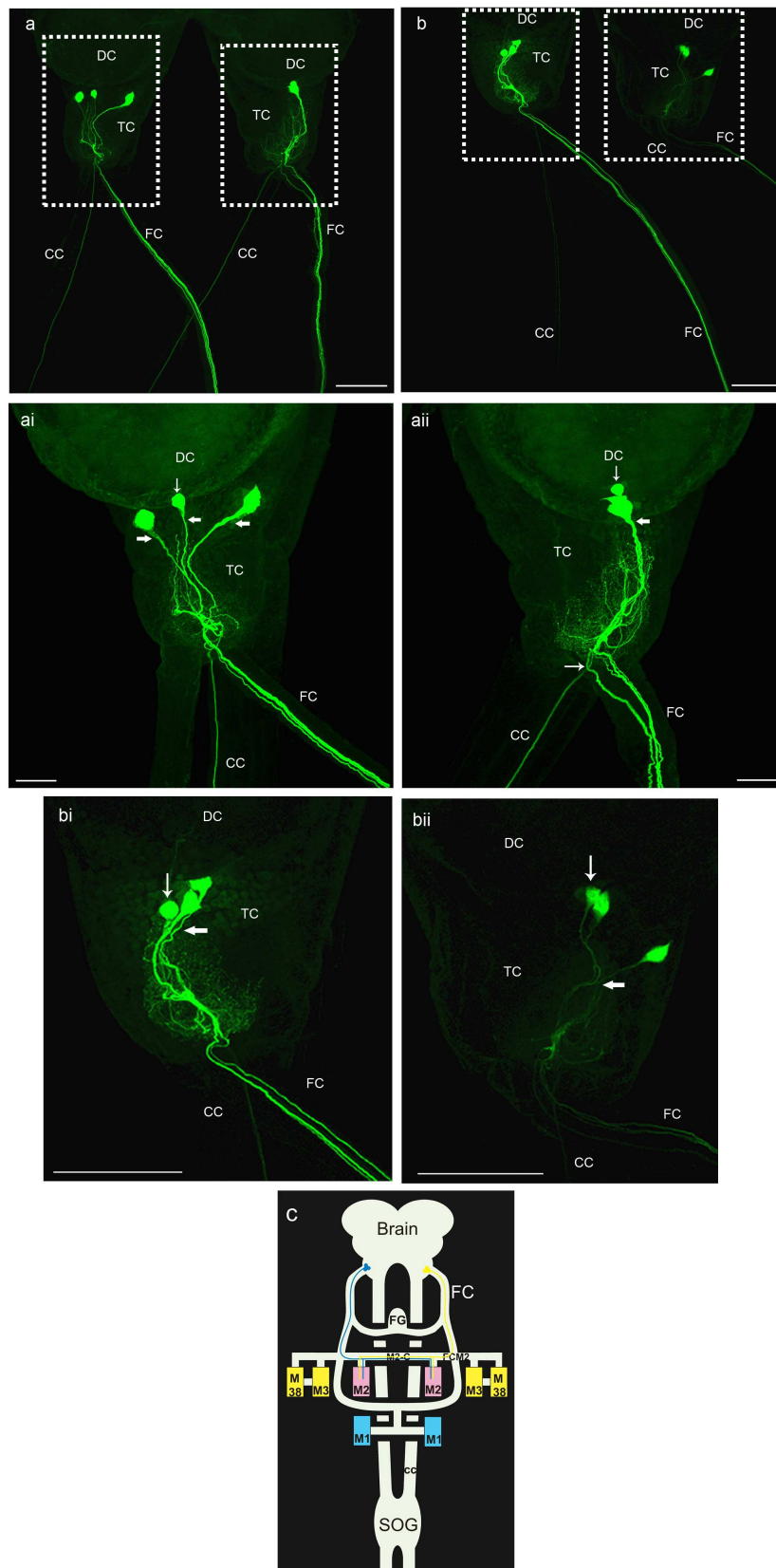


Figure 3.11 Backfilling of motor nerve branches to M2 without severing M2-commissure. (a,b) Confocal images of a whole mount of part of the brain of adult *Locusta migratoria* viewed ventrally, show three motor neurons in each lobe of the tritocerebrum (TC) projecting axons into frontal connectives (FC), stained by retrograde filling of motor nerve branches of left M2 (a) or right M2 (b). Vertical arrows mark small sized soma while thick horizontal arrows mark primary neurites. (ai,aii) Confocal images of contralateral (ai) and ipsilateral (aii) lobe of tritocerebrum shown in inset (a) are

taken using high magnification immersion objectives. Small sized somata are present at the middle of ventral surface of tritocerebral lobe. Larger somata in (ai) are present lateral to smaller one and in (a_{ii}) are posterior to smaller one. Primary neurites run posteriorly by packing together (a_{iii}) or run separately but come close together in neuropilar segment (ai). In (ai, a_{ii}, bi and b_{ii}), part of circumoesophageal connectives (**CC**) shows that axons of ipsi- and contralateral suboesophageal neurons enter into the tritocerebrum and join other axons in frontal connective without making any ramification inside the tritocerebrum (thin horizontal **arrow** in a_{ii}). Ipsilateral (bi) and (b_{ii}) contralateral lobe of tritocerebrum in inset (b) are shown at higher magnification. Small sized somata are present at middle of ventral surface of tritocerebral lobe. Larger somata are on lateral to smaller somata in the direction of outer lateral border of tritocerebrum. Primary neurites in (bi) run in parallel but not packed together while in (b_{ii}) run separately and come close together in neuropilar segment. (c) Schematic figure summarizing the results of M2 motor nerve branch backfilling without severing M2-commissure. Axons of the motor neurons (**blue, yellow**) in either lobe of tritocerebrum project into frontal connective (**FC**) and innervate ipsilateral M2 via FCM2, proximal and distal branches to M2 (Nerve root M2N, Boyan *et al.* 2002) and then further project via M2-commissure to innervate the contralateral M2. Anterior is towards the top of images. Scale bars: 200 μm (a, b, bi, b_{ii}), 80 μm (ai, a_{ii}).

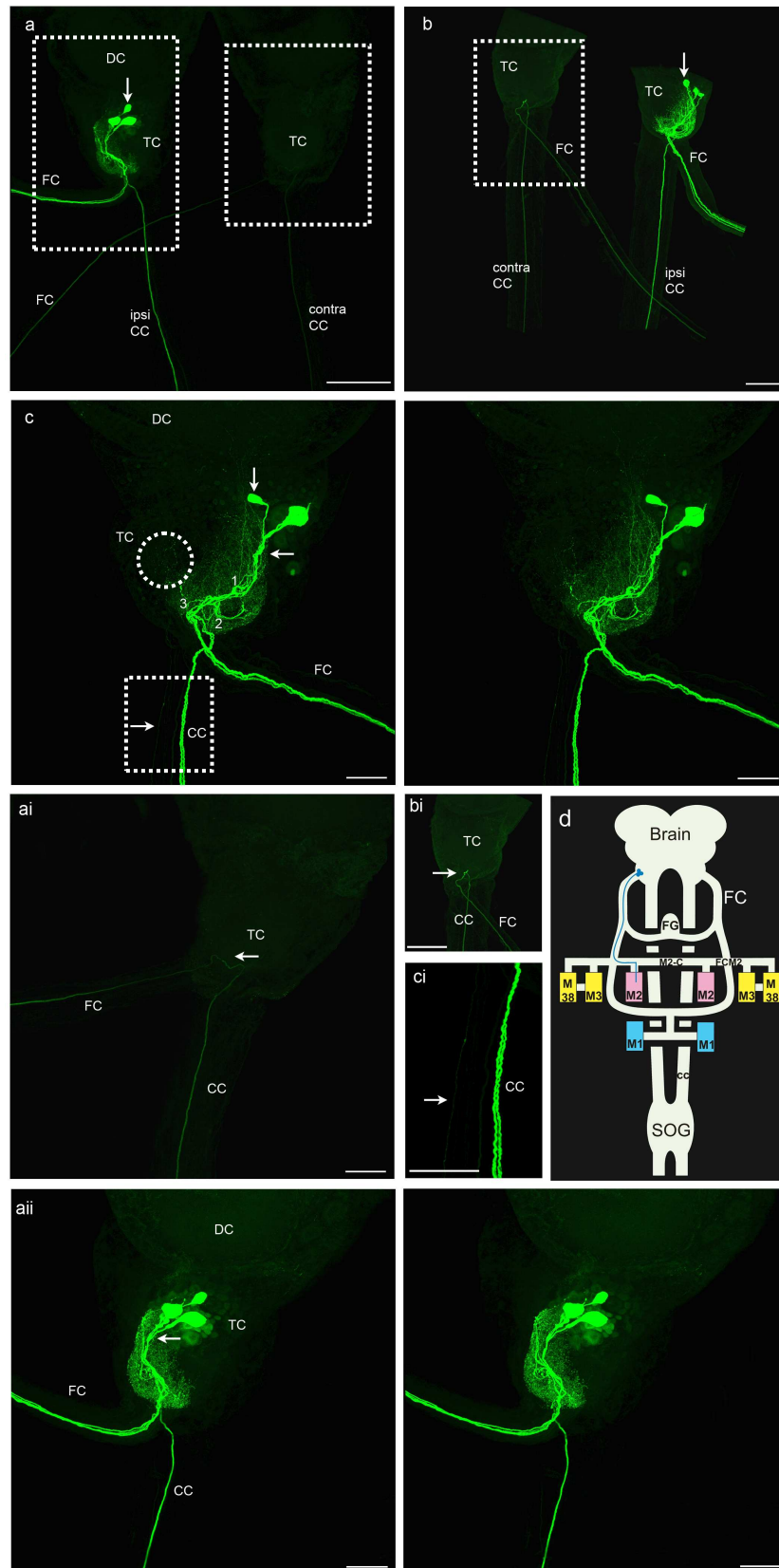


Figure 3.12 Backfilling of motor nerve branch to M2 by severing M2-commissure.

(a, b) Confocal images of a whole mount of part of the brain of adult *Locusta migratoria* viewed ventrally, show three motor neurons in ipsilateral tritocerebrum (TC) projecting their axons into frontal connective (FC), stained by retrograde filling of motor nerve branches of right M2 (a) or left M2 (b, c). Part of ipsilateral and contralateral circumoesophageal connective (ipsiCC, contraCC) shows that axons of suboesophageal neurons project into frontal connectives (FC) via the tritocerebrum. Small

sized somata (vertical **arrows** in, a, b, c) are present at ventral middle surface of tritocerebral lobe. Larger somata in (b, c) are lateral to the smaller one towards the outer lateral border of tritocerebrum while in (a) are posterior to the smaller soma. (ai) confocal image of contralateral lobe of the tritocerebrum shown in inset (a) is taken by using high magnification immersion objective. (bi) contralateral lobe of the tritocerebrum in inset (b) is shown only at high magnification. In both lobes, axons of contralateral suboesophageal neurons do not make any ramification (**arrows**) and project into respective frontal connectives. (aai) Stereo pair of confocal image of ipsilateral lobe of the tritocerebrum showed in inset (a) is taken by using high magnification immersion objective. Primary neurites (**arrow**) run in parallel and get packed before entering in to the neuropile. Integrating segments give rise branches that are projecting dorso-anteriorly and latero-anteriorly. (c) Stereo pair of confocal images. Primary neurites of larger somata (**arrow**) run in parallel close together, join the primary neurite of smaller soma and enter latero-posteriorly into the neuropile. Inside the neuropile, (1, 2, 3) show three sets of overlapping branches at different region of integrating segments. Inset **circle** shows the ramification of dorsal unpaired neuron in the ventral and medio-lateral part of the neuropile. (ci) part of circumoesophageal connective shown in inset (c) is taken at high magnification. A thin axon of DUM neuron (**arrow**) and two axons of SOG neurons are running dorsally into the circumoesophageal connective. (d) Schematic drawing summarising the results of backfill of motor nerve to M2. Only innervation of left side motor neuron is shown. Axons of the motor neurons (**blue**) projects into frontal connective (**FC**) and innervate ipsilateral M2 via FCM2, proximal and distal branches to M2 (Nerve root M2N, Boyan *et al.* 2002). Anterior is towards the top of image. Scale bars: 200 μm (a, b, bi.), 80 μm (ai,aai,c,ci).

Neurons in suboesophageal ganglion:

Backfilling of proximal and distal motor nerves to M2 (Fig.3.6) with or without severing the M2-commissure, maximally stained three neurons in the mandibular neuromere of suboesophageal ganglion. With respect to the muscle from which motor nerve branches were backfilled, two somata were located in the ipsilateral and one was in the contralateral half of the suboesophageal ganglion (Fig.3.13 d, e). Again dendritic field of contralateral soma was not stained in any preparation and only primary neurites and its main branches were faintly stained in few preparations (Fig.3.13 a, bi). Diameter of somata was 21-46 μm . Cell bodies, in ipsilateral and contralateral sides were located ventro-laterally or dorso-laterally or medio-laterally at the border of mandibular and maxillary neuromere. Ipsilateral somata were not lying together. Usually one soma was at dorso-lateral position and second was at ventro-lateral or medio-lateral positions (Fig.3.13 d, e). Primary neurites emerge anteriorly, posteriorly or laterally from the somata and enter into the mandibular neuropile from lateral side. Primary neurites of ventrally located soma first run dorsally and of dorsally located soma run ventrally (Fig.3.13 a, b, c, d and e). At the middle of dorso-ventral plane of ganglion, opposing neurites meet together, turn medially to enter into mandibular neuropile. In neuropile, primary neurites first take turn dorso-laterally, then turn anteriorly and make a loop before entering into the circumoesophageal connective as axons (Fig.3.13 a, bi and c). At point of turn, primary neurites give rise three sets of overlapping branches. Individual branch of each primary neurite was not recognisable. These sets of branches were named as A, B, C respectively and their bifurcation projects into different neuropiles of suboesophageal ganglion.

In set A, small and thin branches emerge from primary neurite and run anteriorly, medially, latero-anteriorly and medio-anteriorly inside the mandibular neuropile. These branches profuse and make a thin layer of ramification in the middle of the mandibular neuropile (A, Fig.3.13 e). In set B, one thick and 1-2 thin branches emerge posteriorly and enter into the maxillary neuropile. Thick branch runs postero-ventrally but more towards the mid line and goes up to the border of maxillary and labial neuromere. After short distance of its emergence, thick branch further give rise to small branches and its diameter become smaller. Its branches run latero-posteriorly and medio-posteriorly. A longer branch also emerges from thick branch that run in parallel. Ramification of thick branch covers anterior middle and posterior ventral area of the maxillary neuropile (Bi in Fig.3.13 e). Thin branches after their emergence from primary neurite run latero-posteriorly for short distance and then turn medially or medio-ventrally. These branches

make fine ramification lateral to the anterior middle ramification of thick branch (Bii in Fig.3.13 e) and few fibers run parallel to the posterior ventral area of thick branch ramification. One of the thin branches runs latero-posteriorly for longer distance and makes ramification in postero-lateral area of maxillary neuropile. In set C, four braches emerge from primary neurite and run latero-posteriorly in maxillary neuropile. Near the border of maxillary and labial neuromeres, these branches get separated. Two branches run posteriorly and enter into lateral area of labial neuropile (Ci in Fig.3.13e) and other two branches run dorso- posteriorly and enter into dorsal area of the labial neuropile (Cii in Fig.3.13e). Posteriorly running branches make thin cylinder shaped ramification at lateral edge of the middle area of labial neuropile while dorso-posteriorly running branches give rise to branches that run medially and posteriorly. Ramification of these branches was not visible.

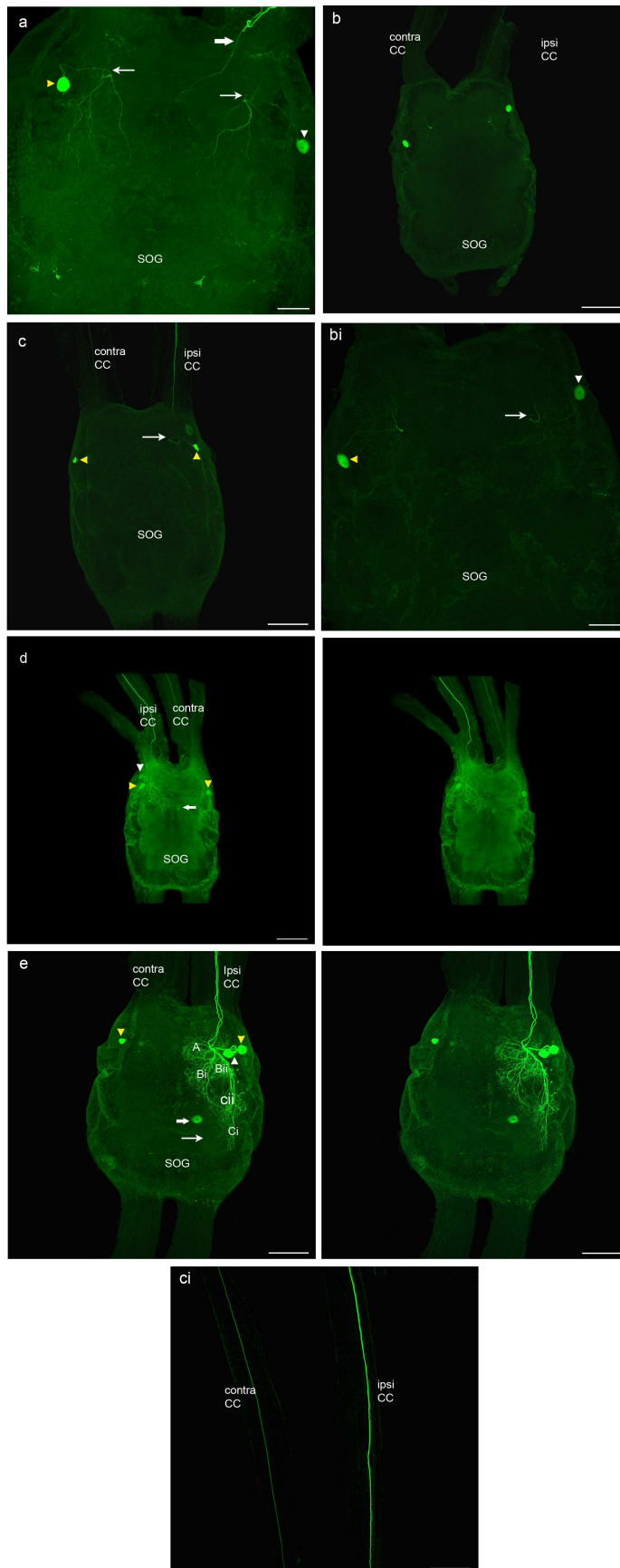


Figure 3.13 Backfilling of M2-commissure and motor nerve branch to M2. Confocal images of a whole mount of subesophageal ganglion (SOG) of adult *Locusta migratoria* viewed ventrally, show motor neurons in ipsilateral and contralateral mandibular neuromere, stained

after retrograde filling of M2-commissure (Boyan *et al.* 2002) or motor nerve branch to M2 with Neurobiotin™. (a) Shows two motor neurons in SOG after retrograde filling of M2-commissure in left direction. Ipsilateral soma (**white arrowhead**) is dorso-laterally located, primary neurite emerges anteriorly and run ventro-medially while contralateral soma (**yellow arrowhead**) is ventro-laterally located, primary neurite emerges anteriorly and run dorso-medially. Thin **arrows** show a loop inside the neuropile made by primary neurite. Thick **arrow** shows the axon of a serotonergic neuron in the mandibular nerve (N4, Altman and Kien, 1979) whose soma was moved anteriorly into circumoesophageal connective (not in focus). (b, c) Each image shows two motor neurons in SOG projecting their axons into ipsilateral and contralateral circumoesophageal connective (**ipsi CC, contra CC** respectively), stained after retrograde filling of motor nerve branch from left M2 without severing M2-commissure (b) or by severing M2-commissure (c). (bi) Anterior part of SOG shown in (b) is scanned by using high magnification oil immersion objective. Ipsilateral soma (**white arrowhead**) is dorso-laterally located, primary neurite emerges posteriorly and run ventro-medially while contralateral soma (**yellow arrowhead**) is ventro-laterally located, primary neurite emerges anteriorly and run dorso-medially. In (c), both somata (**yellow arrowheads**) are ventro-laterally located. Only primary neurite and its main branches were stained for ipsilateral soma. Primary neurite emerges anteriorly and run dorso-medially. Thin **arrows** in (bi, c) show loops of primary neurite inside the neuropile. (ci) Confocal image of a whole mount of anterior part of ipsi- and contralateral circumoesophageal connectives shown in (c). Axon of contralateral neuron is faintly stained while of ipsilateral is brightly stained. (d, e) Stereo pairs of images show two ipsilateral somata and one contralateral soma (**arrowheads**) in SOG, stained after retrograde filling of motor nerve branches from right M2 (d) and left M2 (e) by severing M2-commissure. In (d) one ipsilateral soma (**yellow arrowhead**) is brightly stained and located ventro-laterally while second soma (**white arrowhead**) is faintly stained and located dorso-laterally. Their primary neurites are not visible. Contralateral soma (**yellow arrowhead**) also brightly stained and located medio-laterally but primary neurite and its branches are not stained. Its axon in contralateral circumoesophageal connective is visible. In (e) ipsilateral somata are brightly stained. One soma is dorso-laterally (**white arrowhead**) located and its primary neurite emerges laterally and run ventro-medially while second soma (**yellow arrowhead**) is medio-laterally located and its primary neurite emerges laterally and run straight medially. Two axons are visible in ipsilateral circumoesophageal connective. Ramification of both neurons projects up to labial neuromere. (A, Bi, Bii, Ci, Cii) Show different areas of ramification in mandibular, maxillary and labial neuromeres. Thin **arrow** marks medially and posteriorly running branches inside the dorsal area of labial neuropile. Contralateral soma is also brightly stained and located medio-laterally (**yellow arrowhead**) but primary neurite and its branches are not stained. Thick **arrows** in (d, e) show the faintly stained cell bodies of dorsal unpaired median neurons (DUM). Anterior is towards the top of image. Scale bars: 200 μm (b, c, ci, d, e, ei), 80 μm (a, bi). In (ei) dorsal is towards the left of image.

Axons of suboesophageal ganglion neurons:

Ipsilateral and contralateral suboesophageal ganglion neurons project their axons towards the brain via circumoesophageal connectives. In circumoesophageal connective, axons run on its ventral surface and individual axon can be traced inside it (Fig.3.13 b, c, d and e). But near the tritocerebrum, axons run on the dorsal surface of the circumoesophageal connectives and enter into the tritocerebrum from dorso-posterior side. In the tritocerebrum, axons do not make ramification and turn ventrally to enter into the respective frontal connective (Fig.3.11 aii and 3.12 ai, bii). Axons of suboesophageal ganglion neurons were larger in diameter than those of the tritocerebral neurons. In frontal connective, axons were closely packed together but in some of the preparations, it was possible to trace these axons in whole frontal connective.

Frontal ganglion as a peripheral commissure:

In frontal connectives, axons of ipsilateral and contralateral suboesophageal neurons before entering into their anterior branches to innervate the ipsilateral M2, give rise to branches which turn towards the frontal ganglion and cross the mid line in periphery using it as a commissure, and innervate the contralateral side muscles (Fig.3.14).

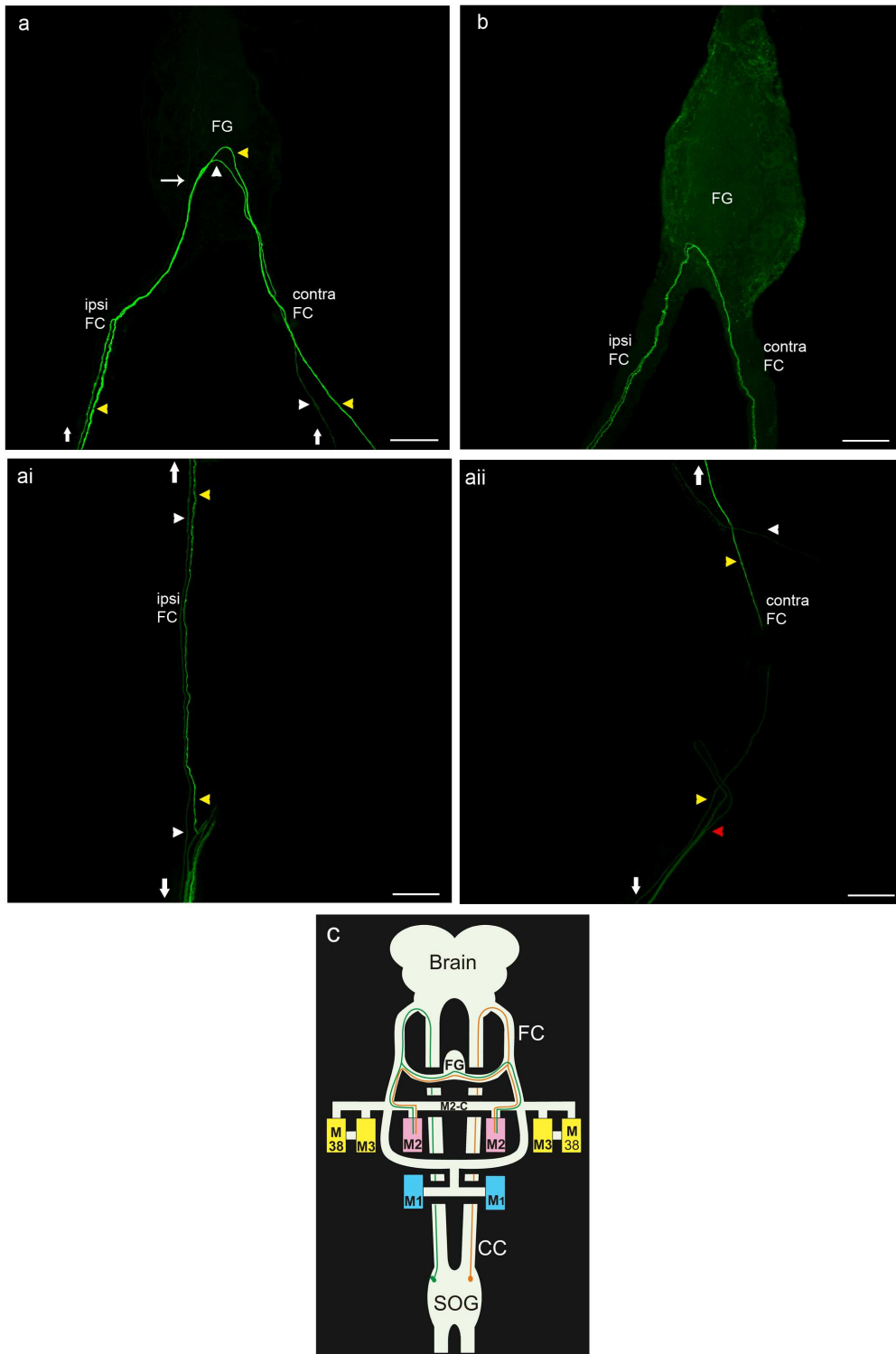


Figure 3.14 Axons of suboesophageal ganglion neurons cross the midline using frontal ganglion as a commissure. (a,ai,aii) Confocal images of ventrally viewed whole mount of frontal ganglion (FG) and ipsilateral (ai) and contralateral (aii) frontal connectives (ipsi FC, contra FC) of adult *Locusta migratoria*, show path of axons of suboesophageal ganglion motor neurons stained after retrograde filling of M2-comisure (Boyan *et al.* 2002). Upward **arrows** mark towards the frontal ganglion and downward **arrows** towards the brain. In (a), two fibers are crossing the frontal ganglion. **White arrowheads** in (ai) show that a thin branch of axon of an ipsilateral suboesophageal ganglion neuron runs towards the frontal ganglion, crosses it (**white arrowheads** in a) and enters into contralateral frontal connective (**white arrowhead** in aii) to innervate contralateral muscles. **Red arrowhead** in (aii) shows division of a thick axon of a contralateral suboesophageal ganglion neuron inside the contralateral frontal connective. One branch (**yellow arrowheads**) run towards the frontal ganglion and projects into ipsilateral frontal connective (**yellow arrowheads** in ai). (b) Confocal image

of a whole mount of frontal ganglion (**FG**) and ipsilateral and contralateral frontal connectives of adult *Locusta migratoria* viewed ventrally; shows crossing of two axons of suboesophageal ganglion motor neurons shown in figure (3.11 b, bi). (c) Schematic drawing summarising the innervation of suboesophageal ganglion motor neurons, stained by backfilling of M2-commissure (**M2-C**) or motor nerve branch to M2. Axons of ipsilateral motor neurons (**green**) project toward the brain via circumoesophageal connective (**CC**) and innervate ipsilateral M2 via frontal connective (**FC**), FCM2, proximal and distal branches to M2. In frontal connective, axons give rise to branches that cross frontal ganglion (**FG**) and innervate contralateral M2 via FCM2, proximal and distal branches to M2. Axons of contralateral motor neurons (**orange**) take similar path to innervate both ipsilateral and contralateral M2. In (a, b) posterior is towards the top of image. Scale bars: 80 μm (a, ai, aii, and b).

Serotonergic and dorsal unpaired median neurons:

Besides the motor neurons in mandibular neuromere, backfilling of distal or proximal motor nerves to M2 (Fig.3.6), with or without severing M2-commissure, also stained some neurons of the satellite nervous system (Bräunig, 1997). In two preparations, soma and axon of one of the dorsal unpaired median neurons in suboesophageal ganglion (Fig.3.13 d, e) was also stained. Axons of DUM neurons ascend towards the brain via circumoesophageal connective (Fig.3.12 c, ci), and make branches in the tritocerebrum and the deutocerebrum were only visible at high magnification.

3.4.2.3. Backfilling of M2-commissure or motor nerve branch to M2 and suboesophageal ganglion neurons:

Backfilling of either M2-C or specific motor branch to M2 revealed motor neurons in the suboesophageal ganglion. With respect to the backfilling direction, their somata were lying in ipsilateral or contralateral half of the suboesophageal ganglion. Backfilling of M2-C showed one soma in ipsilateral and one in contralateral half of suboesophageal ganglion. While backfilling of motor nerve to M2 showed two ipsilateral and one contralateral soma in suboesophageal ganglion. But in both cases, number of fibers crossing the frontal ganglion using it as a commissure was similar. In each case, only two fibers were maximally found to cross the frontal ganglion. Path of an axon of one additionally stained soma, during backfilling of motor nerve to M2, remained unclear. It is not clear whether it crosses the midline using M2-C or frontal ganglion. Possible solution to this problem might was the differential staining of M2-commissure and specific motor nerve to M2. But it was not possible by backfilling technique, as M2-C and motor nerve branches were very close to each other and it was very hard to backfill both ones separately in a single preparation.

3.4.3. Neurons innervating posterior retractor muscles of labrum M3:

3.4.3.1. Backfilling of motor nerve branch to M3:

Ventral branch of FCM3&38 (Fig. 3.7) innervate M3 from its ventral surface. Backfilling of this motor branch with retrograde neuronal tracer Neurobiotin TM, either from right or left M3, stained neurons in the tritocerebrum and suboesophageal ganglion.

Motor neurons in tritocerebrum:

5 backfills of ventral branch of FCM3&38, either from right or left M3, stained variable number of motor neurons in ipsilateral lobe of the tritocerebrum. Their number ranged from 2-8. Neurons project their axons into ipsilateral frontal connective and innervate ipsilateral M3 via FCM3&38 and its ventral branch to M3 (Fig.3.15d). Somata were wrinkled, oval or round in shape and were lying either separately or above each other in the fronto-lateral cell body layer of the tritocerebrum, near the border of the deutocerebrum. Diameter of somata was ranging from 21-34 μm . Like M2 motor neurons, primary neurites of these motor neurons can also be divided into initial segments and integrating segments. Initial segments run latero-posteriorly close to the ventral surface and take turn towards the middle of tritocerebral neuropile to make integrating segments that run deep into the neuropile. Usually primary neurites were not closely packed

together, and were not making any tract outside or inside the neuropile. Only in a few preparations, primary neurites become packed together and run posteriorly at the ventral middle line of the tritocerebral lobe, and enter into the neuropile from its ventral posterior side (Fig. 3.15 a). Integrating segments near to the exit into the frontal connective as axons, give rise to branches which project dorso-anteriorly and latero-dorsally. These branches bifurcate intensively and make fine ramification. Individual branch of a primary neurite and its ramification could not be distinguished. Whole ramification was limited to the tritocerebrum and no fiber was found to project into the deutocerebrum. Similarly, individual axon inside the frontal connective was not traced and all axons were packed together.

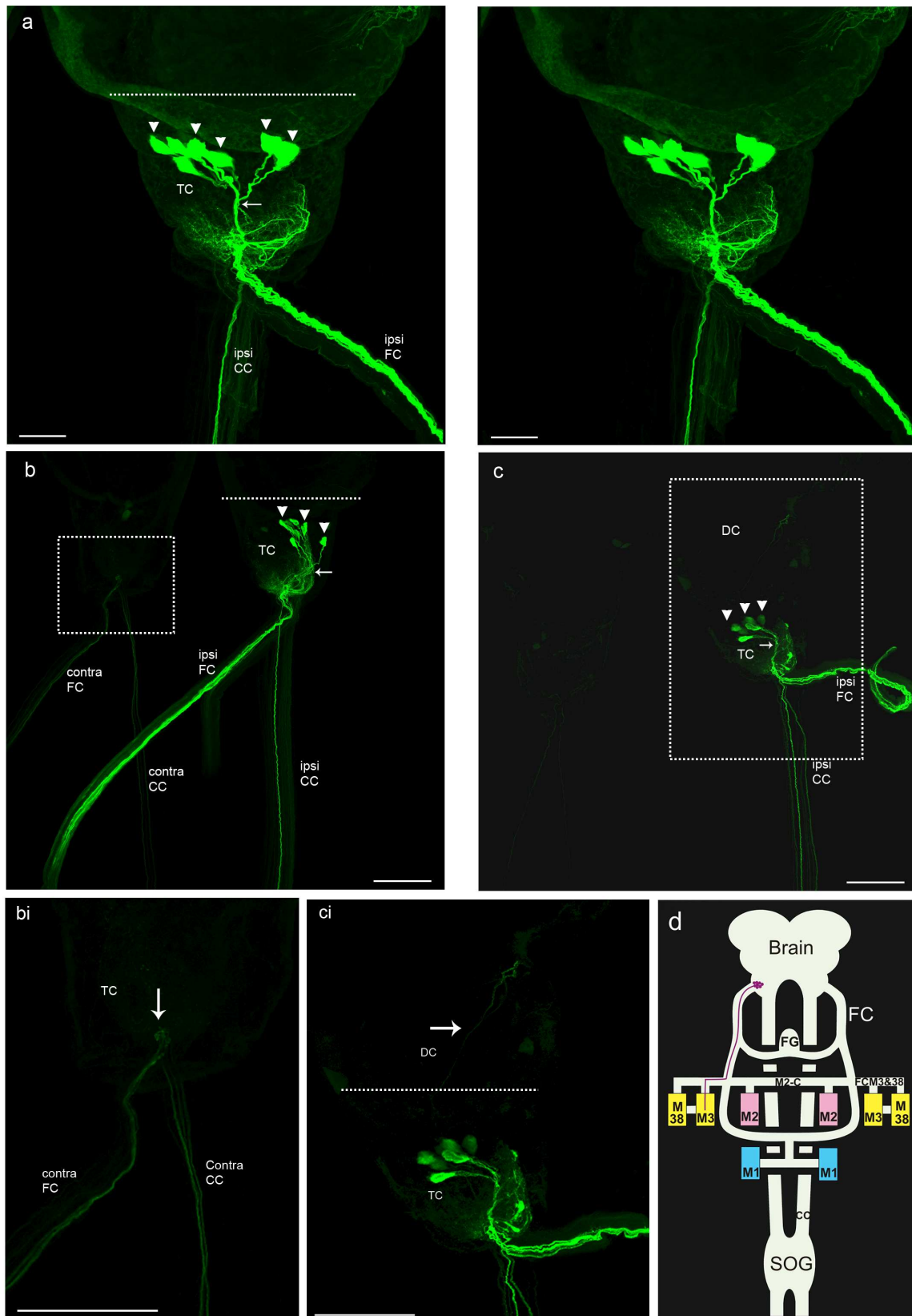


Figure 3.15 Direct backfilling of M3 or its motor nerve branch.

Confocal images of a whole mount of part of the brain of adult *Locusta migratoria* viewed ventrally, show motor neurons in ipsilateral lobe of the tritocerebrum (TC) projecting their axons into frontal connective (FC), stained after direct backfilling of M3 (b, c) or motor nerve branch to M3 (a, stereo pair) with Neurobiotin™. Part of ipsilateral and contralateral circumoesophageal connective (ipsiCC, contraCC) show that axons of suboesophageal neurons project into the tritocerebrum to enter into

frontal connectives (**FC**). **Arrowheads** mark the somata are present close to each other at ventral surface. **Dashed lines** mark the border between the tritocerebrum and deutocerebrum. In (a) Primary neurites (**arrow**) group together, run posteriorly at ventral middle line of the tritocerebral lobe and enter ventro-posteriorly into the neuropile. In (b, c) primary neurites (**arrows**) run latero-posteriorly and enter into the neuropile from lateral side but in (b) primary neurites do not group together as in (c). In (bi) contralateral lobe of the tritocerebrum in inset (b) is shown at high magnification. Arrow marks the axons of contralateral suboesophageal neurons are projecting into contralateral frontal connectives (**contra FC**) with out making ramification inside the tritocerebrum. (ci) Ipsilateral lobe of the tritocerebrum in inset (c) is shown at high magnification. A very thin faintly stained fiber (**arrow**) of dorsal unpaired medial neuron is turning laterally in the deutocerebrum (**DC**) to enter into antennal nerve. (d) Schematic drawing shows the innervation of motor neuron to M3. Axons of the motor neurons (purple) project into frontal connective (**FC**) and innervate only ipsilateral M3 via FCM3&38 and ventral branch to M3. Anterior is towards the top of image. Scale bars: 200 μm (b, c, bi, ci), 80 μm (a).

Neurons in suboesophageal ganglion:

Direct backfilling of M3 or ventral branch of FCM3&38 to M3 also stained motor neurons in suboesophageal ganglion. With respect to backfilling, somata were located in the ipsilateral and the contralateral sides of the suboesophageal ganglion. In case of motor nerve backfilling, two somata on ipsilateral and one on contralateral side of the suboesophageal ganglion were stained (Fig. 3.16a), while in case of direct backfilling of M3, only one additional soma on contralateral side of suboesophageal ganglion was stained (Fig. 3.16b). Dendritic field of contralateral somata was not stained in any of the preparations. Only primary neurite and its main branches were visible. As described in section 3.4.2.1, incomplete stainings may be due to the longer distance. Morphology of these neurons was similar to the neurons stained in suboesophageal ganglion either by backfilling of M2-C or specific motor nerve branch to M2 (see section, 3.4.2.2). Such as somata size, their location, courses of primary neurites, their branching patterns inside the neuropiles of all neuromeres of suboesophageal ganglion were exactly similar to the neurons of M2 (compare Fig. 3.13 and 3.16). Likewise axons were traced inside circumoesophageal connectives that were ascending towards the brain (Fig.3.16ai) and project into respective sides frontal connectives without making any ramification inside the tritocerebrum(Fig. 3.15 bi). Similarly axons give rise to branches inside the frontal connective that cross the frontal ganglion using it as a commissure and innervate contralateral side muscles (Fig.16bi, c, ci).

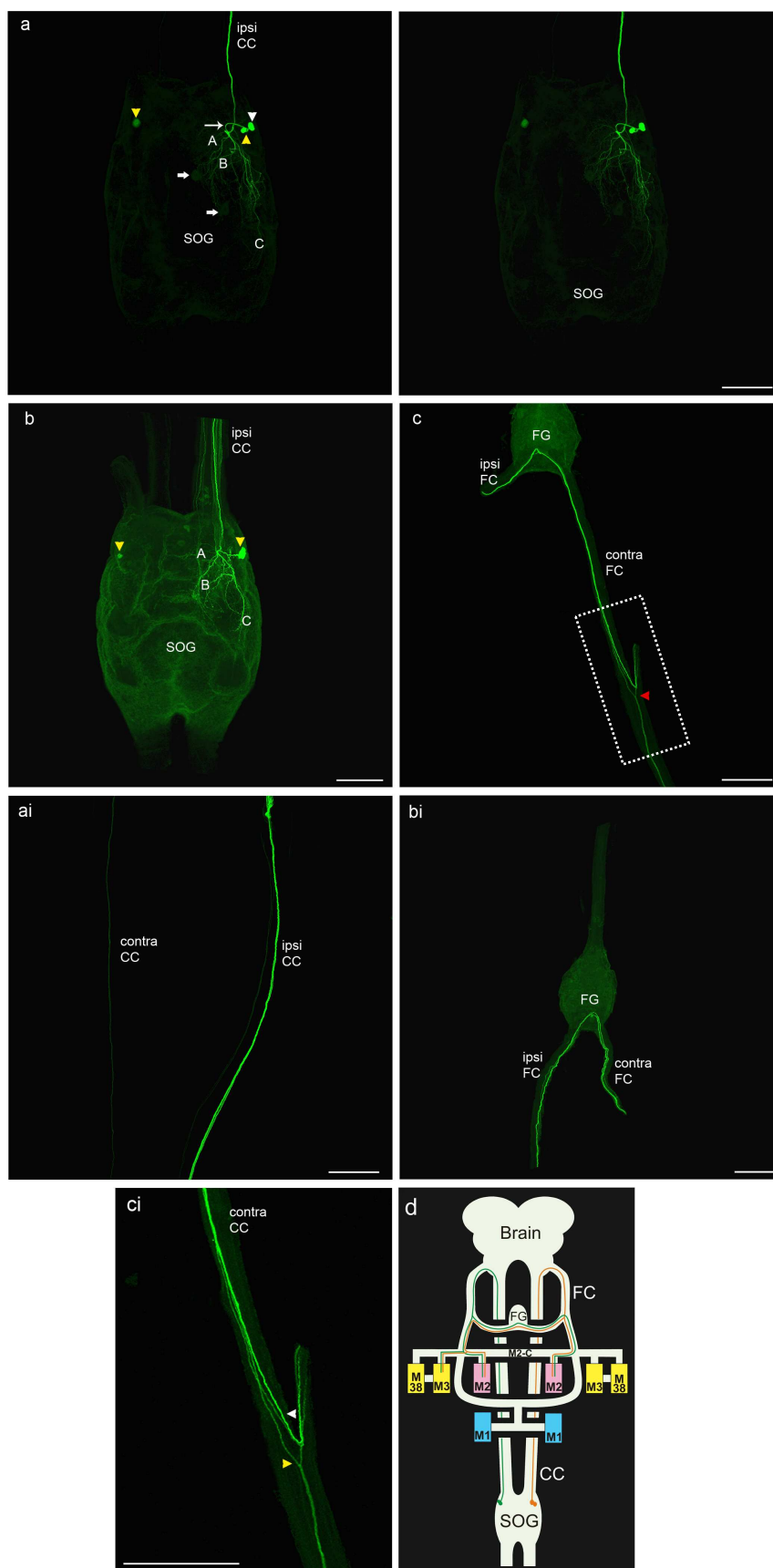


Figure 3.16 Direct backfilling of M3 or its motor nerve branch.

(a, b) confocal images of a whole mount of subesophageal ganglion (SOG) of adult *Locusta migratoria* viewed ventrally, show motor neurons in ipsilateral and contralateral mandibular

neuromere, stained after direct backfilling of M3 (b) or motor nerve branch of M3 (a, stereo pair) with Neurobiotin. (a) Stereo pair of images shows two ipsilateral somata and one contralateral soma (**arrowheads**). One ipsilateral soma is dorso-laterally (**white arrowhead**) located, its primary neurite emerges laterally and run ventro-medially. While second soma (**yellow arrowhead**) is ventro-laterally located, its primary neurite emerges laterally and run dorso-medially. Thin **arrow** shows a loop inside the neuropile made by their primary neurites. On contralateral side, only one soma (**yellow arrowhead**) is faintly stained and is located ventro-laterally. Thick **arrows** show the faintly stained cell bodies of dorsal unpaired median neurons. (b) Shows somata (**yellow arrowheads**) are lying above each other. Two somata are present on ipsilateral side while two are on the contralateral side. Primary neurites of ipsilateral neurons emerge laterally, run straight medially and their ramification projects up to labial neuromere while of primary neurites of contralateral neurons are not stained. (**A, B, C**) shows different areas of ramification in mandibular, maxillary and labial neuromeres. (ai) Confocal image of a whole mount of ipsi- and contralateral circumoesophageal connectives (**ipsiCC, contraCC**) viewed ventrally shows axons of SOG motor neurons of (a). (bi, c) Confocal images of a whole mount of frontal ganglion (**FG**) along with part of ipsi- and contralateral frontal connectives (**ipsi FC and contra FC**) of adult *Locusta migratoria* viewed ventrally. (bi) shows crossing frontal ganglion by three axons of suboesophageal ganglion motor neurons shown in (b). (c) Shows crossing of three axons of suboesophageal ganglion motor neurons stained in another preparation. **Red arrowhead** marks the bifurcation of a thick axon of a contralateral SOG motor neuron inside the contra FC. (ci) Stippled area in (c) is shown at high magnification. **White arrowhead** shows that two axons of ipsilateral suboesophageal ganglion neurons are crossing the frontal ganglion and are projecting into contralateral frontal connective. **Yellow arrowhead** shows that branch of axon of contralateral neuron runs towards the frontal ganglion, crosses it and projects into ipsi FC. (d) Schematic drawing summarising the innervation of motor neurons of **SOG** stained by direct backfilling of M3 or motor nerve branches to M3. Axons of ipsilateral motor neurons (**green**) project towards the brain via circumoesophageal connective (**CC**) and innervate ipsilateral M3 via frontal connective (**FC**), FCM3&38 and ventral branch to M3. In frontal connective, axons give rise to branches that cross the frontal ganglion (**FG**) and innervate contralateral muscle. Axons of contralateral motor neurons (**orange**) take similar path via FG to innervate ipsilateral M3. In (a, b, bi) anterior is towards the top of image. In (bii, c) posterior is towards the top of image. Scale bars: 200 μ m (a, b, c, bi, bii, ci).

Serotonergic and dorsal unpaired median neurons:

Backfilling of motor nerve to M3, either from right or left M3, has not stained any of the neurons of the satellite nervous system (Bräunig, 1997) while in case of direct backfilling of M3, a single neurons was stained, and its axons was visible in mandibular nerve of suboesophageal ganglion (N4, Altman and Kien, 1979). In contrary to the satellite nervous system, two somata of dorsal unpaired neurons were also faintly stained in the suboesophageal ganglion (Fig.3.16a). Their axons enter into the tritocerebrum via circumoesophageal connectives and run on its dorsal surface towards the deutocerebrum. At the border between the deutocerebrum and the tritocerebrum, axons take turn ventro-posteriorly to enter into the frontal connectives. At turning point, axons give rise to the branches which enter into the antennal nerve (Fig.3.15ci). Ramification of DUM neurons was not stained in the suboesophageal ganglion or any of the brain neuromeres.

3.4.3.2. Direct backfilling of M3:

Backfilling of specific motor nerve to M3 revealed variable number of motor neurons in the ipsilateral lobe of the tritocerebrum. This variability might be due to lack of backfilling of all axons in motor nerve to M3 or may be accounted for the common innervation of both M3 and M38 (Fig.3.7). In latter case, axons of motor neurons might first innervate M38 via dorsal branch of FCM3&38 and then innervate M3 (Fig.3.7aii). So backfilling of specific motor nerve branch to M3 could not reveal complete set of its motor neurons. For that M3 was directly backfilled. In total, 8 preparations were made. But direct backfilling of M3 also showed variable number of neurons in ipsilateral lobe of the tritocerebrum. The number of stained neurons was ranging from 3-8 (Fig.3.15b, c, bi, ci) and somata size was ranging from 17-34 μ m.

3.4.4. Neurons innervating anterior dilator muscles of foregut (M38):

To find total number of motor neurons specifically innervating M38 (Fig.3.2b, c, f, e), either dorsal branch of FCM3&M38 or direct M38 was backfilled. Direct backfilling of M38 was difficult. Because M38 was short in length, and secondly its fibers were not arranged on a tendon like the case observed for M3. When muscle was cut near its insertion, it became shorter due to contraction and it was very hard to keep the muscle fibers inside the Vaseline™ container.

Motor neurons in tritocerebrum:

Results regarding the direct backfilling of the M38 were not successful as contraction of the muscle fibers caused leakage of the tracer from Vaseline™ container. But the backfilling of the specific motor nerve to M38 stained neurons in the ipsilateral tritocerebrum and suboesophageal ganglion. Maximum seven neurons were stained in the ipsilateral tritocerebrum. Diameter of neurons was 17-24 µm. Morphology of these neurons was exactly similar to the neurons obtained by direct backfilling of M3 or its specific motor nerve branch (Compare Fig.3.16 and 3.17). Inside the tritocerebral neuropile, like the primary neurites of M2 motor neurons, three sets of overlapping branches were emerging at the start and end of the integrating segments (Fig.3.17a). These sets of branches were also assigned same (1, 2 and 3) numbers. Branches were projecting dorso-anteriorly, latero-dorsally and anteriorly. In set 1, branches emerge at start of the integrating segments while in set 2 and 3, branches emerge by opposing each other on the part of integrating segments close to their exit into frontal connective as axons. In set 1, branches first proceed latero-dorsally towards the outer lateral margin of neuropile and then run anteriorly. These branches profuse and make fine ramification in latero-dorsal region of neuropile. A tuft of branches in set 2 also proceed latero-dorsally towards the outer lateral margin of neuropile, and then run anteriorly to make a characteristic loop inside the neuropile by joining the branches of set 1. Beside the main branches of set 2, many thin branches emerge from the integrating segments and run dorso-anteriorly and cover the posterior dorsal area of the neuropile. Branches in set 3, after their emergence, first proceed latero-ventrally towards the inner medial border of the neuropile and then run anteriorly.

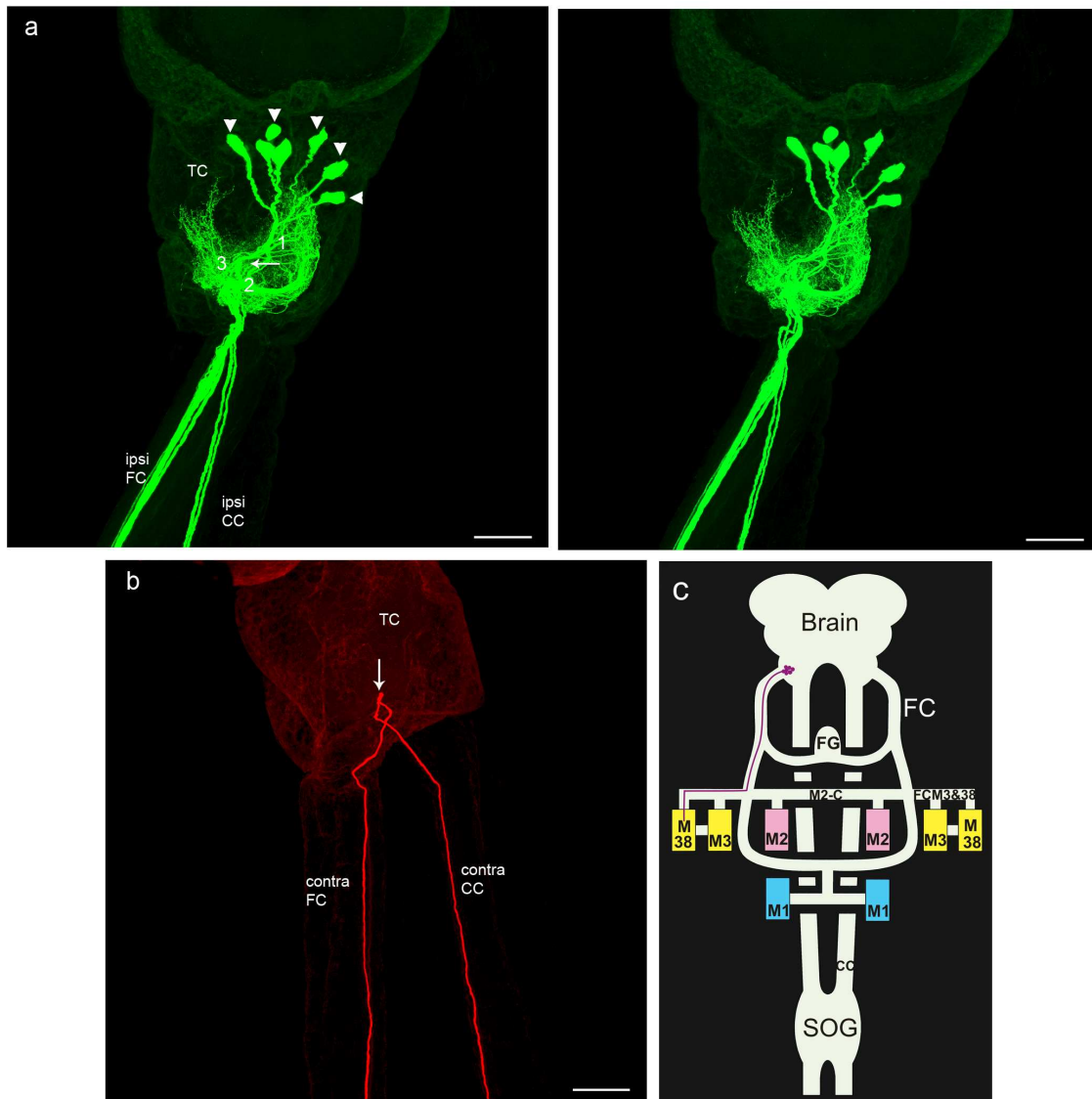


Figure 3.17 Backfilling of motor nerve branch to M38.

(a) Stereo pair of confocal images of a whole mount of ipsilateral lobe of the tritocerebrum (TC) of adult *Locusta migratoria* viewed ventrally, show motor neurons (**arrowheads**) projecting their axons into frontal connective (FC), stained after retrograde filling of motor nerve branches to M38 with Neurobiotin™. Part of ipsilateral circumoesophageal connective (**ipsiCC**) shows that axons of suboesophageal neurons project into the tritocerebrum and enter into ipsilateral frontal connective (**ipsiFC**). Thin **arrow** shows that integrating segments do not group together inside the neuropile and give rise to three sets of overlapping branches (**1, 2, 3**) in different region of the neuropile. Branches in set 2 are making a loop inside the neuropile. (b) Confocal image of ventrally viewed whole mount of contralateral lobe of the tritocerebrum of same preparation shown in (a). **Arrow** indicates that the axon of contralateral suboesophageal neuron projects into contralateral frontal connectives (**contraFC**) without making any ramification inside the tritocerebrum. (c) Schematic drawing showing the innervation of motor neuron to anterior dilator of foregut, M38. Axons of the motor neurons (**purple**) project into frontal connective (FC) and innervate ipsilateral M38 via FCM3&38 and dorsal branch to M38. Anterior is towards the top of image. Scale bars: 80 μ m (a, b).

Motor neurons in suboesophageal ganglion:

Backfilling of specific motor nerve to M38 stained three somata of motor neurons in suboesophageal ganglion whose diameter was ranging from 26-40 μ m. With respect to the muscle from which the motor nerve was backfilled, two somata were located in the ipsilateral and one soma was located in the contralateral sides of the suboesophageal ganglion. Staining showed the complete picture for ipsilateral neurons while for

contralateral neuron, only the course of primary neurite and its main branches was stained. Morphology of all the neurons was exactly similar to the neurons that were stained either by backfilling of M2-commissure or specific motor nerve branches to M2 and M3 (compare figure 3.13e, 3.15a, b and 3.18). But in case here, fine ramification of the three sets of overlapping branches of primary neurites was more clearly stained in mandibular, maxillary and labial neuropiles as compared to the stainings made by backfilling of M2-C or specific motor nerve branch to M2 or M3.

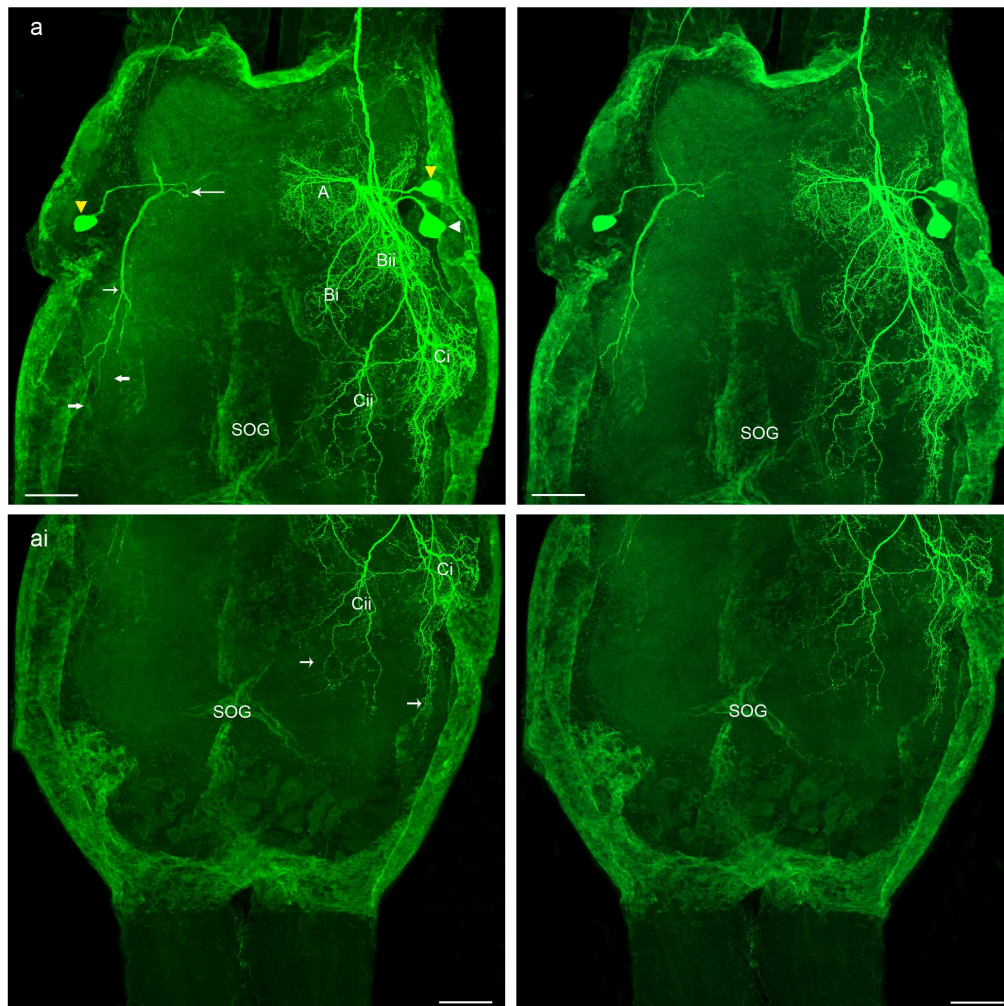


Figure 3.18 Backfilling of motor nerve branch to M38:

Stereo pair of Confocal images of a whole mount of subesophageal ganglion (SOG) of adult *Locusta migratoria* viewed ventrally; show motor neurons in ipsilateral and contralateral mandibular neuromere, stained after retrograde filling of motor nerve branch to M38 with Neurobiotin™. Scanning was made using high magnification immersion oil objective. (a) Anterior half of SOG showing two ipsilateral somata and one contralateral soma (**arrowheads**). Contralateral soma (**yellow arrowhead**) is brightly stained and located ventro-laterally; its primary neurite emerges anteriorly and runs dorso-medially. Long thin **arrow** marks the loop inside the neuropile made by primary neurite. Small thin **arrow** shows that posteriorly running branch bifurcates into the maxillary neuropile, and bifurcating branches project into the dorsal and ventral area of labial neuropile (small thick **arrows**). In ipsilateral half, one soma is dorso-laterally (**white arrowhead**) located. Its primary neurite emerges anteriorly and runs dorso-medially while second soma (**yellow arrowhead**) is medio-laterally located and its primary neurite emerges laterally and runs straight medially. (**A, Bi, Bii, Ci, Cii**) shows different areas of ramification in mandibular, maxillary and labial neuromeres. (ai) Posterior half of SOG shows that ramification of ipsilateral neurons is projecting up to labial neuromere. Small **arrows** mark the ramification into the dorsal and ventral area of labial neuromere. Anterior is towards the top of image. Scale bars: 80 μm (a, ai).

Axons of suboesophageal ganglion neurons:

Axons of suboesophageal neurons were brightly stained both in ipsi- and contralateral circumoesophageal and frontal connectives (Fig.3.19a, ai). Axons do not make ramification inside the tritocerebrum (Fig.3.17b). In ipsilateral frontal connective, axons of tritocerebral neurons were closely packed with axons of suboesophageal ganglion neurons, and individual axon of any neuron could not be distinguished (Fig.3.19b). Inside the frontal connectives, axons give rise to the branches which cross the frontal ganglion and innervate contralateral muscles (Fig.3.19b, c, d). Three axons were crossing the frontal ganglion and no one was making ramification inside the frontal ganglion (Fig. 3.19d, di).

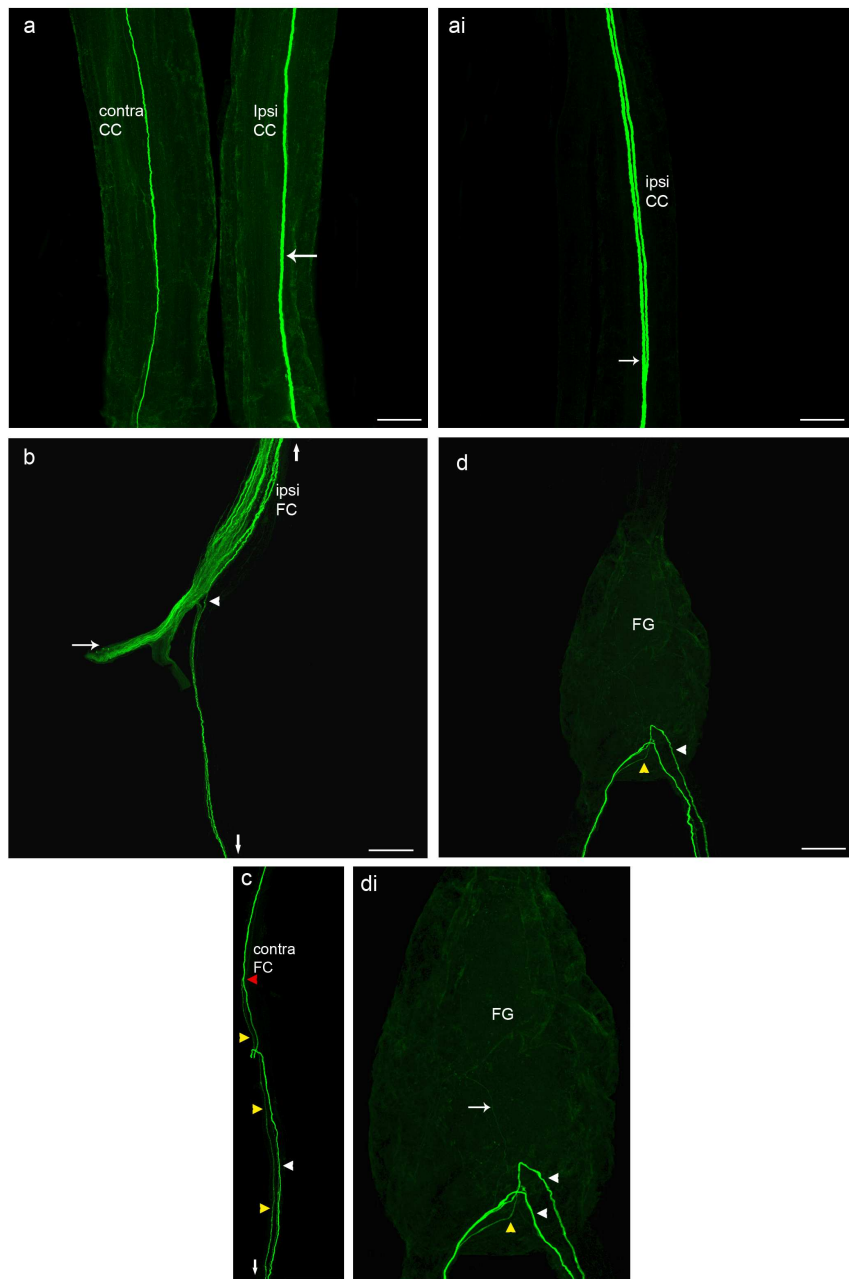


Figure 3.19 Axons of suboesophageal ganglion neurons cross the midline using frontal ganglion as a commissure. (a, ai, b, c) Confocal images of whole mount of ipsi- and contralateral circumoesophageal and frontal connectives (**ipsiCC**, **contraCC**, **ipsiFC**, **contraFC**) viewed ventrally

are showing the projection of axons of suboesophageal ganglion motor neurons of figure 3.18. (a) Shows axonal fibers in the posterior part of both ipsi- and contralateral circumoesophageal connectives. **Arrow** marks that two axons of ipsilateral neurons are running in close association. (ai) anterior part of ipsilateral circumoesophageal connective of same preparation shows separation (**arrow**) of ipsilateral axons that can be traced in rest of the connective. (b) Part of ipsilateral frontal connective along with motor nerve branch being backfilled (horizontal **arrow**) shows that the axons of tritocerebral and suboesophageal ganglion motor neurons are closely packed together and individual axons could not be traced. **White arrowhead** shows that the branch of one of the ipsilateral SOG neurons is projecting towards the frontal ganglion. Downward **arrow** marks towards the frontal ganglion and upward **arrow** marks towards the brain. (c) Part of contralateral frontal connective shows that axon of contralateral SOG neuron bifurcate inside the connective (**red arrowhead**) and one branch runs towards the frontal ganglion (**Yellow arrowheads**). **White arrowhead** marks that the two axons of ipsilateral SOG neurons are projecting into **contra FC** after crossing the frontal ganglion. (d) Confocal image of a whole mount of frontal ganglion (**FG**) of adult *Locusta migratoria* viewed ventrally shows that three axons of suboesophageal motor neurons marked in (b, c) cross the frontal ganglion. **Yellow arrowhead** marks crossing of a thin branch of contralateral axon while **white arrowhead** marks the crossing of two ipsilateral axons. (di) Frontal ganglion in (d) is shown at higher zoom. (**Arrow**) marks that a thin fiber of dorsal unpaired medial neuron is projecting posteriorly into frontal ganglion.

3.4.5. Backfilling of M3 and M38 motor nerves together:

Individual backfilling of M3 or M38 directly or their specific motor nerve branches stained variable number of motor neurons, and it was unclear; whether all of the tritocerebral motor neurons are common to both muscles or there are some specific motor neurons that innervate each muscle. As stated in section 3.4.3.2 that axons of motor neurons might first innervate specifically each muscle via dorsal or ventral branches of FCM3&38 and then innervate second muscle. In these cases, it was hard to reveal the complete set of motor neurons innervating each muscle by backfilling individual motor nerve branch to M3 or M38. So it was better to backfill motor nerves branches to M3 and M38 together in a single preparation and reveals the complete numbers of motor neurons innervating both muscles.

Motor neurons in tritocerebrum:

Backfilling of M3 and M38 motor nerves together stained neurons in the ipsilateral tritocerebrum only. Their number was again variable. We made a total of 14 preparations. In 7 preparations 8 somata were stained while in 6 preparations 5 somata were stained. Only in one preparation, 7 neurons were stained. However, the overall maximum number of neuronal somata found in a single preparation did not exceed the maximum number of cell bodies found in a preparation by individual backfilling of M3 or M38 directly or their specific motor nerve branches. Morphology of these neurons was exactly similar to the neurons found by direct backfilling of M3 or M38 or their specific motor nerve branches and their diameter was ranging from 17-40 μm (compare Fig3.15, 3.17 and 3.20).

Besides the motor neurons in the tritocerebrum, at high magnification, in a total of 5 preparations, a thin axon of dorsal unpaired median neuron running on the dorsal surface of the tritocerebrum was also visible. At the border between the deutocerebrum and the tritocerebrum, axon gives rise to the branches that project into the antennal nerve. One of the branches takes turn ventro-posteriorly and enters into the frontal connective. It is not clear that it gives ramification inside the tritocerebrum or projects directly into the frontal connective (Fig.3.20c).

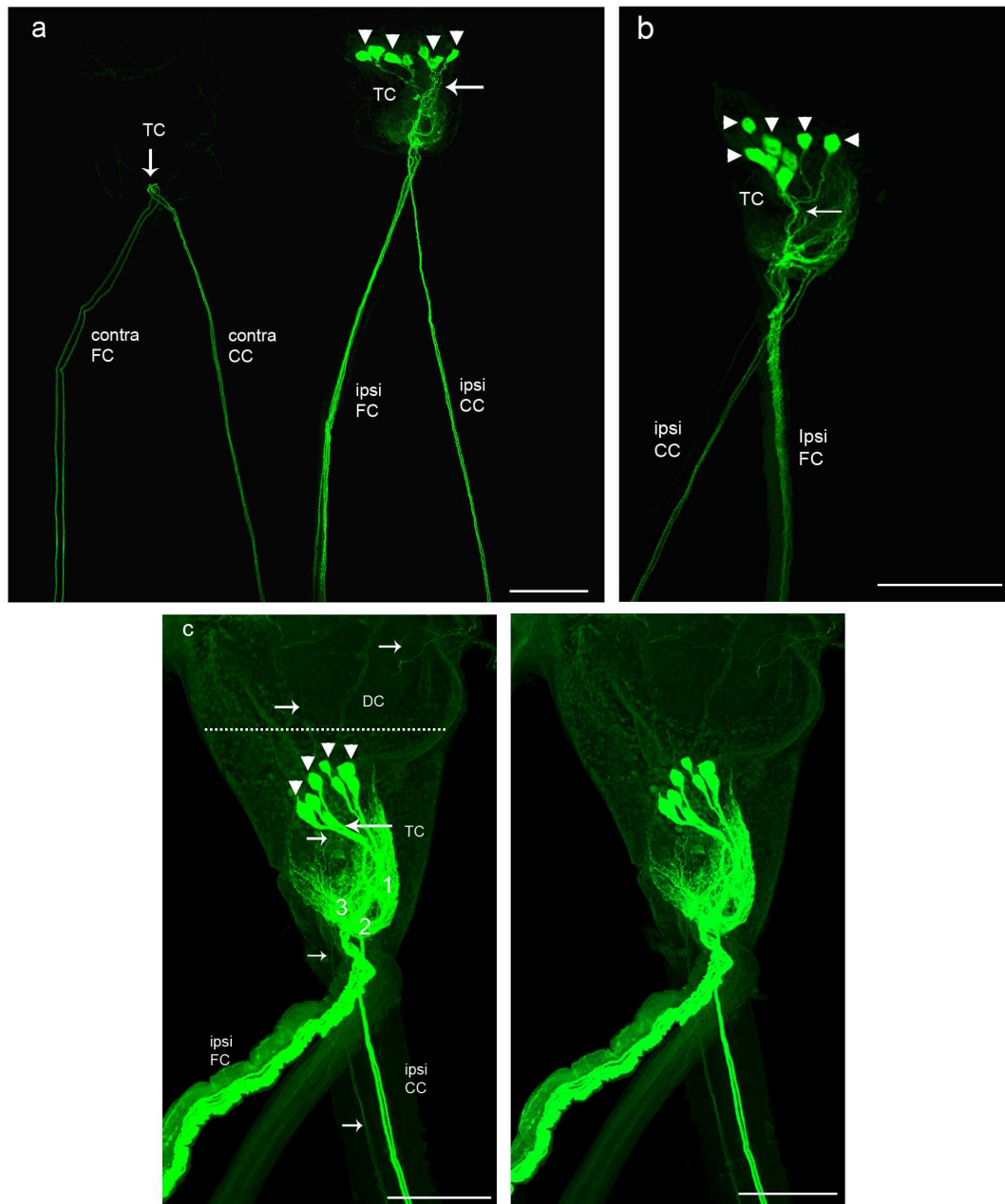


Figure 3.20 Backfilling of M3 and M38 motor nerves together.

(a, b, c) Confocal images of whole mount of the tritocerebrum of three different preparation of the adult *Locusta migratoria* viewed ventrally, show motor neurons in ipsilateral lobe of the tritocerebrum (TC), stained after retrograde filling of M3 and M38 motor nerve branches together with Neurobiotin™. Part of ipsilateral and contralateral circumoesophageal connective (ipsiCC, contraCC) shows that the axons of suboesophageal neurons project into the tritocerebrum to enter into frontal connectives (FC). Somata (arrowheads) are located close to each other at ventral surface of the tritocerebrum. **Dashed line** marks the border between the tritocerebrum and deutocerebrum. Primary neurites (long thin arrows) do not group together, run latero-posteriorly and enter into the neuropile from lateral side. Branches of primary neurites project dorso-anteriorly and latero-dorsally. (a) Vertical **arrow** marks that the axons of contralateral suboesophageal neurons project into contralateral frontal connectives (contra FC) without making ramification inside the tritocerebrum. (c) Stereo pair shows that the integrating segments give rise to three sets of overlapping branches (1, 2, 3) in different region of the tritocerebral neuropile. In set 2, branches make a loop inside the neuropile. Small horizontal **arrows** mark the path of the axon of dorsal unpaired medial neuron which runs anteriorly at the dorsal surface of the tritocerebrum and turns laterally in the deutocerebrum (DC) to enter into antennal nerve. Anterior is towards the top of image. Scale bars: 200 μ m (a, b, c).

Motor neurons in suboesophageal ganglion:

Backfilling of M3 and M38 motor nerves together also stained four neurons in suboesophageal ganglion. With respect to the muscle from which the motor nerve was backfilled, somata were located in the ipsilateral and contralateral half of the suboesophageal ganglion. In a total of 14 preparations, 6 preparations showed 4 somata in the suboesophageal ganglion, with 2 somata in the contralateral half and 2 in the ipsilateral half of the SOG. While 7 preparations showed 3 somata in the suboesophageal ganglion, with two somata in the ipsilateral half and one soma in the contralateral half of the suboesophageal ganglion. Only in one preparation, 2 neurons were stained in the ipsilateral half of the suboesophageal ganglion and no soma was stained in the contralateral half. Like the tritocerebral motor neurons, the overall maximum number of neuronal somata found in a single preparation also did not exceed the maximum number of cell bodies found in preparations by individual backfilling of specific motor nerve branches to M2, M3 or M38.

There were no differences among neuronal morphologies obtained either by backfilling of individual motor nerves to M3 and M38 or by backfilling these nerve together in a single preparation (compare Fig. 3.18 and 3.21).

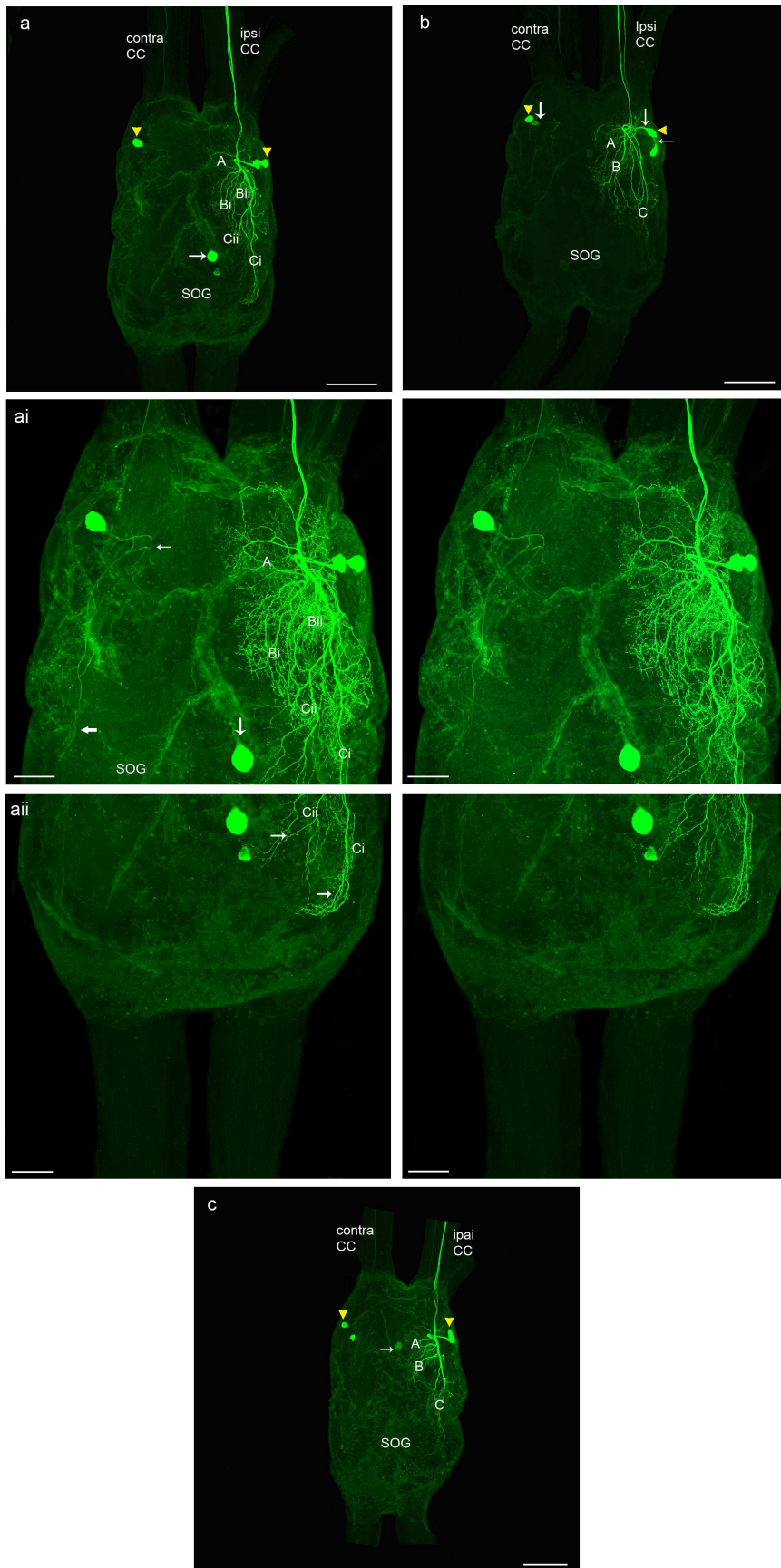


Figure 3.21 Backfilling of M3 and M38 motor nerves together.

(a, b, c) Confocal images of whole mount of subesophageal ganglion (**SOG**) of three different preparations of adult *Locusta migratoria* viewed ventrally; show motor neurons in ipsilateral and

contralateral mandibular neuromere, stained after retrograde filling of M3 and M38 motor nerve together with Neurobiotin™. (a) Shows that in ipsilateral half, one soma is ventro-laterally (**yellow arrowhead**) located while second soma is medio-laterally located. Their primary neurites emerge laterally and run straight medially. In contralateral half, ventro-laterally located soma (**yellow arrowhead**) is brightly stained; its primary neurite emerges laterally and run dorso-medially. **Arrow** marks the brightly stained soma of unpaired medial neuron whose cell body was located on ventral surface of the ganglion. (b, c) Show two somata (**arrowheads**) in ipsilateral half and two in contralateral half of mandibular neuromere. (b) Somata (**yellow arrowheads**) in both half of neuromere are ventro-laterally located. Primary neurites emerge anteriorly (thin horizontal **arrow**) or laterally (vertical **arrow**) and run medially. (c) Ipsilateral somata (**yellow arrowhead**) are lying medio-laterally above each other while contralateral somata are separately lying ventro-laterally. Primary neurites emerge laterally and run straight medially. **Arrow** marks the faintly stained soma of dorsal unpaired medial neuron. (ai, aii) Stereo pairs of confocal images of a whole mount of (**SOG**) shown in (a) are taken by using oil immersion objective. These images show the profused ramification of ipsilateral neuron. (ai) anterior half of SOG. In contralateral half, thin **arrow** shows the loop of primary neurite. Thick **arrow** shows that some of the branches of contralateral primary neurite project posteriorly into the ventral area of the labial neuropile. **Vertical arrow** marks the axon of ventral unpaired median neuron. (aii) Posterior half of SOG shows that the ramification of ipsilateral neurons projects up to labial neuromere. Small **arrows** mark the ramification into the dorsal and ventral area of labial neuromere. In all images (**A, B, Bi, Bii, C, Ci, Cii**) mark different areas of ramification in mandibular, maxillary and labial neuromeres. Anterior is towards the top of image. Scale bars: 200 μm (a, b, c), 80 μm (ai, aii).

Axons of suboesophageal ganglion neurons:

Two fibers in ipsilateral and two in contralateral circumoesophageal connectives were ascending towards the brain and four axons were crossing the frontal ganglion using it as a commissure (Fig. 3.22). Courses of ipsilateral axons inside the tritocerebrum and frontal connective were not traceable. But in one preparation, path of one of the axons of ipsilateral neurons was visible inside the ipsilateral tritocerebrum and it was projecting into the ipsilateral frontal connective without making ramification (data not shown). In contrast to ipsilateral axons, courses of axons of contralateral motor neurons were traceable in all preparations. These axons were projecting into the contralateral frontal connective without making ramification inside the tritocerebrum.

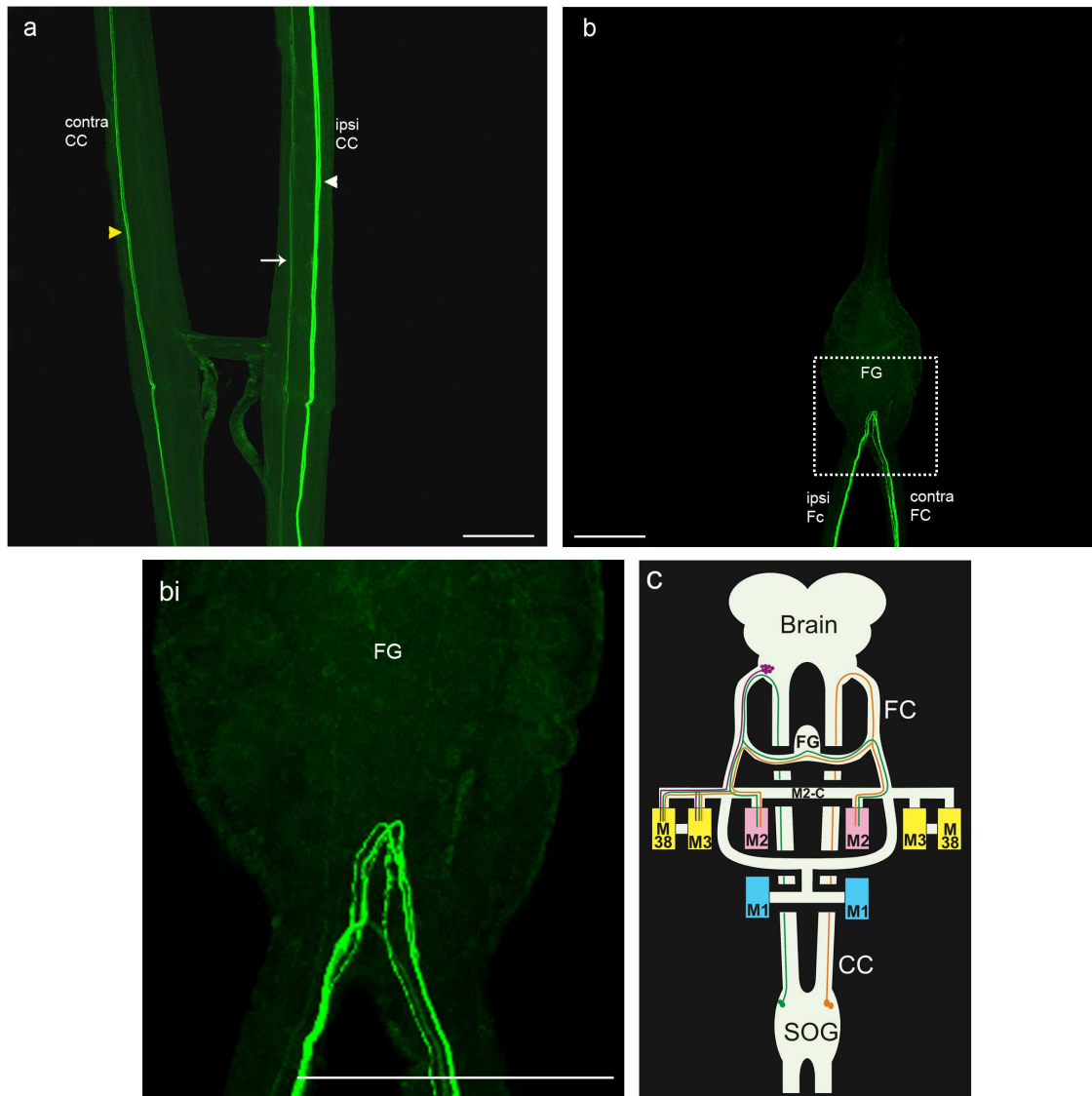


Figure 3.22 Axons of suboesophageal ganglion neurons cross the midline using frontal ganglion as a commissure. (a) Confocal image of a whole mount of ipsi- and contralateral circumoesophageal connectives (**ipsiCC**, **contraCC**) viewed ventrally and shows the projection of axons of suboesophageal ganglion motor neurons of figure 3.21c. **White arrowhead** shows two brightly stained fibers of the ipsilateral neurons while thin **arrow** marks the faintly stained fibers of DUM neurons. **Yellow arrowhead** marks the faintly stained fibers of contralateral neurons. (b) Confocal image of a whole mount of frontal ganglion (**FG**) of adult *Locusta migratoria* viewed ventrally and shows the crossing of four axons of suboesophageal motor neurons stained after retrograde filling of motor nerve branches of M3 and M38 together with Neurobiotin™. (bi) Stippled area in (b) at higher zoom shows that axons do not make ramification inside the ganglion. (c) Schematic drawing summarising the innervation of M3 and M38, obtained by backfilling of motor nerve branches to M3 and M38 together. Axons of the tritocerebral motor neurons (**purple**) project into frontal connective (**FC**) and bifurcate into FCM3&M38 to innervate ipsilateral M3 via ventral branch and M38 via dorsal branch. Axons of ipsilateral motor neurons (**green**) ascend towards the brain via circumoesophageal connective (**CC**), project into frontal connective without making ramification in the tritocerebrum and bifurcate to innervate M3 via ventral branch and M38 via dorsal branch. In frontal connective, axons give rise to branches that cross the frontal ganglion (**FG**) and innervate contralateral muscles. Axons of contralateral motor neurons (**orange**) take similar path to innervate M3 and M38. In (a) anterior is towards the top of image. In (b, bi) posterior is towards the top of image. Scale bars: 200 μ m (a, b).

Serotonergic and dorsal unpaired median neurons:

Backfilling of specific motor nerve branch to M3 and M38 together also stained somata of unpaired median neurons in the suboesophageal ganglion (Fig.3.21a, c, ai). In total, 5 preparations showed unpaired medial neurons. In 4 out of 5 preparations, two somata were faintly stained on dorsal surface of the ganglion while in one preparation; two somata were stained on ventral surface of the SOG. Primary neurites of ventrally lying neurons first runs towards the dorsal surface and then bifurcate to project into both circumoesophageal connectives.

3.4.6. Contralateral targets of suboesophageal neurons:

Backfilling of specific motor nerve branches to M2, M3 and M38 stained neuronal somata in ipsilateral and contralateral half of the suboesophageal ganglion. Their axons ascend towards the brain via circumoesophageal connectives and project into the respective side frontal connective to innervate different muscles in either half of the labrum. But before projecting into specific motor nerve branches, each axon divides and crosses the midline via the frontal ganglion and innervates the muscles in the contralateral half of the labrum. It was not clear whether all of the contralateral muscles are innervated by SOG neurons or they have some specific contralateral targets. For that, motor nerve branches to M3 and M38 were backfilled together. After incubation; brain, suboesophageal ganglion, frontal ganglion, ipsilateral M2, contralateral M2, M3 and M38 altogether were dissected out of the head and cleared in methyl salicylate using the similar histological methods as described in chapter2.

In total, 4 experiments were conducted. In two preparations, motor nerve branches of right M3 and M38 were incubated while in other two preparations; motor nerve branches of left m3 and M38 were incubated. Either case stained maximally four neurons in suboesophageal ganglion. Two somata were lying in ipsilateral half and other two were in contralateral half of the SOG. Confocal scanning of these preparations showed axonal terminals only in ipsilateral M2, contralateral M2 and M38. In none of the preparations, axonal terminals were found in contralateral M3 (Fig.3.23).

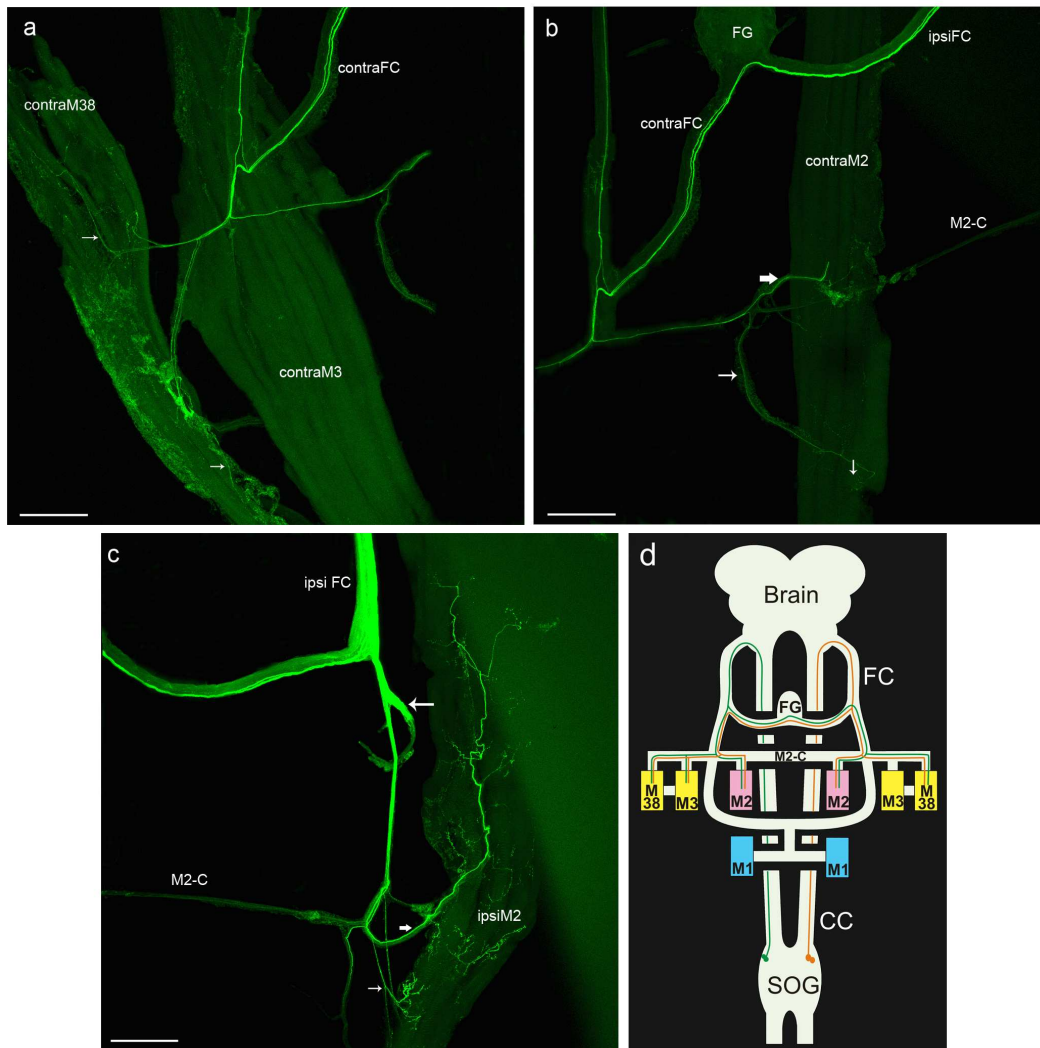


Figure 3.23 Contralateral targets of suboesophageal ganglion neurons.

Confocal images of whole mount of labral muscles of an adult *Locusta migratoria* show the innervation of suboesophageal ganglion motor neurons, stained after retrograde filling of M3 and M38 motor nerve together with Neurobiotin™. (a) Dorsal view of contralateral M3 (**contraM3**) has not shown any stained fiber while ventro-lateral view of contralateral M38 (**contraM38**) shows anteriorly and posteriorly branches and their terminals inside the muscle (thin **arrows**). (b) Dorsal view of contralateral M2 (**contraM2**) shows axonal staining inside the proximal (thin **arrow**) and distal (thick **arrow**) nerve branches and their terminals inside the muscle fibers (**vertical arrow**). (c) Dorsal view of ipsilateral M2 (**ipsiM2**) shows axonal staining inside the proximal (thin **arrow**) and distal (thick **arrow**) nerve branches. Distal branch is running posteriorly and give rise to many lateral branches. Large horizontal **arrow** shows the motor nerve branch being backfilled. (b) Schematic drawing summarising innervation of suboesophageal ganglion (**SOG**) neurons to M2, M3 and M38. Axons of ipsilateral motor neurons (**green**) ascend towards the brain via circumoesophageal connective (**CC**) and project into the branch of frontal connective. Inside this branch, each axon divides into two branches. One branch enters into FCM2 and second branch enters into FCM3&38. Axonal branches running into FCM2 innervate ipsilateral M2 while axonal branches running into FCM3&38 further bifurcate to innervate M3 via ventral branch and M38 via dorsal branch. All axons before projecting into the branch of frontal connective, give rise to branches that cross frontal ganglion (**FG**) and innervate only the contralateral M2 and M38. Axons of contralateral motor neurons (**orange**) take similar path to innervate M3 and M38. Ipsilateral frontal connective (**ipsiFC**), contralateral frontal connective (**contraFC**), M2-commissure (**M2-C**), frontal ganglion (**FG**). In (a, b, c) posterior is towards the top of images. Scale bars: 200 µm (a, b, c).

3.5. Action of motor neurons innervating labral muscles:

In the light of our results of backfilling, intracellular recordings were made from the fibers of M2, M3 and M38 to know:

1. Are all motor neurons that innervate a particular muscle spontaneously active?
2. Do left and right side muscles show any synchrony in their motor potentials?
3. Like the innervation of legs muscles, are labral muscles also innervated by inhibitory neurons?

3.5.1. Intracellular recording from anterior retractor muscles of labrum (M2):

M2 are innervated by 6 tritocerebral motor neurons, with 3 somata located in each tritocerebral lobe, and by four suboesophageal ganglion motor neurons (section, 3.4). Simultaneous intracellular recordings were made from right and left M2. To avoid movement artefacts, all recordings were made near to the origin of the muscles. All in vivo preparations have not shown activity inside the muscles. Only in a few preparations, it was possible to make intracellular recordings from both M2. These preparations showed variable results and probing of microelectrode into each fiber of a muscle did not reveal PSPs. In one preparation, a recording of 165 seconds showed occasional burst of excitatory PSPs in both M2. Duration of burst activities was ranging from 0.36s – 9s while pauses during bursting activity were ranging from 0.40s – 94.91s (Fig. 3.24). This occasional burst activity showed variable number of neurons was firing at different times and frequencies and there was a temporal summation of PSPs (Fig. 3.24Ai). PSPs were of variable size and shape but in principle were supporting our anatomical data. Their amplitude was ranging from 0.74 mV to 15.82 mV while Intervals between two successive PSPs in a single burst were ranging from 6.58-117.83 ms.

According to our anatomical data, tritocerebral neurons cross the midline in periphery through M2-commissure and innervate both ipsi- and contralateral M2. In general, when a single neuron in either lobe of the tritocerebrum will spike, its PSPs will be recorded from both M2, and PSPs in one muscle will appear after a short constant delay. But keeping in the view that the distance between right and left M2 is less than one millimeter, and the estimated velocity of action potentials is 4.1 m/s in periphery of the ganglion is 4.1 m/s (Gwilliam and Burrows, 1980). As a consequence, the action potentials of a neuron will require approximately $1/4^{\text{th}}$ of one ms to travel from one M2 to second M2. This very short time delay may be undetectable during recording and PSPs in right and left M2 will occur at the same time.

Simultaneous intracellular recordings of PSPs from both M2 showed similarity in their patterns. PSPs occurring in one muscle were accompanied by PSPs in other muscle. But extended time scale analysis showed variations in the latencies among PSPs of right and left M2. At some time PSPs appeared first in right M2 and then after a short varying latency in left M2 and vice versa. While on other time there was no time lag between the appearance of a PSP in right and left M2. Similarly, at another occasion a single PSP occurring in one M2 was not accompanied by simultaneous spike in second muscle (Fig. 3.24Ai). Latencies among PSPs of both M2 were ranging from 1.1 ms to 2.2 ms. Varying latencies among PSPs of both M2, and occasional independent occurrence of PSPs in one muscle indicate that neurons in both lobes of tritocerebrum were independently active.

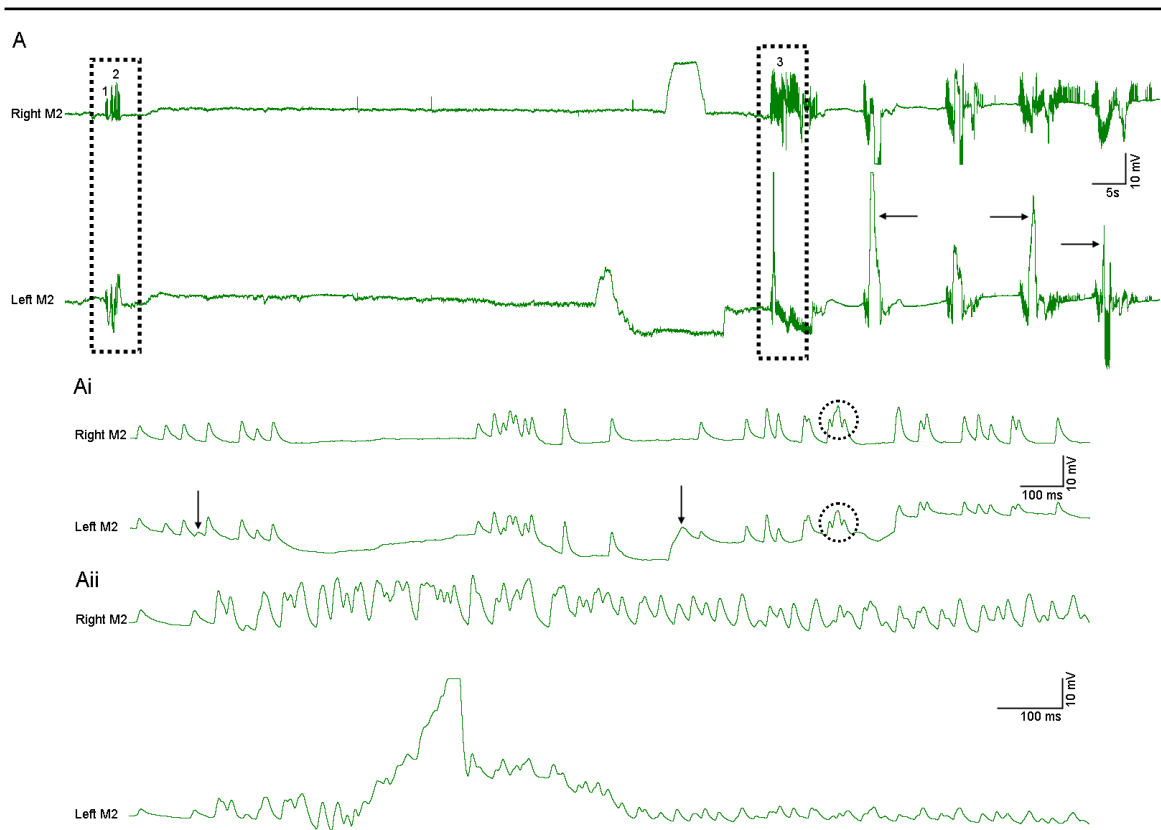


Figure 3.24 Intracellular recordings from right and left M2.

(A) Simultaneous intracellular recording from fibers of right M2 (upper trace) and left M2 (lower trace) in semi-intact preparation shows occasional bursts of excitatory post synaptic potentials. **1, 2** and **3** marks the PSPs bursts shown at extended time scale. Large baselines (**arrows**) deflections are movement artefacts. (Ai, Aii) Stippled areas marking 1, 2 and 3 burst of PSPs in (A) are shown at extended time scale. This extended time resolution indicates that all PSPs are excitatory and most of them occurred at similar time in right and left M2. There is also summation among different PSPs (**dotted circles**). **Arrows** in lower trace of (Ai) show the failure of an excitatory PSP in right M2.

3.5.2. Intracellular recording from posterior retractor muscles of labrum (M3):

Simultaneous intracellular recordings of PSPs from right and left M3 were not successful in all in vivo preparations. But recording made from one preparation showed that different numbers of motor neurons were firing in each M3 and not all the anatomically described motor neurons were active spontaneously, and active units were firing at different frequencies (Fig. 3.25). There was no synchrony among the active motor neurons of both muscles. In each muscle, all PSPs were excitatory and none was inhibitory. There were temporal summations among the PSPs of different spiking motor neurons (Fig. 3.25Ai). Size and shape of PSPs were variable and there were many small, intermediate and large PSPs. Amplitude of different PSPs recorded from left M3 was ranging from 0.19 mV – 4.42 mV while of right M3 were ranging from 0.17 mV – 5.49 mV.

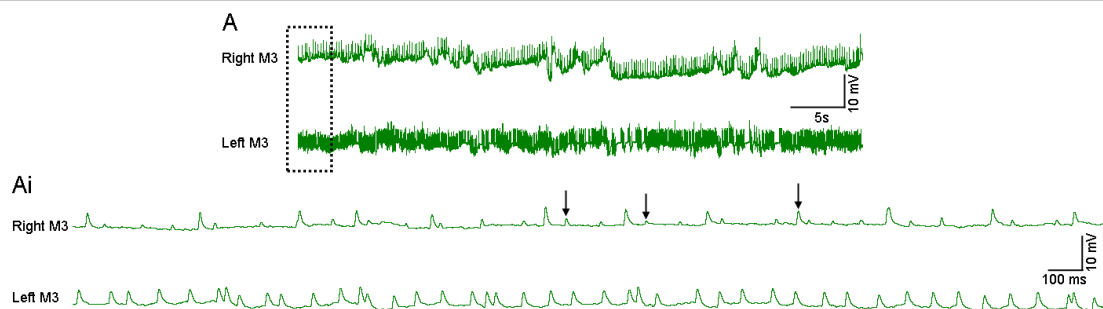


Figure 3.25 Intracellular recordings from right and left M3.

(A) Simultaneous intracellular recording from muscle fibers of right (upper trace) and left M3 (lower trace) shows that motor neurons in both muscles are firing independently with varying rate. (Ai) Extended time scale of stippled area shown in (A) indicates that all PSPs are excitatory and their amplitude is variable (**arrows** in upper trace). PSPs of right and left M3 are asynchronous and there is summation among different PSPs (**circle** in lower trace).

3.5.3. Intracellular recording from ipsilateral M2 and M3:

Simultaneous intracellular recordings from right M2 and M3 were made to reveal the activity of suboesophageal motor neurons. Both muscles are present in close approximation to one another, and the length of frontal connective branches innervating each muscle is very short. So, time required for the conduction of action potential to both muscles would be similar and simultaneous intracellular recordings of PSPs from both muscles will show one to one correlation.

However simultaneous recording of different fibers of M2 and M3 showed no common PSPs (Fig. 3.26). But recording revealed that different number of motor neurons was firing in each muscle, and not all the anatomically described motor neurons were active spontaneously. All PSPs were excitatory and none was inhibitory. There was no synchrony among the PSPs of both muscles and different PSPs were summated. PSPs were small, intermediate and large in size. The amplitudes of different PSPs recorded from M2 were ranging from 0.61mV – 5.01 mV while of M3 were ranging from 0.24 mV– 6.31 mV.

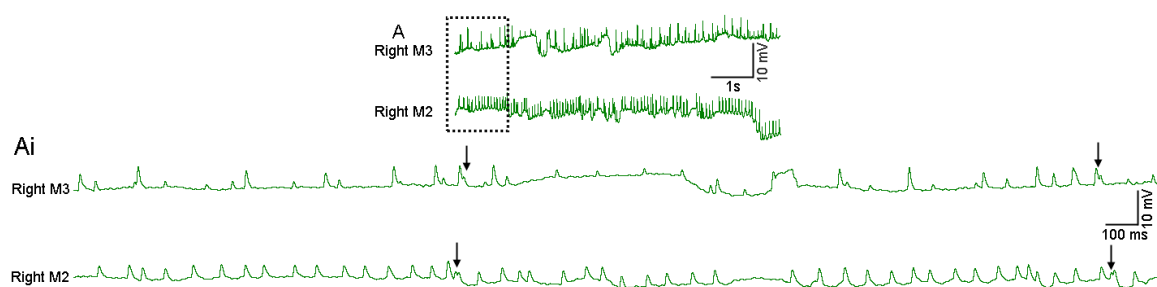


Figure 3.26 Intracellular recordings from right M2 and M3.

(A) Simultaneous intracellular recording from muscle fibers of ipsilateral M3 (upper trace) and M2 (lower trace) shows that different number of motor neurons in each muscle is independently active at varying firing rate. (Ai) Extended time scale of stippled area shown in (A) indicates that all PSPs are excitatory and there is no correlation between PSPs of right M3 (upper trace) and right M2 (lower trace). **Arrows** in upper and lower trace marks the summation of PSPs.

3.5.4. Intracellular recording from ipsilateral M3 and M38:

Simultaneous intracellular recording from ipsilateral M3 and M38 were made to reveal whether all motor neurons stained during the backfilling experiments are common to both muscles or there are some specific motor neurons to each muscle. If neurons were common to M3 and M38 then intracellular recordings of PSPs from both muscles will show one to one correlation. Secondly, as both muscles were also innervated by suboesophageal ganglion, so simultaneous recording might reveal inhibitory inputs to both muscles.

Different muscle fibers of M3 and M38 were recorded simultaneously but no recording showed one to one correlation between any of PSPs of both muscles (Fig. 3.27Ai). Different number of motor neurons was firing in each muscle which implies that not all the anatomically described neurons are common to both muscles, and there are some motor neurons specific to each muscle. The size and shape of PSPs in both traces were also variable. Recording from M38 fibers showed tonic and phasic occurrence of PSPs. Their amplitudes were ranging from 0.46mV – 4.6 mV. Duration of phasic PSPs were ranging from 0.33 - 0.44 s while of tonic PSPs were ranging from 2.17 - 2.70 s. Recording from M3 showed only phasic PSPs, and their duration was ranging from 0.51 - 0.72 s. However, a few sporadic PSPs of varying amplitude also occur in M3 during the occurrence of tonic PSPs in M38. Amplitude of M3 PSPs was ranging from 0.37 mV to 4.7 mV.

Recording showed that PSPs in both muscles were in synchrony. PSPs in M38 were driving the PSPs in M3. When phasic activity appeared in M38, then after a short variable time delay, phasic activity appear in M3. Phasic activity of M38 neurons started 0.05 - 0.21s before the phasic activity of M3 and ended 0.16 – 0.45s before the activity of M3. Both M3 and M38 traces also showed the summation of different PSPs. All PSPs were excitatory and none was inhibitory.

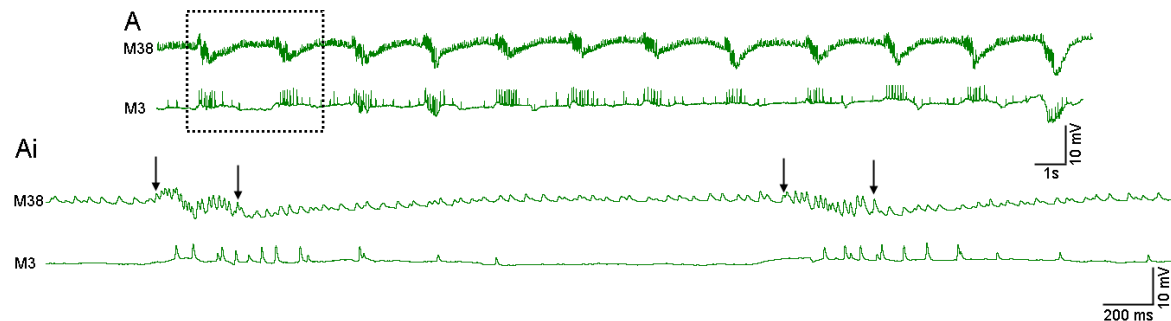


Figure 3.27 Intracellular recordings from M3 and M38.

(A) Simultaneous intracellular recording from muscle fibers of right M3 (lower trace) and right M38 (upper trace) shows that different number of motor neurons are active in both muscles. Recording from fibers of M38 (upper trace) shows tonic and phasic PSPs while of M3 (lower trace) shows only phasic PSPs. (Ai) Extended time scale of stippled area shown in (A) indicates all PSPs are excitatory and there is no correlation between PSPs of right M3 (lower trace) and right M38 (upper trace). **Arrows** in upper trace shows that PSPs in M38 start and end before the PSPs of M3.

3.6. Physiological properties of suboesophageal ganglion motor neurons:

Role of suboesophageal ganglion neurons and physiological confirmations of existence of their common innervation to labral muscles were studied. Neurons were recorded from one side of suboesophageal ganglion and no neuron was recorded from the contralateral side. In total six successful experiments were conducted. In two preparations, neurons were identified by application of both antidromic and orthodromic stimuli while in other four preparations, antidromic stimuli did not work and neurons were identified by correlating muscle PSPs with soma responses evoked spontaneously or by application of depolarised current. The failure of antidromic stimuli might be accounted for the damage caused to axons terminals by insertion of stimulus wires. Likewise, in three out of six preparations, iontophoretic application of Neurobiotin™ successfully stained the recorded somata. More striking feature of results was the absence of inhibitory input to muscle fibers and all PSPs recorded from different fibers of M2, M3 and M38 were excitatory.

Results of different experiments are described separately as it was not possible to make recording from all labral muscles at one time due to technical availability of only two microelectrodes. Secondly, muscle movements hindered the individual recording of all muscle in a single preparation. Thirdly, the discharge patterns of recorded neurons were variable in different preparations.

3.6.1. Simultaneous intracellular recording from fibers of M2, M3 and suboesophageal ganglion motor neurons:

In two preparations, simultaneous intracellular recordings from SOG motor neuron and labral muscles M2 and M3 were successfully made. While in one preparation, only simultaneous intracellular recording from M3 and SOG neurons was made.

Experiment No. 1

In this experiment, neuron was identified both by the application of antidromic and orthodromic stimuli, and turn by turn recording was made from different fibers of M2 and M3 (Fig. 3.29 and 3.30).

Application of antidromic stimuli:

On probing the neuronal soma by glass microelectrode, no spontaneous activity was recorded. While application of voltage stimuli to axonal terminals caused an action potential that travelled in antidromic way to the cell body, and passively invading action potential was recorded from the soma. Electrode used to record from the soma at the same time also recorded stimulus artefacts. Latencies between stimulus onset and rising phases of passively invading soma spikes were measured. Figure 3.28 shows ten consecutive overlapped passive soma spikes triggered by stimulus onset time. The latency between the stimulus artifacts and passive soma spike was constant and its value was 7 ms. Amplitude of the passively invading soma spike was 10.6 mV and their duration at half amplitude was 4.41-4.84 ms.

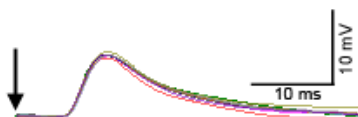


Figure 3.28 Identification of SOG neuron by application of antidromic stimuli.

Ten passively invading soma spikes evoked by stimulation of axonal terminals in muscle are superimposed. Signals are triggered by on set time of stimulus artefacts (**arrow**).

Application of orthodromic stimuli and simultaneous intracellular recording from M3 and SOG motor neuron:

Antidromically identified soma was depolarized by application of current through the recording electrode and simultaneous intracellular recordings from soma and M3 fibers were made (Fig. 3.29). As cell was not spiking spontaneously, on the application of depolarising current, it started to spike, and passively invading spikes were recorded from soma. Initial response in soma appeared after 100 ms of current application. First it gave only two spikes and after a time of 2.6 s, neuron started to spike in bursts. A total of 240 s recording trace initially showed 1-2 spikes in each burst but with passage of time, duration and spikes in burst get increased. Burst durations were ranging from 0.04 - 21.45 s. Inter-burst intervals were ranging from 0.59 - 8.85 s. Firing rate of neuron in each burst was also variable. Within each burst, it was tonically increasing or decreasing. After a time periods of 90 s, neuron changed bursting activity to long duration tonic spikes. At this point, when current application was stopped, neuron immediately stopped to fire (vertical arrow in lower trace of Fig. 3.29Ai). After 6 seconds, again current was applied to the soma and it again started to fire tonically. But initial response time of neuron after current application get decreased and first passive spike in soma was recorded after 55 ms. With passage of time, the amplitude of passively invading soma spikes were also changed. Amplitudes of passive soma spikes and their half height durations were measured for first 10 spikes shown in figure 3.29A, B. Maximum amplitude of passive soma spike was measured 8.80 mV and their half height duration was ranging from 3.28 ms to 11.35 ms.

When neuron was depolarized to cause spikes, at the same time, a second glass microelectrode was impaled near the origin of M3 muscle fibers, and simultaneously passively invading soma spikes and their evoked PSPs from M3 fibers were recorded (Figure 3.29A, B, upper trace). All PSPs were excitatory and showed 1:1 correlation with the passively invading soma spikes. Each PSP in M3 was following a passive soma spike of the impaled SOG neuron. As neuronal firing rate changed, same shift in M3 PSPs were observed. Latencies between first 10 passively invading soma spikes and their corresponding M3 PSPs shown in traces of figure 3.29A were measured. Latencies were measured between rising phases of both passive soma spikes and PSPs. Measured latencies were constant with a value of 8.16 ms. Moreover, first five consecutive passively invading soma spikes and their evoked PSP were overlapped by triggering the rising phase of passive soma spikes, and it showed no time lag between passive soma spikes and their corresponding PSPs evoked in M3 (Fig. 3.29Aii).

Amplitudes of evoked PSPs were slightly variable and it might be due to the muscle movement's artefacts. Amplitude of PSPs and their half height durations were measured for first 10 PSPs in each trace of M3 recordings shown in figure 3.29A, B. Maximum amplitude of PSPs measured was 34.7 mV and their half height duration was ranging from 8.16 ms to 11.57 ms.

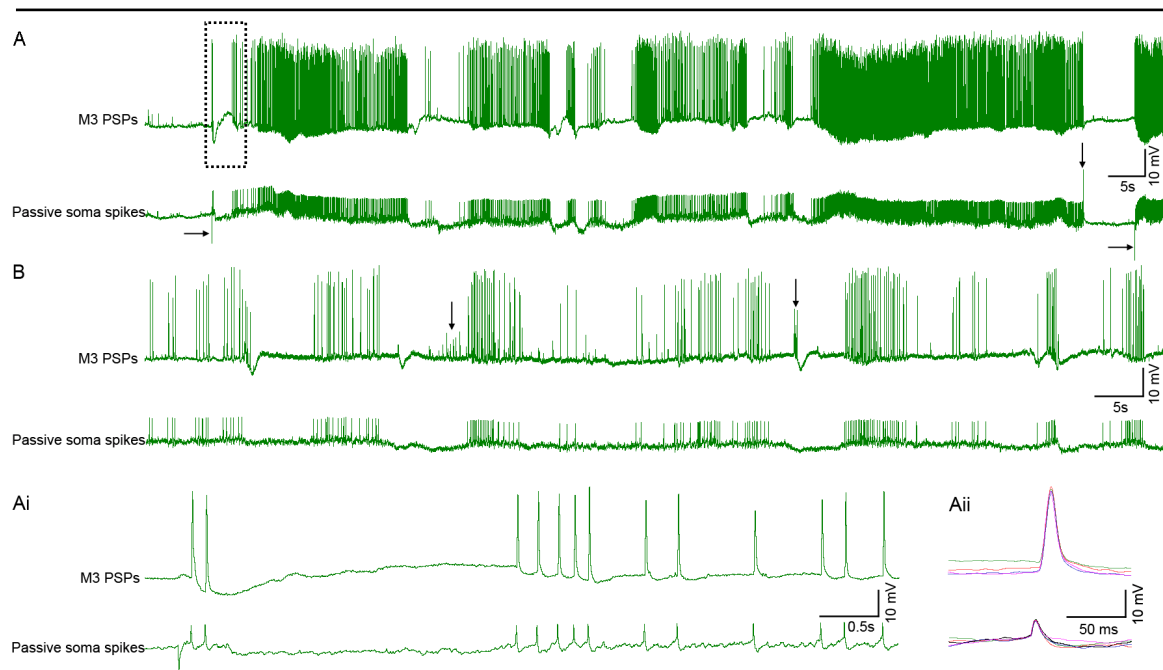


Figure 3.29 Simultaneous intracellular recording from M3 and SOG motor neuron.

(A, B) lower traces show the passively invading soma spikes evoked by application of depolarising current (horizontal **arrow** showing the downward deflection of base line) to the soma of SOG motor neuron. Upper traces show the simultaneous recordings of PSPs from the fibers of M3. All PSPs are excitatory. On application of current, neuron started to spike in bursts and same shifts was recorded from fibers of M3. Downward deflections (**circles**) of base lines are movement artefacts. Vertical arrow in lower trace of (A) marks the upward deflection on stop of depolarising current while **arrows** in upper trace of (B) show PSPs of other motor neurons. (Ai) Extended time scale of stippled area shown in (A) indicates each passively invading soma spike is in 1:1 correlation with M3 PSPs. (Aii) First five consecutive passively invading soma spikes and M3 PSPs shown in (Ai) are superimposed. Triggering of signals by rising phases of passive soma spikes (lower trace) showed fixed latency between passive soma spikes and their evoked EPSPs in M3.

Post synaptic potentials of other neurons in M3:

Intracellular recordings of PSPs from M3 evoked by SOG neuron have also showed some other PSPs (Fig. 3.29B). These were not correlating with passively recorded soma spikes. Other type of PSPs appeared at the time when there was no activity inside the impaled neuron. These may be due to the activity of other SOG neuron or may belong to ipsilateral tritocerebral neurons that also innervate M3.

Simultaneous intracellular recording from M2 and SOG neuron:

After simultaneous recording from fibers of M3 and soma, electrode was pulled out from fibers of M3 and impaled near to the origin of fibers of M2, and simultaneous intracellular recordings from passive soma spikes of same SOG neuron and their corresponding PSPs in M2 fibers were made (Fig.3.30). On the application of current (downward deflection in lower traces of Fig.3.30A, Ai) neuron started to spike and it evoked PSPs into M2. Again all post synaptic potentials recorded from the fibers of M2 were excitatory and showed 1:1 correlation with the passively invading soma spikes. Latencies between rising phases of 10 consecutive passive soma spikes and their corresponding PSPs in M2 were measured. Measured latencies were constant with a value of 8.21 ms. Moreover, first five PSPs of M2, evoked after application of depolarising current to the soma, were overlapped by triggering the rising phase of passive soma spikes, and there was no time lag between passive soma spikes and corresponding PSPs (Fig.3.30Aii).

Amplitude of M2 PSPs of M2 was very low and variable. The variability may be due to muscle movements and low amplitude of these PSPs indicates that neurons might make few synaptic terminals into the fibers of M2. Amplitude of PSPs and their half height durations were measured for first 10 PSPs recorded after application of current. Maximum amplitude of PSPs measured was 1.95 mV and their half height duration was ranging from 6.26 ms to 6.65 ms.

At the end of recordings, neuron was stained with iontophoretic injection of Neurobiotin™ contained in the tip of the recording electrode. But stainings did not work.

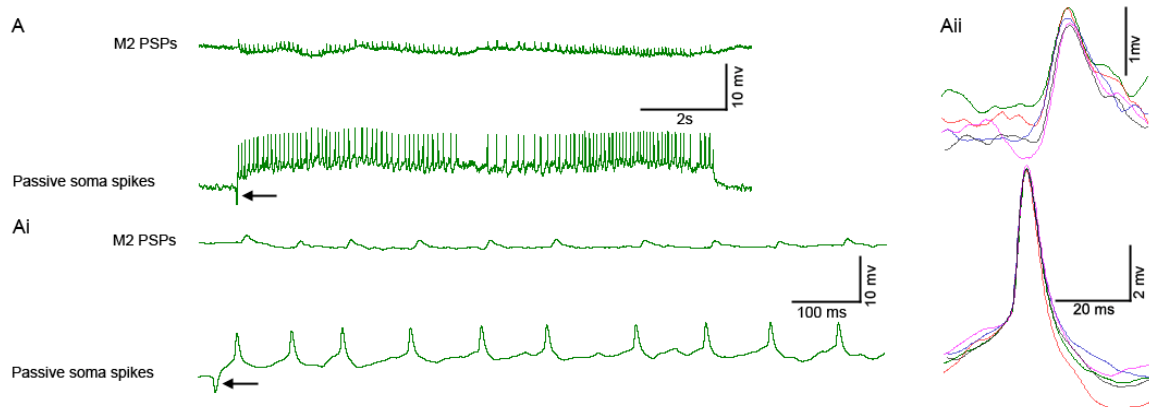


Figure 3.30 Simultaneous intracellular recording from M2 and SOG neuron:

(A) Lower trace shows the passively invading soma spikes evoked by application of depolarising current (**arrow** showing downward deflection of base line in lower traces) to the soma of SOG motor neuron. Upper trace shows the simultaneous recordings of PSPs from the fibers of M2. On application of current neuron started to spike and caused low magnitude PSPs in M2. (Ai) First ten passive soma spikes and their corresponding PSPs in M2, taken from the start of traces of (A), are shown at extended time scale. Each passively invading soma spike is in 1:1 correlation with recorded PSPs of M2 and all PSPs are excitatory. (Aii) First five passively invading soma spikes and their evoked M2 PSPs shown in (Ai) are superimposed by triggering the rising phases of passive soma spikes (lower trace) which shows fixed latency between them.

Experiment No. 2:

Application of orthodromic stimuli and simultaneous intracellular recording from M3 and SOG motor neuron:

In second preparation, neuronal soma was impaled with glass micro electrode and no spontaneous activity was recorded. Application of voltage stimuli did not evoke the action potential and no soma response was recorded.

On application of depolarised current through the recording electrode, neuron started to spike, and simultaneous intracellular recording of passive soma spikes and PSPs from fibers of M3 was made (Figure 3.31). Amplitudes of passive soma spikes and their half height durations were measured for first 10 spikes shown in figure 3.31A. Maximum amplitude of passive soma spike measured was 2.73 mV and their half height duration was ranging from 3.67 ms to 15.50 ms.

Initially neuron started to spike in burst and number of spikes within each burst was variable (Fig.3.31A). At this time, burst durations calculated for 35 s recordings were ranging from 0.03 - 2.11 s and pauses between burst were ranging from 0.37 - 1.25 s. Latter neuron started to spike tonically with varying inter spike intervals (Fig.3.31B, lower trace). During tonic activity, neuron fired sporadic doublet of spikes. After few seconds, neuron again changed its firing behaviour from tonic to occasional burst activity and number of spikes in each burst gradually increased. Initially in each burst, singlet or doublet of spikes were present (Fig.3.31C). Latter burst occurred with doublet, triplet or

fourlet of spikes, and finally burst occurred with large number of spikes (Fig.3.31D, E). As number of spikes in each burst increased, their duration also increased. At this time, the longest burst duration calculated was 1.20 s and the longest interval between two burst was 0.71 s. Similarly muscle contraction and relaxation rate also increased and at that it became impossible to make stable recording from muscle fiber.

Simultaneous intracellular recordings of passively invading soma spikes and their corresponding PSPs from M3 fibers showed having 1:1 correlation. As neuronal firing rate changed, same shift in M3 PSPs were observed. Latencies were measured between rising phases of 10 consecutive passively invading soma spikes and their corresponding PSPs in M3. Measured latencies were constant with a value of 6.53 ms. Moreover five consecutive PSPs of M3 were overlapped by triggering the rising phase of passive soma spikes and they showed no time lag between passive soma spikes and their corresponding M3 PSPs (Fig.3.31F).

Amplitudes of PSPs were slightly variable and it might be due to muscle movement. Amplitude of PSPs and their half height durations were measured for first 10 PSPs shown in figure 3.30A. Maximum amplitude of PSPs measured was 8.63 mV and their half height duration was ranging from 6.94 ms to 8.57 ms.

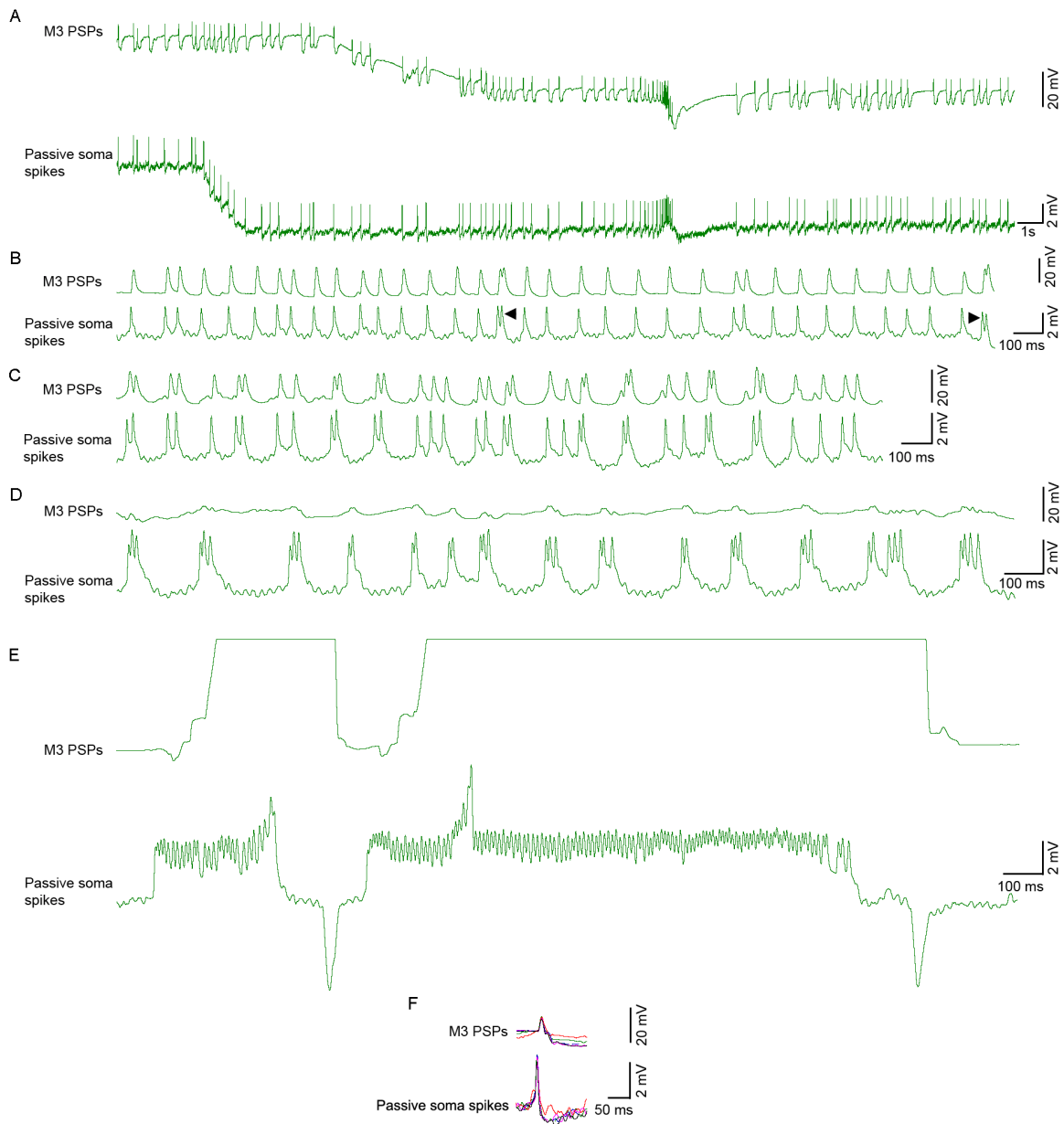


Figure 3.31 Different spiking patterns of SOG motor neuron.

(A-F) lower traces show the passively invading soma spikes evoked by application of current to the soma of SOG motor neuron. Upper traces show the simultaneous recordings of PSPs from the fibers of M3. (A) Application of depolarizing current to neuron caused to fire in bursts with long inter-spike intervals, (B) tonic activity with sporadic doublet of spikes (**arrowheads** in B). (C) Shows both tonic and phasic activity. (D) Shows doublet, triplet or fourlet of spikes. In (A, B, C) same shifts of neuronal spiking were also recorded from fibers of M3. (E) Shows long duration burst with increasing number of spikes. Downward deflections of base lines of lower trace are movement artefacts while upper trace shows increased contraction and relaxation rate of M3 which hindered the stable recordings by microelectrode. (F) First five passively invading soma spikes and their evoked M3 PSPs shown in (A) are superimposed by triggering the rising phase of passive soma spikes (lower trace) which shows fixed latency between passive soma spikes and M3 PSPs.

Intracellular staining:

At the end of recordings, neuron was stained with iontophoretic injection of NeurobiotinTM contained in the tip of the recording electrode. Intracellular staining revealed similar morphology of neuron as was obtained by backfilling of specific motor nerve branches to

M2, M3 and M38 (section, 3.4). But staining was not as sharp as obtained during anatomical study (compare figure 3.21 and 3.32). However, course of primary neurite and their branches were clearly visible. Primary neurite was making similar loop inside the neuropile before projecting into circumoesophageal connective as an axon. Similar pattern of three branches of primary neurites (A, B, C) were visible. Axon was ascending toward the brain via circumoesophageal connective and was projecting into the ipsilateral frontal connective without giving any branch into the tritocerebrum. In frontal connective, axon was faintly stained and it could not be traced further towards the frontal ganglion.

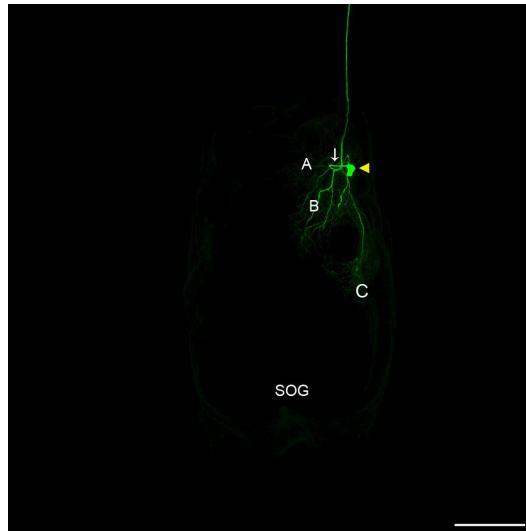


Figure 3.32 Intracellular staining of SOG motor neuron

Confocal image of a whole mount of suboesophageal ganglion (**SOG**) of adult *Locusta migratoria* viewed ventrally; show motor neuron in mandibular neuromere, stained with iontophoretic injection of Neurobiotin™. Soma (**yellow arrowhead**) is ventro-laterally located. Primary neurite emerges laterally, runs straight medially and makes a loop inside the neuropile (**arrow**) before entering into circumoesophageal connective (**CC**). (A, B, C) mark three branches of primary neurite into mandibular, maxillary and labial neuromeres. Anterior is towards the top of image. Scale bars: 200 μm .

Experiment No. 3:

Application of orthodromic stimuli and simultaneous intracellular recording from M3 and SOG motor neuron:

In third preparation, probing of microelectrode into the soma of suboesophageal ganglion neuron has also not revealed any spontaneous activity and application of antidromic stimuli was also not successful.

Application of depolarised current caused to spike neuron tonically after a time delay of 21 ms and passively invading spikes were recorded from the soma (Fig.3.33A, lower trace). Amplitudes and half height durations measured for 10 consecutive passive soma spikes were variable. Maximum amplitude of passive soma spike was 3.23 mV and their half height duration was ranging from 2.40 ms to 3.61 ms. Simultaneous intracellular recording from the soma and fiber of M3 showed 1:1 correlation and all recorded PSPs were excitatory. Latencies between 10 consecutive passively invading soma spikes and their corresponding PSPs in M3 were measured. Measured latencies were constant with a value of 6.32 ms. Moreover, first five consecutive PSPs from M3 evoked after application of depolarising current to the soma of neuron were overlapped by triggering the rising phase of passive soma spikes. This overlapping showed no time lag between passive soma spikes and their corresponding PSPs evoked in M3 (Fig.3.33Ai). Maximum

amplitude of PSPs measured for first 10 PSPs was 0.68 mV and their half height duration was ranging from 4.08 ms to 5.90 ms.

Simultaneous intracellular recording from M2 and SOG motor neuron:

Now glass micro electrode was pulled out from M3 fibers and was impaled into muscle fibers of M2. Simultaneous intracellular recordings from previously impaled SOG neuron and their evoked PSPs from M2 fibers were recorded (Fig.3.33B). Simultaneous intracellular recordings showed that now neuron was spontaneously active and each PSP in M2 trace was in 1:1 correlation with passively invading soma spikes. Application of depolarizing current to soma (downward deflection in lower trace of Fig.3.33B) increased its firing rate and similar shift was observed in recording trace of PSPs of M2 fibers. Latencies between first 10 passively invading soma spikes recorded after application of current and their corresponding PSPs in M2 were measured. Latencies were constant with a value of 7.00 ms. Moreover, first five PSPs of M2 evoked after application of depolarising current to the soma were overlapped by triggering the rising phase of passive soma spikes and it showed no time lag between passive soma spikes and their corresponding M2 PSPs (Fig.3.33Bi).

Amplitude of PSPs of M2 was again very low. Amplitude of PSPs and their half height durations were measured for the same first 10 PSPs for which latencies were measured. Maximum amplitude of PSPs measured was 3.81 mV and their half height duration was ranging from 7.70 ms to 9.80 ms.

At the end of recordings, neuron was stained with iontophoretic injection of Neurobiotin™ contained in the tip of the recording electrode. But staining was not successful.

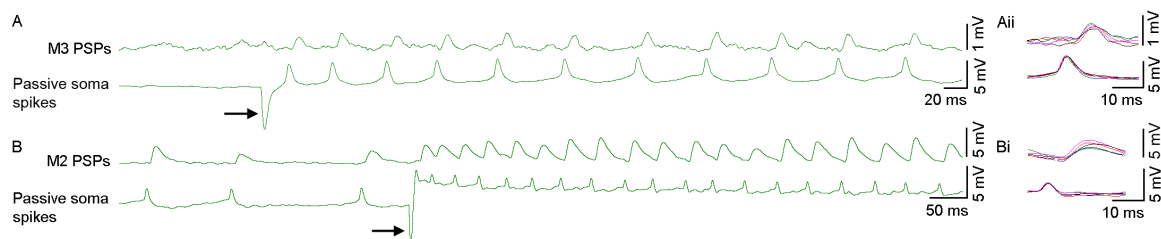


Figure 3.33 Simultaneous intracellular recording of passive soma spikes of SOG motor neuron and PSPs of M2 and M3.

In (A, B) upper traces show intracellular recordings of PSPs from M3 and M2 respectively while lower traces show the passive soma spike of a SOG which have common innervation to both muscles. On application of current (arrow showing downward deflection of base line in lower traces) neuron started to spike tonically and caused PSPs in fibers of M3 and M2. In (B) both spontaneous and depolarized activity of SOG motor neuron is recorded. Application of current increased the neuronal firing rate and same shift in M2 PSPs is recorded. (Ai, Bi) First five passively invading soma spikes and their evoked PSPs in M3 and M2 shown in (A, B) are superimposed by triggering the rising phase of passive soma spikes (lower trace) which indicates 1:1 correlation between passive soma spikes and PSPs in M3 and M2 respectively.

3.6.2. Simultaneous intracellular recording from fibers of M38 and SOG neuron:

Only in one preparation, simultaneous intracellular recording from M38 and SOG neuron was successful. Probing of neuronal soma revealed no spontaneous activity but on application of depolarising neuron started to spike tonically, and passive responses were recorded from the neuronal soma. In this experiment, deflection in baseline caused by application of current could not be completely balanced. Intracellular recordings of PSPs from fibers of M2 and M3 were also not successful. However, intracellular recordings from fibers of M38 showed 1:1 correlation. All PSPs were excitatory and latencies between first 10 passively invading soma spikes and their corresponding PSPs in M38 were 14.92 ms.

Moreover, overlapping of five consecutive PSPs by triggering the rising phase of passive soma spikes also showed 1:1 correlation between passive soma spikes and their corresponding PSPs evoked in M3 (Fig.3.34Ai).

Amplitude and half height durations of ten consecutive passive soma spikes and their evoked PSPs were calculated. Maximum amplitude of passive soma spikes and their evoked PSPs were 7.44 mV and 12.42 mV respectively while half height durations of passive soma spikes were ranging from 8.95 ms to 16.41 ms and of their PSPs were ranging from 8.35 ms to 11.94 ms.

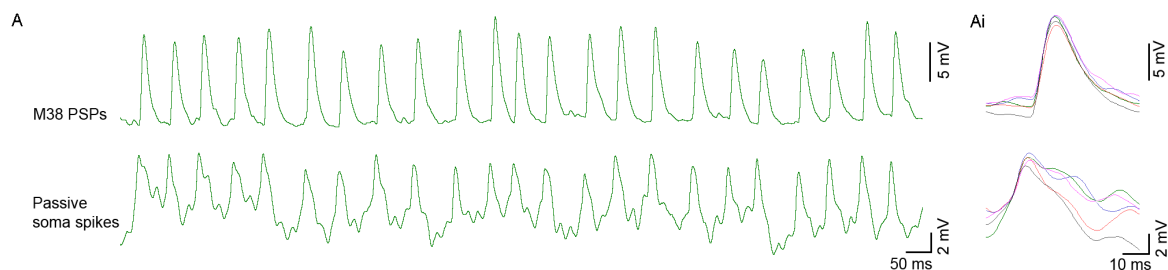


Figure 3.34 Simultaneous intracellular recording from M38 and SOG neuron:

(A) Shows tonic activity was recorded after application of depolarizing current to neuronal soma and each passively invading soma spike (lower trace) is in 1:1 correlation with M38 PSPs (upper trace). (Ai) Five consecutive passively invading soma spikes and their corresponding PSPs in M38 shown in (A) are superimposed by triggering the rising phase of passive soma spikes (lower trace) which shows fixed latency between passive soma spikes and M38 PSPs.

Intracellular staining:

At the end of recordings, neuron was stained with iontophoretic injection of Neurobiotin™. Staining revealed similar morphology as was in preceding intracellular staining (compare figure 3.35 and 3.32). But iontophoretic injection of Neurobiotin™ also stained some other neurons in the ganglion. These were the artefacts caused by tissue movements. As it might possible that during current application, movements of tissues caused the electrode to get out of the recorded neuron and probed it into the neighbouring neuron.

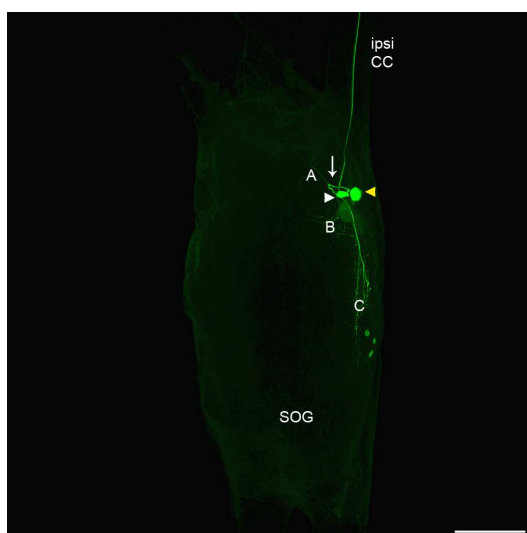


Figure 3.35 Intracellular staining of SOG motor neuron

Confocal image of whole mount of suboesophageal ganglion (SOG) of adult *Locusta migratoria* viewed ventrally; show motor neuron in mandibular neuromere, stained with iontophoretic injection of Neurobiotin. Soma (Yellow arrowhead) is ventro-laterally located. Primary neurite emerges laterally and run dorso medially and makes a loop inside the neuropile (arrow) before entering into circumoesophageal connective (CC). (A, B, C) mark three branches of primary neurite projecting in

mandibular, maxillary and labial neuromeres. **White arrowhead** shows another soma stained during application of current pulses. Anterior is towards the top of image. Scale bars: 200 μm .

4. Discussion:

In contrast to the neuromuscular systems of thoracic and abdominal structures controlling walking and flight of locust, very little is known about the motor system of feeding apparatus. In study here, we have investigated first time a systematic detail of innervation pattern of labral musculature of migratory locust *Locusta migratoria*. Specifically backfilling of motor nerve branches of individual muscle with neuronal tracer Neurobiotin™ and taking images with confocal laser scanning microscopy, we have characterised the anatomical features of neurons such as position and size of somata, course of primary neurites, their branching patterns and paths of axons. Electrophysiological properties of the motor neurons having common innervation to labral muscles were also studied.

4.1. Innervation pattern of labral muscles:

Locust labrum has one intrinsic (M1) and two extrinsic muscles (M2 and M3). First description of muscles of labrum was described by Snodgrass, 1928 in Carolina locust (*Dissostertia carolina*). He described three pairs of bilaterally symmetrical muscles which were named and numbered as compressor of labrum (M1), anterior (M2) and posterior retractor of labrum (M3). In present study, similar sets of three pairs of bilaterally symmetrical muscles in the labrum of adult locust were found and same name and numbers were used. Besides labral muscles, a closely related anterior dilator muscle of foregut (M38) was also studied. Although previous studies (Boyan *et al.* 2002; Ayali *et al.*, 2002; Gundel and Penzlin, 1978 and Aubele and Klemm, 1977) described that labral muscles are innervated by branches of frontal connectives, but never mentioned the details of innervation pattern. To know this, frontal connective was stained with nickel chloride in an anterograde fashion, and a great deal of variation was found in its branching pattern. But for ease of description, a general branching pattern was devised (Fig. 3.8). Branching pattern of frontal connective was bilaterally symmetrical. Each frontal connective anteriorly gives off 2-3 branches which were named according to the muscle being innervated; FCM1, FCM2 and FCM3&M38. Frontal connective branches innervating each M1 fuse together in the clypeus and make labral median nerve (LMN). This median nerve runs ventrally and again bifurcates to make nerve root to M1 (M1N). At the level of muscle, each M1N further divides into dorsal and ventral branches to innervate M1. While each FCM2 after innervating the respective side M2 proximally and distally, projects towards the midline, and fuses with each other in periphery to make M2-commisssure. However, M3 and M38 of either half of labrum are innervated by ventral and dorsal branches of a short common nerve of frontal connective. These branches exchange their innervation pattern on muscles but do not cross the midline.

In previous studies, Schachtner and Bräunig, 1993, during the investigation of activity pattern of serotonergic neurons, described the innervation pattern of M1 and Boyan *et al.* 2002 mentioned the innervation of M2. Innervation pattern described by these authors could be in general confirmed except for the additional findings of dorsal and ventral branches for M1, and proximal and distal branches for M2. For M3 and M38, innervation pattern is described first time in present study and shows both muscles share a unique common exchangeable nerve pattern (Fig. 3.7). Additional findings of branching pattern of nerves at level of individual muscle seem to mark the compartmentalization of muscle fibers that receive innervation from different numbers of motor neurons. This is in accord with the model presented by Hoyle, 1955; all skeletal muscles of locust may fit into one of the three categories. According to Hoyle, insect muscles are composed of many fibers that group together to form different muscle units. A single muscle unit may form a complete muscle and could have multiple innervations. In second category, several units form a muscle and attach to a common apodeme but each unit has independent

innervation. In third category, muscle is also formed of several units attached to a common apodeme but all are innervated by a single common axonal source.

4.2. Organization of motor neurons:

A fundamental purpose of neuronal mapping is to chart anatomical connection within the nervous system. However, the topographical organization of a neuron requires a tracer, capable of resolving fine morphological detail and permitting analysis of the projection either from whole tissue or selected areas under bright field microscopy. In this case, retrograde filling of nerves with Neurobiotin™ has proved an advantageous method for mapping neurons projecting their axons into the peripheral nerves. Neurobiotin™ is a derivative of biotin and is detected with avidin or streptavidin labelled with fluorochrome. It has much smaller molecules that could travel for long distance. It does not leak out of the cells and is non toxic to them.

In present study, backfillings of specific motor nerves of individual labral muscles revealed 20 motor neurons. M1 is innervated by two motor neurons, with one soma located in each lobe of the tritocerebrum (Fig. 3.9). The axons of both neurons bifurcate in the periphery to innervate ipsi- and contralateral M1. Labral retractor muscles (M2) are innervated by 6 tritocerebral motor neurons, with 3 somata located in each tritocerebral lobe (Fig. 3.11). Their axons cross the midline in a distinct commissure between the two muscles. M3 and M38 have common innervation and their somata are located in the ipsilateral tritocerebrum only. Both muscles together receive 8 motor axons (Fig. 3.20). In addition; M2, M3 and M38 also receive common innervation from 4 motor neurons located in the suboesophageal ganglion (SOG). In relation to the muscle, their somata are located on the ipsi- and the contralateral sides of the SOG (Fig. 3.21). Their axons ascend through the circumoesophageal connectives and proceed into the frontal connectives without forming ramifications in the tritocerebral lobes, and cross the midline in the periphery to innervate contralateral set of muscles. They cross the midline via M2-commissure or through the frontal ganglion (Fig. 3.22 and 3.23).

No comparable description of the morphology of the labral neurons in other insects has been yet published. However, our morphological descriptions are in accord with a few studies conducted in adult locust. Schachtner and Bräunig, 1993 backfilled labral medial nerve and described two motor neurons for M1, one in each tritocerebral lobe of the brain. Boyan *et al.* 2002 made a cobalt backfill of a branch of labral medial nerve; nerve root to M1 (M1N), and described that a single soma in the ipsilateral lobe of the tritocerebrum innervates both ipsi- and contralateral M1. In same study, cobalt backfill of a branch of FCM2 revealed three motor neurons in the ipsilateral lobe of the tritocerebrum and a single motor neuron in the ipsilateral half of the mandibular neuromere. Neurons were innervating ipsi-and contralateral M2 via M2-commissure. In cockroach, Gundel and Penzlin, 1978, and in cricket, Kirby *et al.* 1984, mapped the connection of stomatogastric nervous system with central nervous system by cobalt and nickel chloride infusion of peripheral nerves of frontal ganglion and branches of the frontal connective, and stated frontal ganglion contains the motor neurons that innervate clypeolabral muscles. They also described that some motor neurons in the mandibular neuromere of suboesophageal ganglion project their axons into branches of the frontal connectives. But on the contrary, in present findings, no neuron was stained inside the frontal ganglion. This implies the labrum has no connection with stomatogastric nervous system. Neurons crossing the frontal ganglion using it as a commissure indicate the anterior commissure of the tritocerebral neuromere (Boyan, *et al.* 2003). Auble and Klemm, 1977 during his study of mapping the connection of tritocerebral neurons in locust also stated that some neurons in the mandibular neuromere of suboesophageal ganglion project into frontal connectives. But no author described their peripheral targets. In backfilling of frontal connective with Neurobiotin™ in the direction of the tritocerebrum, Bräunig, 2008 stated a total of 60 neurons in ipsi- and contralateral neuromeres of suboesophageal ganglion. He ascribed them in nine distinct groups (a-i) containing from three to more than 20 neurons. But during that study, only one group consisting of DUM

neurons was identifiable, and neurons belonging to group “b” were assumed to innervate labral muscles. Present study confirms this notion and characterizes some of the suboesophageal neurons. Four somata stained in ipsi- and contralateral half of suboesophageal ganglion belongs to the neurons of group “b” and “c” of Bräunig, 2008.

Neuronal somata stained in the tritocerebrum are located in the outer cortex of the neuropile and single processes emerge from them, enter into the neuropile and give rise to a profusion of branches before entering into frontal connective as axons. Whole ramification is limited to the tritocerebral neuropile. No fibers are found into the deutocerebrum, and also none of the fibers crosses the midline in brain to enter into the contralateral lobe of the tritocerebrum. Ramification of motor neurons of both halves of the tritocerebrum does not overlap but dendritic arborisation of all motor neurons within each half overlaps, and individual neuron cannot be identified on the basis of its morphology. Organization of motor neurons within the tritocerebrum is similar to the bauplan of motor neurons located in other ganglia of locust. Such as somata and ramification of motor neurons innervating thoracic and abdominal musculatures are found exclusively in the ipsilateral hemisphere of ganglia, and neurons innervating same muscle or projecting their axons in same nerve have somata clustered together and their ramification overlap with each other (Burrows, 1973; Wilson, 1979a, b; Siegler *et al.*, 1991). However, the homology of individual neuron with those innervating legs or wing muscles is very difficult. Because, the complexity of fusion of the tritocerebrum with other brain neuromeres, and structural and functional differences between thoracic appendages and labrum complicate a direct comparison. But future studies implying the cell lineage analysis and studying the fate of progeny of individual neuroblast of the tritocerebrum might resolve the problem, and can show how the shape and synaptic contacts of motor neurons are changed during development to innervate functionally different structures.

This organization is also extendable to the motor systems of head appendages used for feeding and sensory information collection, whose ganglia have been fused and innervate highly modified appendages. For example, Baines *et al.* 1990 described that 8 motor neurons for mandibular closer muscle of locust are located dorso-laterally in the mandibular neuromere of suboesophageal ganglion. All neurons have similar morphology and their ramification is confined to the ipsilateral mandibular neuropile. But one exception was stated by Tyrer *et al.* 1984. They described that 12 motor neurons for mandibular closer muscle of locust are located anteriorly between the connectives but their ramification projects both ipsi- and contralaterally into the ventral neuropile of mandibular neuromere. Similarly the antennal muscles are innervated by highly modified brain neuromere, the deutocerebrum, which follow the same principle of central organization of the neurons. In insects, the deutocerebrum is divided into dorsal and ventral lobes. Dorsal lobe is also known as antennal mechano-sensory and motor centre (AMMC); it receives projection not only from motor neurons but also from antennal mechanoreceptors. The antennal motor system has not been studied only in locust (Bauer and Gewecke, 1990) but a great deal of antennal motor system is also available for cricket (Honegger, *et al.* 1990a, b; Allgäuer and Honegger, 1993), honeybee (Kloppenburger, 1995), moth (Kloppenburger, *et al.* 1997), stick insect (Dürr *et al.* 2001) and cockroach (Baba and Comer, 2008). In the antennal motor system of all insects studied so far, somata are mostly located in the dorsolateral and medial layers of neurons that surround the dorsal lobe. Primary neurites of closely located somata run together and arborize in AMMC. Ramification of individual neuron overlaps together but whole ramification is limited to the ipsilateral neuropile.

Although the dendritic arborisation of all motor neurons of a neuromuscular system of locust extensively overlaps in ipsilateral neuropile but there exists no monosynaptic contacts among them. Only one exception lies in neuromuscular system controlling the hind leg of locust, where fast extensor tibiae motor neuron was found to make monosynaptic contacts with the flexor motor neurons (Hoyle and Burrows, 1973). Similarly, some sensory projections making reflexive pathways in control of flight and

walking of locust has been reported to make monosynaptic connections with motor neurons (Burrows, 1975; Skorupski and Hustert, 1991). In antennal motor system, no direct evidence of monosynaptic connection between sensory and motor neurons has been described. But from the overlapping of dendritic arborisation of motor neurons with projection of several antennal mechanoreceptors like the campaniform sensilla, the Johnston's organ (Gewecke, 1979) and antennal strand receptors (Bräunig, 1985), it is assumed that the information to air currents reach to the motor neurons by monosynaptic connection.

Monosynaptic connections among labral motor neurons also seem less probable. Because labrum is not involved in any postural control behaviour during walking or flight. Secondly, it is part of feeding apparatus and its movements are controlled by feeding circuitry located in suboesophageal ganglion (Seath, 1977; Rast and Bräunig, 2001b). But overlapping dendritic field of its motor neurons suggests that they may receive common synaptic inputs from interneurons located in the suboesophageal ganglion for fine coordination of its movements during feeding behaviour. This suggestion seems true for labral musculature as dendritic field of motor neurons innervating muscles of one half of the labrum is limited to only ipsilateral hemisphere of ganglia and none of the dendritic branches crosses the midline. This interpretation is also in accord with the findings of Rast and Bräunig, 2001b. They described that muscarinic agonist pilocarpine induced feeding related rhythms in deafferented preparations of suboesophageal ganglion, and motor outputs to all mouthparts muscles were not only strongly coupled with mandibular motor pattern but bilateral coupling was also of similar strength. And for labral motor pattern, these authors concluded that the tritocerebral motor neurons act as an output structure for premotor neurons of suboesophageal ganglion. In present study, although staining of 2 neurons in each half of the mandibular neuromere do not seem the possible candidates for the connection of the two motor centres as these neurons were not found to have any ramification in the tritocerebrum. But on the basis of their morphology, at least, it could be stated that in parallel to the premotor neurons of suboesophageal ganglion, these neurons also take part in the fine coordination of labral muscle movements during feeding activity.

Like their distinct peripheral innervation, these motor neurons also have unique dendritic arborisation. Their somata are located in outer cortex of each half of the mandibular neuromere. Primary neurites run together and gives off branches in mandibular neuropile. Some branches also project posteriorly up to the labial neuromere and make profound overlapping arborisation in maxillary and labial neuropiles. Whole ramification is limited only to the ipsilateral neuropils and do not cross the midline. This unique pattern of arborisation has not been found for any of the motor neurons in all the neuromuscular systems studied so far in locust, and comparison of their ganglionic architecture is further limited by less studied neuromuscular system of feeding apparatus. In this regard, only a few studies describe the morphology of mandibular motor neurons.

Tyrer *et al.* 1984 has described that motor neurons controlling the locust mandibular closer muscle are located between the connective, and their dendritic arborisation projects in ipsi- and contralateral mandibular neuropiles. But dendritic arborisation is limited only to the mandibular neuromere and does not into the maxillary and labial neuropiles. The only notable exception in this regard is the dendritic arborisation of the mandibular motor neurons of *Manduca sexta* which seems to some extent comparable with that of labral common motor neurons. Griss, 1990 described that 12 motor neurons in *Manduca* innervate mandible closer muscle and 8 motor neurons innervate mandible opener muscle. All neurons have their somata in mandibular neuromere but their ramification projects ipsilaterally beyond the mandibular neuromere. However, on the basis of such limited studies, it is very hard to draw any conclusion whether this unique dendritic arborisation is only destined to labral motor neurons or it is a general feature of all the motor neurons of suboesophageal ganglion. In this context, comparable studies of motor neurons controlling the feeding apparatus in different insects will lead to draw any final conclusion.

The involvement of motor neurons from the mandibular neuromere in the control of labral muscles itself raises the question of segmental origin of this part of the suboesophageal ganglion. Doe and Goodman, 1985; Zacharias, 1993 and Urbach, *et al.* 2003 have described that anterior of the mandibular neuromere is derived from the neuroblast forming the third brain neuromere, the tritocerebrum (see conclusion). It might be concluded that during the course of evolution of the neuronal circuitry of mouthparts, labral neurons also went under modification and become well integrated with other neuromere of suboesophageal ganglion to cope with the requirements of feedings. Similar to this interpretation, Rast and Bräunig, 2001b during their course of study of bilateral coupling of motor output to different mouthparts muscles in deafferented preparation described that in contrast to the legs, for the stable coordination of all mouthparts muscles movement sensory feedback is not essential. They concluded that during the evolutionary process which led to derived feature of mouthparts, central nervous network controlling these structures was also reconfigured accordingly.

4.3. Neurosecretory and neuromodulatory innervation:

All neuromuscular systems studied so far in locusts have innervation by various types of neurosecretory and neuromodulatory neurons. These neurons are located either in the central nervous system or in the periphery, and release a messenger that affects groups of neurons or effectors cells that have appropriate receptors. The act of neuromodulation unlike that of neurotransmission does not necessarily carry excitation or inhibition from one neuron to another, but instead changes the cellular or synaptic properties of certain neurons, so that neurotransmission between them is changed (Burrows, 1996). Among neuromodulators, the innervation of efferent dorsal unpaired medial neurons (DUM) and peripheral neurosecretory cells are well described. DUM neurons have been found to innervate muscles of legs (Hoyle, 1978), wings (Stevenson and Meuser, 1997), abdomen (Pflüger and Watson, 1988; Ferber and Pflüger, 1990), mouthparts (Bräunig, 1988) and antennae (Bräunig, *et al.* 1990; Allgäuer and Honegger, 1993). Their somata are located on the dorsal midline of the segmental ganglion of ventral nerve cord and axons project bilaterally into the peripheral nerves to innervate structures on both sides of the body. However, the brain of locust apparently has no segmental DUM neurons and appendages of head are innervated from DUM neurons located in the suboesophageal ganglion or from more posteriorly located ganglia (Bräunig, 1990 and 1991). In study here, backfilling of motor nerve branches to labral muscles partially stained 2 somata of suboesophageal ganglion DUM neurons. Although their exact morphology was not stained, but it seems these neurons are the members of DUM Sap 1, 2 and 7. Morphology of these three DUM neurons was previously described by backfilling of other brain nerves or by intracellular staining of individual neuron (Bräunig, 1990, 1991, 1997). According to Bräunig, DUM Sap1 and 2 ascend axons towards the brain and project into peripheral nerve of the brain such as frontal connectives, antennal nerves, the *nevus corporis cardiac III*, and the tritocerebral ventral nerve which innervates pharyngeal dilator muscles. While DUM Sap 7 was found to be exclusively projecting into the frontal connectives. In this context, future studies emphasizing on simultaneous intra-and extracellular recordings from DUM neurons of suboesophageal ganglion and motor nerve branches of labral muscles might reveal their exact number and nature. In study here, it is also very hard to establish the behavioural relevance of these neurons. However, all the DUM neurons studied so far have been described to release octopamine on terminals of motor neurons and skeletal muscles. Their exact role during specific behaviour has not been yet established but it is thought that they alter the performance of the muscles and their response to particular feature of their motor innervation (Burrows, 1996; Bräunig and Pflüger, 2001).

Does staining of no DUM neuron during backfilling of M1 motor nerve branches really imply the complete lack of their innervation? It is very hard to conclude, as axons of DUM neurons are very thin, it may be possible that due to long distance from periphery to the somata of these neurons, a tracer may fail to stain these neurons or simply axons might fail to take up the tracer due to their damages during dissection. On the other hand, M1 is

a small muscle and is innervated only by two motor neurons, and does not actively take part in the feeding behaviour. So it might not require fine control mechanism during behavioural orchestration. Hence simplicity of its nature and work imply that it might not be innervated by DUM neurons.

Apart from the innervation of segmentally located DUM neurons, some peripherally located neurosecretory cells have also been found to innervate skeletal muscles of insects (Finlayson and Osborne, 1968; Fifield and Finlayson, 1978; Swales, et al. 1992; Bräunig, 1998). These cells are present on the peripheral nerves and make varicose terminals on motor branches innervating the muscles and release various peptides into the haemolymph. During the course of tracing of motor nerve branches of labral muscles, such type of peripherally located neurons has also been observed. These cells form a small ganglion like structure which is attached anteriorly to the frontal ganglion. A large number of small thin fibers emerge from it and anastomosis with motor nerves innervating labral and foregut muscles (Fig. 3.8). These cells were not stained specifically and their neurosecretory nature could not be identified. But from their location and by comparing their branching pattern with extensive branches of cervical peripheral neurosecretory cells of crickets (Honegger, *et al.* 1988; Gracia-Scheible and Honegger, 1989), it might be assumed that these cells are neurosecretory in nature. It is also very hard to conclude about their possible role. Like the other peripheral neurosecretory cells, a general assumption of their function could be their usage in modulation of contraction and relaxation rates of muscles. However, specific staining of these neurons along with the muscles being innervated with antibodies raised against different neurotransmitters and peptides might reveal their exact nature and will shed light on their possible role during behaviour.

Another category of neurosecretory cells making neurohaemal network; satellite nervous system, was described in parallel in locust (Bräunig, 1987) and cockroach (Davis, 1987). It consists of three pairs of somata located in each half of suboesophageal ganglion. All these neurons show serotonin like immunoreactivity. Their axons establish an extensive network of neurohaemal terminals on periphery of nerves innervating mouthparts and labrum. During study here, in a number of stainings, a few cells of satellite nervous systems were weakly stained and their axons were visible in mandibular nerve. But failure of staining of all cells in a single preparation could be explained in the context of the inherent variability of peripheral branching pattern of the system, as all neurons do not project their axonal branch on every nerve innervating mouthparts and labrum (Bräunig, 1987). The second possibility may be the technical problem of backfilling technique as is discussed for DUM neuron innervation. However, in general our results are in accordance with findings of Schachtner and Bräunig, 1993. They investigated the activity pattern of satellite neurons by backfilling the labral medial nerve (LMN) with cobalt chloride, and found similar weak stainings in one out of six preparations only. They also discussed their role during behaviour and concluded satellite neurons become active during feeding behaviour and modulate the muscular and sensory systems involved in the orchestration of feeding behaviour.

4.4. Physiology of labral musculature:

Labrum is broad oval shaped structure hanging on the anterior of mandibles (Figure3.1). It is active during feeding behaviour and its movements are controlled by action of its anterior (M2) and posterior (M3) retractor muscles (Fig.3.2). During feeding, when mandibles are opened for a bite, contraction of anterior retractor muscles raises the labrum from the mandibles, and when mandibles are closed for chewing the food, contractions of posterior retractors close the labrum against the mandibles (Seath, 1977). In vivo preparations have also shown that labrum is active in close synchrony with the mandibular opening and closing movements (Rast and Bräunig, 2001b). But, morphology and physiology of neuronal entities controlling labral movements were still unknown. In study here, backfilling of motor nerve branches to labral muscles revealed large number of motor neurons in the tritocerebral lobe of the brain and the mandibular neuromere of

the suboesophageal ganglion. Physiological confirmation of existence of all anatomically described motor neurons could not verify during present study due to the necessity of massive dissection of the head capsule to expose the ganglia for intracellular recordings from all motor neurons in intact animal. Second, topography of the neurons did not allow intracellular recordings. Hence, physiological characterization of labral motor neurons into slow, intermediate and fast motor neurons was also not possible, as well described for leg motor neurons (Hoyle and Burrows, 1973; Wilson, 1979b; Phillips, 1980; Sasaki and Burrows, 1998; Nishino, 2003).

However, intracellular recording made from muscle fibers to know the spontaneity and synchrony of labral motor neurons in general supported our anatomical findings and showed commonalities of innervation pattern with other well studied neuromuscular systems of locust. We made intracellular recordings from muscles of both halves of the labrum. No postsynaptic potentials (PSPs) were elicited on probing the microelectrode into different fibers of a muscle. This finding was in accord to the previous studies that the isolated brain and suboesophageal ganglion preparations do not show spontaneous activity (Rast and Bräunig, 2001b). However, in a few preparations, spontaneous activities of some of the neurons were recorded. These recording showed that not all the anatomically identified neurons were firing spontaneously, and active units were firing at different rates. Spontaneous activity of neurons could be due to intrinsic membrane properties. But it seems less probable because PSPs of different firing units were summated, and implied they were centrally generated. Central propagation could be explained in the context of observed overlapping dendritic arborization of neurons which imply that they may receive input from a common source of driver interneurons. In this case, different intrinsic membrane properties of neurons innervating same muscles might cause them to fire at different rate and time, like the phenomenon observed in the neuromuscular systems of legs and spiracles of locust (Hoyle and Burrows, 1973; Wilson, 1979b; Burrows, 1978). It also seems to be true from the paired recordings of PSPs from right and left M2. These recording showed that PSPs occurring in one muscle were accompanied by PSPs occurring in second muscle. But their extended time scale analysis showed variation in latencies among PSPs of both M2, and at some occasions, a complete lack of corresponding PSPs was observed in one M2 trace (Fig. 3.24).

Paired intracellular recordings from M3 and M38 fibers revealed their complex innervation pattern but in general supported our anatomical findings. Simultaneous recording of PSPs from fibers of both muscles revealed that indeed some neurons specifically innervate M3 and M38. PSPs recorded from both muscles have not shown 1:1 correlation among active units. However, recording revealed that first phasic activity occurs in M38, then after a short delay, phasic activity occurs in M3 (Fig. 3.27). This may indicate that as mandibles start to close, at the same time motor neurons of M38 become active to open the mouth to enter food into the gut and after short while activity of motor neurons in M3 closes the labrum against the mandibles. However, to accept this functional explanation is very hard, because recording was made only from one preparation, and secondly there was no feeding related activity in semi-intact preparation. Most probably, it seems a mere chance that neurons controlling both muscles were active at similar time. But this could also happen due to the overlapping dendritic arborisation of motor neurons receiving common inputs but different innate properties of motor neurons cause them to fire at different rate and time. In second case, it might also possible that neurons receive independent input from two different sources of interneurons.

As in the starting section of this chapter was stated that innervation pattern seems to mark the compartmentalisation of muscles fibers receiving input from different types and number of motor neurons. Our physiological data confirms this assumption and shows labral muscle innervation is complex. First, PSPs of low, medium and high amplitudes were recorded from muscles fibers. Second, during the recording of PSPs, microelectrodes were probed into different muscle fibers but the activity of firing units could not be recorded from all of the fibers being probed. Third, recorded PSPs were summated that implied polyneuronal innervation of individual muscle fibers. These local

innervation features of labral muscles, revealed by recordings of PSPs, are comparable with other neuromuscular systems of locust, where various types of muscles are adapted to meet different functional requirements. In all these neuromuscular systems, three types of excitatory motor neurons (low, intermediate and fast) were found to innervate different units of a single muscle. Beside excitatory motor neurons, at least, one common or specific inhibitory neuron was also found to innervate the muscles. Only exception lies for mandibular muscles (Griss, 1990), which have no inhibitory innervation (see latter in discussion). Among these neuromuscular systems, the most extensively studied muscles are extensor and flexor tibiae muscles of hind leg (Hoyle and Burrows, 1973; Wilson, 1979b; Sasaki and Burrows, 1998; Theophilidis and Burns, 1983). Extensor tibiae is a large muscle and used for jumping. It receives innervation from 2 excitatory motor neurons (slow and fast) and one inhibitory motor neuron. On the basis of innervation, muscle body is divided into anterior and posterior region. Fast neuron innervates only anterior fibers of muscle while slow and inhibitory neurons innervate posterior fibers (Hoyle and Burrows, 1973; Theophilidis, 1983). On the other hand, flexor tibiae is smaller than its antagonistic extensor tibiae muscle in hind leg, and is innervated by a pool of nine excitatory (Sasaki and Burrows, 1998; Philips, 1980) and two inhibitory motor neurons (Hale and Burrows, 1985). Muscle body is divided into proximal, middle and distal parts. Each neuron in pool innervates only a restricted array of muscle fibers and none innervates throughout the muscle (Sasaki and Burrows, 1998). Although such details of innervation at ultra structural level of muscles have not been investigated during study here but our physiological data imply that future investigation utilizing extensive electrophysiological experiment and making recordings simultaneously from muscle fibers and neuronal somata might reveal the complexity lying under the innervation pattern at local level.

4.5. Absence of inhibitory innervation:

Hoyle, 1974 described that if skeletal muscles are innervated by 3 or more motor neurons then innervation pattern often include slow, fast and inhibitory motor neurons. Inhibitory motor neurons speed up the mechanical response of a muscle to changes in excitatory motor neuron discharge through the selective pre-and postsynaptic inhibition of slow motor neuron activity, and through its effect on the muscle fibers (Schmäh and Wolf, 2003). Thus common inhibitors facilitate rapid limb movements required during escape and defence behaviour. Intracellular recordings from labral muscle fibers revealed excitatory PSPs and none of them was inhibitory. This was in contrast to our anatomical findings that showed labral muscles were commonly innervated by suboesophageal ganglion motor neurons. Common motor neurons have also been found in motor systems controlling thoracic (Hale and Burrows, 1985; Burrows, 1973; Wolf, 1990; Watson, *et al.* 1985; Bräunig, *et al.* 2006), abdominal (Schmäh and Wolf, 2003) and antennal muscles (Bauer and Gewecke, 1990) of locust, and their electrophysiological studies showed that these neurons cause inhibitory PSPs, and have GABA like immunoreactivity. While simultaneous intracellular recordings made from somata of suboesophageal ganglion neurons and fibers of M2, M3 and M38 have not revealed any inhibitory input (Fig.3.29). However, Like a feature common to invertebrate motor neurons (Burrows, 1973), all recorded somata were inexcitable and invaded by attenuated spikes, evoked distantly in spike initiating zone. Each spike produced a twitch contraction in muscle fibers, and all PSPs correlating in 1:1 fashion with passive soma spike were excitatory and no inhibitory post synaptic potential (IPSP) was observed. This unique phenomenon of common excitatory post synaptic potential (CEPSPs) has not been found in any other neuromuscular system studied so far.

Absence of inhibitory input to labral muscles can be explained in the context of behavioural requirements. Labrum actives only during feeding behaviour and its movements are entrained by mandibular activity, and occur in close synchrony to mandible rhythmic movements (Seath, 1977; Rast and Bräunig, 2001b). Like other mouthparts, it does also not involve in the posture control behaviour and its movement

does not affect the position of the locust. This simplicity of action may imply lack of inhibitory input to labral muscles. However, question arises, why labral muscles have complex excitatory innervation? A simple answer to this question might be explained on the basis of fusion of two appendages. It seems, originally motor neurons were innervating only their respective appendages. During course of evolution, two appendages get fused, and rather changing central neuronal circuit, their axonal growth pattern in periphery get changed to cope the new functional requirements of the developing structure that might had demanded more force to lift fused structure.

On the basis of simplicity of action, lack of inhibitory input was also put forward for mandibular muscular system of *Manduca sexta* (Griss, 1990). In moth caterpillar, like locust, mandibular movements are controlled by closer and opener muscles. Both muscles are innervated by division of mandibular nerve. By cobalt backfilling of these nerves, Griss described 12 motor neurons for closer muscle and 8 for opener muscle in the mandibular neuromere. No motor neuron was common to both muscles. Intra- and extracellular recordings from both muscles were made during feeding behaviour or during electrical stimulation of the mandibular nerve or by directly depolarizing neuronal somata by penetrating microelectrode. All of the muscle fibers examined were of fast twitch type and none of the penetrated neuron was inhibitory. Further, no GABA like immunoreactive axons were found in mandibular nerve, and an assumption to the lack of inhibitory input to mandibular muscles was made on the basis of its simple pattern of movements and presence of only twitch type muscle fibers.

An assumption of lack of inhibitory inputs to the muscles, on the basis of simplicity of function, can also be explained by reduction in number of inhibitory motor neurons to antennal motor system. Both legs and antennae are part of reflex actions, e.g. Escape or avoidance behaviour, and faster movements are required to accomplish these behaviours. In such cases, inhibitory inputs to the muscles fibers increase their relaxation rate and provide basis to achieve greater velocity of movements. However, due to less functional complexity of antennae, only one inhibitory motor neuron innervates antennal muscles in comparison to the three inhibitory motor neurons of leg muscles. This number is conserved among all the insects studied so far, and it is assumed to reveal the evolutionary mechanism of specific neuromuscular control circuits (Baba and Comer, 2008). Hence, on the basis of results presented here, it may be assumed that during the course of evolution of labrum and mandibles, underlying inhibitory neuronal circuitry completely changed.

To accept this conclusion, at the present state of knowledge of physiology of labral muscles, is very hard. First, neurons were recorded only from one half of the suboesophageal ganglion and no neuron was recorded from the contralateral side. Second, intracellular stainings of recorded neurons showed similar morphology, and it is difficult to conclude whether recordings were made from both neurons or all recordings represent the activities of same single neuron. But, the number of six successful experiments made it less probable that each time same neuron was probed. However, future electrophysiological studies emphasizing the paired intracellular recording of two neurons in either half of the mandibular neuromere and simultaneously from labral muscle fibers might reveal the exact nature of their functions. Third, phenomenon of co-localization of neurotransmitter can also not be ruled out (Marder, 1999), and neurons with similar morphology may differ in release of their contents. For example, in locust, the innervation pattern of closer muscles of mesothoracic spiracles is to lesser extent similar to labral musculature. These muscles are innervated by branches of mesothoracic median nerve which have the axons of two motor neurons. Axons of these neurons bifurcate inside the medial nerve and innervate left and right spiracle muscles. Morphology of both neurons is similar but only differs in the contents of dense cored vesicle in their synaptic terminals, and represents the co-localization of neurotransmitter (Swales, *et al.* 1992). In this context, staining of labral muscle fibers, their nerves and neurons with antibody raised against GABA will further reveal the basic properties of neuromuscular transmission. Lastly, like the other body appendages, the possibility of

specific inhibitory neurons can also not be ruled out. But to find this feature, extensive electrophysiological studies are required that will utilize simultaneous intracellular recordings from individual soma and all fibers of a single muscle.

5. Conclusion:

The aim of present thesis was to investigate the innervation pattern of muscles of the labrum to decide whether it represents a structure that developed during the evolution by fusion of paired appendages associated with the intercalary segment. Our analysis of neuromuscular system of labrum in adult locust supports this notion by showing that the morphological and physiological features of motor neurons are comparable with those innervating other body appendages. For example, the number and the size of somata are in the same range as for all other body appendages. Their motor pattern is centrally generated and many of the neurons receive common synaptic input. Intracellular recordings from muscle fibers shows that all PSPs are excitatory and individual muscle fibers are polyneuronally innervated. However, excitatory motor neurons do not provide any surprises; there are clear differences between the innervation of the labrum and other appendages. First, we could not find any evidence for inhibitory innervation. Second, there are common excitatory motor neurons. These obvious differences are regarded as evolutionary implication for this highly derived structure, hypothesized as composed of pair of appendages associated with the intercalary segment. Arguments in the support of this hypothesis are presented in the proceeding discussion.

5.1. Sequence of labral muscles:

According to the defining criterion of a segment, each body segment also has pair of appendages and their accompanying musculature. Likewise labrum has 3 pairs of bilaterally symmetrical muscles. Snodgrass, 1935 tried to homologize the structures on basis of musculature but left many of the controversial points that are still unsettled. In general, to draw homology among the muscles of different body appendages is very difficult. Because appendages may get lost during evolution or adapted to a new shape to meet environmental constrains. As a consequence, homologous muscles can change their articulation and function. Similarly, origin or insertion ends of a muscle may shift to a new place and completely differ from its original connection. Finally, a muscle may span to more than one segment, and in this case, it also becomes difficult to know its original segmental affiliation. In case of labrum, muscle homology is further limited by the difficulty to identify that from which part of an appendage it was derived. Boyan *et al.* 2002 described that it represents coxal and trochanter part of an appendage. Haas *et al.* 2001a considered it as fusion of only endites of coxal part. Kukalova-Peck, 1998 stated that it represents subcoxa, coxa and trochanter of an appendage. But, beside all of these complications, arrangement of muscles in each half of the labrum indicates originally there were two separate appendages with bilaterally symmetrical sets of muscles and during evolution, these appendages get fused. Second, lack of active participation of M1 in moving the labrum also supports the notion of fusion of appendages by retaining its original position but losing its role in appendage movements.

5.2. Innervation pattern:

Our data also shows that motor innervation pattern is in accordance with symmetrical arrangements of three sets of muscles. First, labral muscles are innervated from both sides of central nervous system. Second, innervation pattern is bilaterally symmetric as that of other appendages. There are two symmetrical sets of motor neurons located in each half of the tritocerebral and mandibular neuromeres. But the conspicuous feature differentiating these motor neurons is that their axons cross the midline in periphery to innervate both ipsi- and contralateral muscles. Axons of motor neurons innervating M1 divide at midline in periphery close to the muscles. Axons of motor neurons innervating M2 cross midline by using a unique peripheral M2-commissure, located between both muscles. While axons of motor neurons located in mandibular neuromere cross the midline by using frontal ganglion as a commissure.

Peripheral crossing of midline of motor axons has not been found in any of the neuromuscular system studied so far in the insects. Only few examples lie where motor axons have been shown to cross the midline inside the ganglion but not in the periphery. In locust, thoracic and abdominal dorsal and ventral longitudinal muscles are innervated by two groups of motor neurons. With respect to the muscle being innervated, somata of one group are located in the next anterior ganglion while of other are located in segment specific ganglion. Two of the segment specific motor neurons have unusual morphology. Their somata are located contralateral to the muscle they innervate and primary neurites cross the midline inside the ganglion, and exit as an axon in the most anterior contralateral peripheral nerve (Kutsch and Heckman, 1995a, b; Steffens and Kutsch, 1995). Homologs of these motor neurons innervating neck region muscles also have similar morphology (Honegger, *et al* 1984). Some neurosecretory neurons releasing crustacean cardioactive peptide have also contralaterally projecting somata, and occur with similar segmental branching pattern in all neuromere from suboesophageal ganglion to the seventh abdominal ganglion (Dirksen, *et al.* 1991; Breidbach and Dirksen, 1991). Motor neurons of thoracic spiracle muscles innervate both ipsi-and contralateral muscles (Swales *et al.* 1992; Burrows, 1982). These muscles are innervated by branches of thoracic median nerves. Motor neurons project their axons into the median nerve and immediately divide into two branches near the ganglion to innervate right and left spiracle muscles.

Thus, unique innervation pattern destined for labral muscles supports the idea that the labrum derives from fused appendages, and indicates, during the evolution of labrum, its motor innervation pattern was reconfigured in the periphery while original bilateral sets of central neurons remained unchanged.

5.3. Appendage of intercalary segment:

If labrum is an appendage then it must belong to a segment. But its segmental affiliation was controversial among various workers. Eastham, 1930; Roonwal, 1939; Rempel and Church, 1971; Repel, 1975 and Scholtz, 2001 described labrum as fused appendage of first head segment, secondarily innervated by the tritocerebrum. According to these authors, the tritocerebrum had shifted from posterior to preoral position. Ferris, 1942 and Henry, 1947 regarded the labrum as a complete segment, innervated primarily from the tritocerebrum which had shifted phylogenetically posteriorly. However, Butt, 1960 concluded the labrum as highly modified appendage of intercalary segment and is innervated from the tritocerebrum. By maintaining the neuraxes as reference point, Boyan *et al.* 2002 analysed expression pattern of segmental polarity gene; *engrailed (en)*, in the brain of 30% embryo of locust. They described that head consists of six segments, topologically arranged from anterior to posterior as follows; ocular, antennal, intercalary, mandibular, maxillary and labial segments housing protocerebrum, deutocerebrum, tritocerebrum, mandibular, maxillary and labial as their neuromeres respectively. Further, following the HRP immunoreactivity, it was shown that from each embryonic neuromere a segmental nerve runs in a corresponding homologous series to innervate eye, antennae, labrum, mandible, maxillae and labium. Thus, during the embryonic development, topologically the labrum is located posterior to the antennae and anterior to the mandible, and is innervated from the tritocerebrum. In accordance to this embryonic head segmentation model, present analysis of motor innervation of adult labrum also shows motor neurons only in the tritocerebrum and the mandibular neuromere of the suboesophageal ganglion. Both the tritocerebrum and the mandibular neuromere are considered as a neuromere of intercalary segment, (Doe and Goodman, 1985; Zacharias *et al.*, 1993; Urbach *et al.* 2003, also see latter discussion).

Our findings reject the previous studies implying the labrum as part of stomatogastric system and innervated from fontal ganglion (see review, Bitsch and Bitsch, 2010). Snodgrass, 1960 stated tritocerebral innervation of locust labrum is sensory and its musculature is innervated from fontal ganglion. By making cobalt infusion of nerves of frontal ganglion in cockroach, Gundel and Penzlin, 1978 also stated that labrum is

innervated from frontal ganglion. In study here, we could not confirm any of the statements presented by these authors. Backfilling of specific motor nerve branch to labral muscles did not stained a single neuron in any part of the stomatogastric nervous system.

Rempel, 1975 studied the embryonic development of *Lytta viridana*, and stated labrum is a fused pair of appendages affiliated to first head segment. The neuromere of this segment was the prosocerebrum, consisted of protocerebral bridge and central complex. This conclusion was made on the basis that central complex and protocerebral bridge are absent in annelids and present only in arthropods. Rempel described that the original mode of the innervation of labrum was via nervus connectivus, frontal ganglion and nervus procurrens (N4 of Gundel and Penzlin, 1978), and innervation via the labral nerve was secondary acquisition. But recent immunocytochemical investigation of the brain of polychaete worm by Heuer *et al.* 2010 described a mid line neuropile equivalent to the arthropod central complex. Second, nervous connectivus has been found only in a few species of Heimetabolous insects such as cockroach (Gundel and Penzlin, 1978) and cricket (Kirby *et al.* 1984). Nervous connectivus connects medio-dorsal region of fontal ganglion with protocerebrum. Cobalt infusion of nervus connectivus stained two somata in the protocerebrum. Their axons arborize in the neuropile of frontal ganglion. Inside the neuropile, each axon divides into three branches. One branch runs off posteriorly into the nervus recurrens and other two run anteriorly towards the fontal connectives. Branches running into the frontal connective penetrate the anterior surface of the tritocerebrum and arborize in the tritocerebral neuromere. During course of tracing of motor nerves to labral nerves, we could not find any nerve like nervus connectivus. Therefore it is considered that nervus connectivus is an autapomorphic feature of cockroach and cricket brains only. Second, if it was the original mode of innervation of clypeolabral complex then retrograde fillings should at least show some motor neurons in the protocerebrum. But during our study, no neuron was stained in the protocerebrum. Hence, it seems illogical that despite the presence of both labrum and so called its neuromere prosocerebrum; labral innervation lost its original mode during evolution and secondarily gets innervated from the tritocerebrum.

Present findings of motor neurons in the tritocerebrum and the mandibular neuromere are also in accord to the early neurogenesis of the insect brain. These embryonic studies supports to the splitting of the intercalary neuromere, and compliments tritocerebrum and anterior of mandibular neuromere as a neuromere of intercalary segment. In insect embryo, nervous system arises from a bilateral sheet of cells called the neuroectoderm. From this neuroectoderm, neuronal stem cells; the neuroblasts (NBs) develop. Neuroblasts divide asymmetrically to generate a chain of ganglion mother cells, each of which then divides symmetrically to produce a pair of postmitotic sibling neurons. Doe and Goodman, 1985 studied the neurogenesis of suboesophageal, thoracic and abdominal segments in *Schistocera americana*, and described that most of the segments have 25-30 NBs in each hemiganglion, arranged in rows of from 2-5 NBs and one median NB. They observed four NBs groups in suboesophageal ganglion, and named them as S0 to S3. According to them, S2 and S3 were following typical number and pattern of NBs while the anterior most segments, S0 and S1 were having reduced number of both types of neuronal precursor cells. There were 13 NBs in a hemisegment of S0 and their arrangement did not resemble a particular portion of the typical segmental portion. Latter on Zacharias, *et al.* 1993 studied the neurogenesis of the brain in *Schistocera gregaria*, and described 130 NBs in each brain hemisphere at 30-40% embryonic stage. According to these authors, during early neurogenesis, NBs generate their progeny through the mechanism similar to those that occur in the segmental ganglion, and complex mature brain derives from a simple and stereotyped set of neuronal precursor cells and their number is not much larger than the total numbers of NBs and midline precursors found in the three thoracic ganglia. They found 86 NBs in the protocerebrum, 32 NBs in the deutocerebrum and only 12 NBs in the tritocerebrum. By comparing the brain NBs numbers with that described by Doe and Goodman, 1985, they concluded that three

gnathal as well as posterior segments clearly have their own well defined neuromeres, each consisting of 24-30 segmentally homologous neuroblasts. While 12 NBs of the tritocerebrum do not have typical segmental pattern like the 13 NBs of S0 group anterior to mandibular neuromere S1. They suggested that each hemisphere of the intercalary segment first comprised of 25 neuroblast, which later become segregated into the tritocerebral group and S0 group due to gut invagination. Urbach *et al.* 2003 studied the segmental composition of embryonic brain in *Tenebrio molitor* by examining the *engrailed* (*en*) expression pattern in the head ectoderm and in the deriving components of the central nervous system, and provided a detailed description of spatial and temporal pattern of the brain neuroblasts during 18-60% of embryonic development. They identified 125 NBs in each brain hemisphere at about 40% of embryonic development, and observed that in contrast to the remaining parts of the brain, the number of tritocerebral NBs becomes diminished from about 21 NBs at 35% stage to about 13 NBs at 40% stage. They further described that with the formation of connective between the brain and suboesophageal ganglion, part of neuronal cells deriving from *engrailed* positive tritocerebral NBs become displaced and secondarily fused with most anterior part of suboesophageal ganglion.

Hence, in the light of arguments presented above caution seems warranted in inferring that the labrum is a fused pair of appendages of the intercalary segment, and is innervated by its own neuromere; the tritocerebrum, which splits off in two parts during development due to invagination of the gut. The anterior part becomes fused with other brain neuromere while the posterior part makes the anterior part of mandibular neuromere. Secondly, innervation pattern indicated that during the evolution of labrum, the motor innervation pattern was reconfigured in the periphery, while the original bilateral sets of central neurons remained unchanged.

6. Summary:

Major animal taxa, known as phyla, each represents a basic bauplan. Among the diversity of phyla, arthropods are the most dominant on the earth. The conspicuous feature of the arthropod bauplan is the grouping of body segments into specialized units by the phenomenon of tagmosis which in insect has given rise to three body regions; head, thorax and abdomen. But the number and the nature of segments involved in composition of the insect head is still a matter of dispute among today's evolutionary biologists. From the beginning of the dispute, there was general agreement that three mouthparts segments (mandible, maxillae, and labium) take part in the head composition, and their ganglia fuse to form the suboesophageal ganglion of the insect nervous system. However, the nature of the segments anterior to the mandible (labral/ocular, antennal, and intercalary segments) remained controversial. Modern molecular, palaeontological, and neuroanatomical studies showed that the insect head is composed of six segments; ocular, antennal, intercalary, and three gnathal segments. But conflicting views are still present regarding the nature and segmental affiliation of the insect labrum. Several such modern studies imply that the labrum is a highly modified appendage of the intercalary segment, and sensory innervation of the embryonic and the adult labrum shares many similarities with that of head and thoracic appendages. However, defining criterion of an appendage implies that every appendage must be innervated by its own segmental ganglion, and the innervation pattern must include both sensory and motor elements. The aim of thesis is to investigate the motor innervation pattern of muscles of the labrum in the adult locust to reveal the evolutionary changes underlying neuronal circuitry, which might help to decide whether the labrum represents a structure that has developed during the evolution by fusion of paired appendages associated with the intercalary segment.

Using Neurobiotin as a retrograde neuronal tracer, specific motor nerves of individual labral muscles were stained. Results show that all labral muscles receive innervation from both the tritocerebral lobes of the brain and the suboesophageal ganglion, except for M1, the labral compressor muscle. M1 is innervated by two motor neurons. Both tritocerebral lobes contain one soma. The axons of both neurons branch in the periphery to innervate ipsi- and contralateral muscles. The labral anterior retractor muscles, M2, are innervated by 6 tritocerebral motor neurons, with 3 somata located in each tritocerebral lobe. Their axons cross the midline in a distinct commissure between the two muscles. The labral posterior retractor muscles, M3 and anterior dilator muscles of foregut, M38, are innervated from the ipsilateral tritocerebrum only. Both muscles together receive 8 motor axons and there are some common motor neurons that innervate both muscles. In addition, M2, M3 and M38 also receive common innervation from neurons located in the suboesophageal ganglion (SOG). In relation to the muscle, their somata are located on the ipsi- and the contralateral sides of the SOG. Their axons ascend through the circumoesophageal connectives and proceed into the frontal connectives without forming ramifications in the tritocerebral lobes. These axons also cross the midline in the periphery to reach muscles on both sides of the head. They either cross within the commissure between muscles M2, or through the frontal ganglion. Further more, electrophysiology of labral muscles in isolated insect heads was investigated by intracellular recordings from the fibers of individual muscles. The recordings showed that all postsynaptic potentials were excitatory and no inhibitory synaptic inputs to labral muscles were found during the present study. Similarly simultaneous intracellular recording from fibers of labral muscles and suboesophageal ganglion motor neurons also revealed no inhibitory synaptic inputs to labral muscles, and showed that suboesophageal neurons are common excitatory motor neurons.

The innervation pattern was compared with that of the other body appendages of locust, and it was concluded that labral muscles are innervated from both sides of the CNS and their innervation pattern is bilaterally symmetric as that of other appendages.

The participation of both tritocerebral and suboesophageal ganglion motor neurons supports the notion that the labrum is innervated by the so-called intercalary segment. The innervation pattern also supports the idea that the labrum derives from fused appendages: There are two symmetrical sets of motor neurons. Some of them cross the midline in the periphery. This indicates that during the evolution of the labrum its motor innervation pattern was reconfigured in the periphery, while the original bilateral sets of central neurons remained unchanged.

7. References:

- Abbott, M. K. & Kaufman, T. C. (1986). The relationship between the functional complexity and the molecular organization of the *Antennapedia* locus of *Drosophila melanogaster*. *Genetics*, 114, 919-942.
- Abzhanov, A. & Kaufman, T. (2004). Hox gene and tagmatization of the higher Crustacea. In G.Scholtz (Ed.), *Evolutionary developmental biology of crustacea* (pp. 43-74). Balkema, Lisse.
- Abzhanov, A. & Kaufman, T. C. (1999). Homeotic genes and the arthropod head: Expression patterns of the *labial*, *proboscipedia*, and *deformed* genes in crustaceans and insects. *Proceedings of the National Academy of Sciences of the United States of America*, 96, 10224-10229.
- Aguinaldo, A. M. A., Turbeville, J. M., Linford, L. S., Rivera, M. C., Garey, J. R., Raff, R. A. et al. (1997). Evidence for a clade of nematodes, arthropods and other moulting animals. *Nature*, 387, 489-493.
- Allgäuer, C. & Honegger, H. W. (1993). The antennal motor system of crickets - modulation of muscle contractions by a common Inhibitor, DUM Neurons, and proctolin. *Journal of Comparative Physiology A-Sensory Neural and Behavioral Physiology*, 173, 485-494.
- Altman, J. S. & Kien, J. (1979). Subesophageal neurons involved in head movements and feeding in locusts. *Proceedings of the Royal Society of London Series B-Biological Sciences*, 205, 209-227.
- Anderson, D. T. (1973). *Embryology and Phylogeny in Annelids and Arthropods*. Pergamon Press, Oxford.
- Arias, A. M., Baker, N. E., & Ingham, P. W. (1988). Role of segment polarity genes in the definition and maintenance of cell states in the *Drosophila* embryo. *Development*, 103, 157-170.
- Aubele, E. & Klemm, N. (1977). Origin, destination and mapping of tritocerebral neurons of locust. *Cell and Tissue Research*, 178, 199-219.
- Ayali, A., Zilberstein, Y., & Cohen, N. (2002). The locust frontal ganglion: a central pattern generator network controlling foregut rhythmic motor patterns. *Journal of Experimental Biology*, 205, 2825-2832.
- Baba, Y. & Comer, C. M. (2008). Antennal motor system of the cockroach, *Periplaneta americana*. *Cell and Tissue Research*, 331, 751-762.
- Baines, R. A., Lange, A. B., & Downer, R. G. H. (1990). Proctolin in the innervation of the locust mandibular closer muscle modulates contractions through the elevation of inositol trisphosphate. *Journal of Comparative Neurology*, 297, 479-486.
- Baker, N. E. (1987). Molecular cloning of sequences from *wingless*, a segment polarity gene in *Drosophila* - the spatial distribution of a transcript in embryos. *Embo Journal*, 6, 1765-1773.

-
- Bauer, C. K. & Gewecke, M. (1991). Motoneuronal control of antennal muscles in *Locusta migratoria*. *Journal of Insect Physiology*, 37, 551-562.
- Bitsch, J. & Bitsch, C. (2010). The tritocerebrum and the clypeolabrum in mandibulate arthropods: segmental interpretations. *Acta Zoologica*, 91, 249-266.
- Bowerman, R. F. & Burrows, M. (1980). The morphology and physiology of some walking leg motor neurons in a Scorpion. *Journal of Comparative Physiology*, 140, 31-42.
- Boyan, G. S., Bräunig, P., Posser, S., & Williams, J. L. D. (2003). Embryonic development of the sensory innervation of the clypeo-labral complex: further support for serially homologous appendages in the locust. *Arthropod Structure & Development*, 32, 289-302.
- Boyan, G. S., Williams, J. L. D., Posser, S., & Bräunig, P. (2002). Morphological and molecular data argue for the labrum being non-apical, articulated, and the appendage of the intercalary segment in the locust. *Arthropod Structure & Development*, 31, 65-76.
- Bräunig, P. (1985). Mechanoreceptive neurons in an insect brain. *Journal of Comparative Neurology*, 236, 234-240.
- Bräunig, P. (1987). The satellite nervous system - An extensive neurohemal network in the locust head. *Journal of Comparative Physiology A-Sensory Neural and Behavioral Physiology*, 160, 69-77.
- Bräunig, P. (1988). Identification of a single prothoracic dorsal unpaired median (DUM) neuron supplying locust mouthpart nerves. *Journal of Comparative Physiology A-Sensory Neural and Behavioral Physiology*, 163, 835-840.
- Bräunig, P. (1990). The morphology of subesophageal ganglion cells innervating the nervus corporis cardiaci-III of the locust. *Cell and Tissue Research*, 260, 95-108.
- Bräunig, P. (1991). Subesophageal DUM neurons innervate the principal neuropils of the locust brain. *Philosophical Transactions of the Royal Society of London Series B-Biological Sciences*, 332, 221-240.
- Bräunig, P. (1997). The peripheral branching pattern of identified dorsal unpaired median (DUM) neurones of the locust. *Cell and Tissue Research*, 290, 641-654.
- Bräunig, P. (1998). Networks of neurosecretory (neurohemal) endings. In Locke, M. (Ed.), *Insecta* (11b ed., pp. 539-549). New York: Wiley-Liss.
- Bräunig, P. (2008). Neuronal connections between central and enteric nervous system in the locust, *Locusta migratoria*. *Cell and Tissue Research*, 333, 159-168.
- Bräunig, P., Allgäuer, C., & onegger, H. W. (1990). Subesophageal DUM neurons are part of the antennal motor system of locusts and crickets. *Experientia*, 46, 259-261.
- Bräunig, P. & Pflüger, H. J. (2001). The unpaired median neurons of insects. *Advances in Insect Physiology*, Vol 28, 28, 185-266.
-

-
- Bräunig, P., Schmäh, M., & Ioff, H. (2006). Common and specific inhibitory motor neurons innervate the intersegmental muscles in the locust thorax. *Journal of Experimental Biology*, 209, 1827-1836.
- Breidbach, O. & Dirksen, H. (1991). Crustacean cardioactive peptide immunoreactive neurons in the ventral nerve cord and the brain of the meal beetle *Tenebrio molitor* during postembryonic development. *Cell and Tissue Research*, 265, 129-144.
- Brook, W. J. & Cohen, S. M. (1996). Antagonistic interactions between *Wingless* and *decapentaplegic* responsible for dorsal-ventral pattern in the *Drosophila* leg. *Science*, 273, 1373-1377.
- Brusca, R. C. & Brusca, G. J. (2003). *Invertebrates*. (2nd ed.) Sinauer Associates, Inc. 461-700pp.
- Budd, G. E. (2002). A palaeontological solution to the arthropod head problem. *Nature*, 417, 271-275.
- Budd, G. E. & Telford, M. J. (2009). The origin and evolution of arthropods. *Nature*, 457, 812-817.
- Burrows, M. (1973). Physiological and morphological properties of metathoracic common inhibitory neuron of locust. *Journal of Comparative Physiology*, 82, 59-78.
- Burrows, M. (1975). Monosynaptic connections between wing stretch receptors and flight motoneurons of locust. *Journal of Experimental Biology*, 62, 189-219.
- Burrows, M. (1978). Sources of variation in output of locust spiracular motoneurons receiving common synaptic driving. *Journal of Experimental Biology*, 74, 175-186.
- Burrows, M. (1982). The physiology and morphology of median nerve motor neurons in the thoracic ganglia of the locust. *Journal of Experimental Biology*, 96, 325-341.
- Burrows, M. (1996). *The Neurobiology of an Insect Brain*. Oxford University Press, Oxford.
- Burrows, M. & Hoyle, G. (1973). Neural mechanisms underlying behavior in locust *Schistocerca gregaria* III. Topography of limb motoneurons in metathoracic ganglion. *Journal of Neurobiology*, 4, 167-186.
- Butt, F. H. (1957). The role of the premandibular or intercalary segment in head segmentation of insects and other arthropods. *Transaction of the American Entomological Society*, 83, 1-30.
- Butt, F. H. (1960). Head Development in the Arthropods. *Biological Reviews of the Cambridge Philosophical Society*, 35, 43-91.
- Chapman, R. F. (1998). *The insects: Structure and function*. (4th ed.) Cambridge university press, Cambridge.
- Chen, J. Y., Waloszek, D., & Maas, A. (2004). A new 'great-appendage' arthropod from the lower cambrian of China and homology of chelicerate chelicerae and raptorial antero-ventral appendages. *Lethaia*, 37, 3-20.

-
- Chipman, A. D., Arthur, W., & Akam, M. (2004). Early development and segment formation in the centipede, *Strigamia maritima* (Geophilomorpha). *Evolution & Development*, 6, 78-89.
- Clements, A. N. & May, T. E. (1974). Studies on locust neuromuscular physiology in relation to glutamic acid. *Journal of Experimental Biology*, 60, 673-705.
- Cohen, S. & Jürgens, G. (1991). *Drosophila* headlines. *Trends in Genetics*, 7, 267-272.
- Cohen, S. M. (1990). Specification of limb development in the *Drosophila* embryo by positional cues from segmentation genes. *Nature*, 343, 173-177.
- Damen, W. G. (2002). Parasegmental organization of the spider embryo implies that the parasegment is an evolutionary conserved entity in arthropod embryogenesis. *Development*, 129, 1239-1250.
- Damen, W. G., Hausdorf, M., Seyfarth, E. A., & Tautz, D. (1998). A conserved mode of head segmentation in arthropods revealed by the expression pattern of Hox genes in a spider. *Proceedings of the National Academy of Sciences of the United States of America*, 95, 10665-10670.
- Davis, N. T. (1987). Neurosecretory neurons and their projections to the serotonin neurohemal system of the cockroach *Periplaneta americana* (L), and identification of mandibular and maxillary motor neurons associated with this system. *Journal of Comparative Neurology*, 259, 604-621.
- Dewel, R. A. & Dewel, W. C. (1996). The brain of *Echiniscus viridissimus* Peterfi, 1956 (Heterotardigrada): A key to understanding the phylogenetic position of tardigrades and the evolution of the arthropod head. *Zoological Journal of the Linnean Society*, 116, 35-49.
- Diaz-Benjumea, F. J., Cohen, B., & Cohen, S. M. (1994). Cell interaction between compartments establishes the proximal-distal axis of *Drosophila* legs. *Nature*, 372, 175-179.
- Diederich, R. J., Pattatucci, A. M., & Kaufman, T. C. (1991). Developmental and evolutionary implications of *labial*, *deformed* and *engrailed* expression in the *Drosophila* head. *Development*, 113, 273-281.
- Dinardo, S., Kuner, J. M., Theis, J., & Ofarrell, P. H. (1985). Development of embryonic pattern in *Drosophila melanogaster* as revealed by accumulation of the nuclear *engrailed* protein. *Cell*, 43, 59-69.
- Dirksen, H., Muller, A., & Keller, R. (1991). Crustacean cardioactive peptide in the nervous system of the locust, *Locusta migratoria* : An immunocytochemical study on the ventral nerve cord and peripheral innervation. *Cell and Tissue Research*, 263, 439-457.
- Doe, C. Q. & Goodman, C. S. (1985). Early events in insect neurogenesis .1. Development and segmental differences in the pattern of neuronal precursor cells. *Developmental Biology*, 111, 193-205.
- Dong, Y. & Friedrich, M. (2005). Comparative analysis of *wingless* patterning in the embryonic grasshopper eye. *Development Genes and Evolution*, 215, 177-197.
-

- Dove, H. & Stollewerk, A. (2003). Comparative analysis of neurogenesis in the myriapod *Glomeris marginata* (Diplopoda) suggests more similarities to chelicerates than to insects. *Development*, 130, 2161-2171.
- Duporte, E. M. (1957). The comparative morphology of the insect head. *Annual Review of Entomology*, 2, 55-70.
- Dürr, V., König, Y., & Kittmann, R. (2001). The antennal motor system of the stick insect *Carausius morosus* : anatomy and antennal movement pattern during walking. *Journal of Comparative Physiology A-Neuroethology Sensory Neural and Behavioral Physiology*, 187, 131-144.
- Eastham, L. E. S. (1930). The embryology of *Pieris rape* - Organogeny. *Philosophical Transactions of the Royal Society B-Biological Sciences*, 219, 1-50.
- Eriksson, B. J. & Budd, G. E. (2000). Onychophoran cephalic nerves and their bearing on our understanding of head segmentation and stem group evolution of Arthropoda. *Arthropod Structure & Development*, 29, 197-209.
- Eriksson, B. J., Tait, N. N., & Budd, G. E. (2003). Head development in the onychophoran *Euperipatoides kanangrensis* with particular reference to the central nervous system. *Journal of Morphology*, 255, 1-23.
- Eriksson, B. J., Tait, N. N., Budd, G. E., Janssen, R., & Akam, M. (2010). Head patterning and Hox gene expression in an onychophoran and its implications for the arthropod head problem. *Development Genes and Evolution*, 220, 117-122.
- Farris, S. M. & Strausfeld, N. J. (2003). A unique mushroom body substructure common to basal cockroaches and to termites. *Journal of Comparative Neurology*, 456, 305-320.
- Ferber, M. & Pflüger, H. J. (1990). Bilaterally projecting neurons in pregenital abdominal ganglia of the Locust : Anatomy and peripheral targets. *Journal of Comparative Neurology*, 302, 447-460.
- Ferris, G. F. (1942). Some observations on the head of insects. *Microentomology*, 7, 25-62.
- Ferris, G. F. (1943). The basic materials of the insect cranium. *Microentomology*, 8, 8-24.
- Fifield, S. M. & Finlayson, L. H. (1978). Peripheral neurons and peripheral neurosecretion in stick insect, *Carausius morosus*. *Proceedings of the Royal Society of London Series B-Biological Sciences*, 200, 63-85.
- Finlayson, L. H. & Osborne, M. P. (1968). Peripheral neurosecretory cells in stick insect (*Carausius morosus*) and blowfly larva (*Phormia terraenovae*). *Journal of Insect Physiology*, 14, 1793-1801.
- Fleig, R. (1994). Head segmentation in the embryo of the colorado Beetle *Leptinotarsa decemlineata* as seen with anti-*en* immunostaining. *Roux's Archives of Developmental Biology*, 203, 227-229.
- Folsom, J. W. (1899). The segmentation of the insect head. *Psyche*, 280, 391-394.

-
- Garcia-Scheible, I. & Honegger, H. W. (1989). Peripheral neurosecretory cells of insects contain a neuropeptide with Bursicon-like activity. *Journal of Experimental Biology*, 141, 453-459.
- Gewecke, M. (1979). Central projection of antennal afferents for the flight motor in *Locusta migratoria* (Orthoptera, Acrididae). *Entomologia Generalis*, 5, 317-320.
- Giribet, G. (2003). Molecules, development and fossils in the study of metazoan evolution; Articulata versus Ecdysozoa revisited. *Zoology*, 106, 303-326.
- Goodrich, E. S. (1897). On the relation of the arthropod head to the annelid prostomium. *Quarterly Journal Of Microscopical Science*, 40, 247-268.
- Grimaldi, D. & Engel, M. S. (2005). Arthropods and the Origin of Insects. In *Evolution of the Insects* (1st ed., pp. 93-118). Cambridge University Press, Cambridge.
- Griss, C. (1990). Mandibular motor neurons of the caterpillar of the Hawk moth *Manduca sexta*. *Journal of Comparative Neurology*, 296, 393-402.
- Gundel, M. & Penzlin, H. (1978). Neuronal connections of frontal ganglion of cockroach *Periplaneta americana* - Histological and iontophoretical study. *Cell and Tissue Research*, 193, 353-371.
- Gwilliam, G. F. & Burrows, M. (1980). Electrical characteristics of the membrane of an identified insect motor neuron. *Journal of Experimental Biology*, 86, 49-61.
- Haas, M. S., Brown, S. J., & Beeman, R. W. (2001a). Homeotic evidence for the appendicular origin of the labrum in *Tribolium castaneum*. *Development Genes and Evolution*, 211, 96-102.
- Haas, M. S., Brown, S. J., & Beeman, R. W. (2001b). Pondering the procephalon: the segmental origin of the labrum. *Development Genes and Evolution*, 211, 89-95.
- Hale, J. P. & Burrows, M. (1985). Innervation patterns of inhibitory motor neurons in the thorax of the Locust. *Journal of Experimental Biology*, 117, 401-413.
- Hanström, B. (1928). *Vergleichende anatomie des nervensystems der wirbellosen tiere unter besonderer berücksichtigung seiner funktion*. Springer, Berlin. 628pp.
- Harzsch, S. (2006). Neurophylogeny: Architecture of the nervous system and a fresh view on arthropod phylogeny. *Integrative and Comparative Biology*, 46, 162-194.
- Harzsch, S. & Waloszek, D. (2000). Serotonin-immunoreactive neurons in the ventral nerve cord of Crustacea: a character to study aspects of arthropod phylogeny. *Arthropod.Struct.Dev.*, 29, 307-322.
- Henry, L. M. (1947). The nervous system and the segmentation of the head in the Annelata. *Microentomology*, 12, 65-110.
- Henry, L. M. (1947). The nervous system and the segmentation of the head in the Annelata. *Microentomology*, 13, 1-48.
- Heuer, C. M. (2010). *Comparative Neuroanatomy within the context of deep Metazoan Phylogeny*. Ph.D Thesis. RWTH Aachen, Germany.
-

-
- Heuer, C. M., Muller, C. H. G., Todt, C., & Loesel, R. (2010). Comparative neuroanatomy suggests repeated reduction of neuroarchitectural complexity in Annelida. *Frontiers in Zoology*, 7, 1-21.
- Heymons, R. (1901). *Die Entwicklungsgeschichte der Scolopender*. Verlag E. Nägele, Stuttgart.
- Holmgren, N. (1916). Zur vergleichenden anatomie des gehirns von Polychaeten, Onychophoren, Xiphosuren, Arachniden, Crustaceen, Myriapoden und Insekten. *Kungliga Svenska Vetenskapsakademiens Handlingar, Stockholm*, 56, 1-303.
- Honegger, H. W., Allgäuer, C., Klepsch, U., & Welker, J. (1990). Morphology of antennal motoneurons in the brains of two crickets, *Gryllus bimaculatus* and *Gryllus campestris*. *Journal of Comparative Neurology*, 291, 256-268.
- Honegger, H. W., Altman, J. S., Kien, J., Mullertautz, R., & Pollerberg, E. (1984). A comparative study of neck muscle motor neurons in a cricket and a locust. *Journal of Comparative Neurology*, 230, 517-535.
- Honegger, H. W., Bruninger, B., Bräunig, P., & Elekes, K. (1990). GABA-like immunoreactivity in a common inhibitory neuron of the antennal motor system of crickets. *Cell and Tissue Research*, 260, 349-354.
- Hoyle, G. (1955). The anatomy and innervation of locust skeletal muscle. *Proceedings of the Royal Society of London Series B-Biological Sciences*, 143, 281-292.
- Hoyle, G. (1974). Neuronal control of skeletal muscle. In K. Rockstein (Ed.), *The physiology of insecta* (pp. 175-236). Academic Press, New York.
- Hoyle, G. (1978). Dorsal, unpaired, median neurons of locust metathoracic ganglion. *Journal of Neurobiology*, 9, 43-57.
- Hoyle, G. & Burrows, M. (1973). Neural mechanisms underlying behavior in locust *Schistocerca gregaria* .I. Physiology of identified motoneurons in metathoracic ganglion. *Journal of Neurobiology*, 4, 3-41.
- Hughes, C. L. & Kaufman, T. C. (2002). Exploring myriapod segmentation: the expression patterns of *even-skipped*, *engrailed*, and *wingless* in a centipede. *Developmental Biology*, 247, 47-61.
- Janssen, R., Prpic, N. M., & Damen, W. G. (2004). Gene expression suggests decoupled dorsal and ventral segmentation in the millipede *Glomeris marginata* (Myriapoda: Diplopoda). *Developmental Biology*, 268, 89-104.
- Jiang, J. & Struhl, G. (1996). Complementary and mutually exclusive activities of *Decapentaplegic* and *Wingless* organize axial patterning during *Drosophila* leg development. *Cell*, 86, 401-409.
- Jockusch, E. L., Williams, T. A., & Nagy, L. M. (2004). The evolution of patterning of serially homologous appendages in insects. *Development Genes and Evolution*, 214, 324-338.
- Kadner, D. & Stollewerk, A. (2004). Neurogenesis in the chilopod *Lithobius forficatus* suggests more similarities to chelicerates than to insects. *Dev. Genes Evol.*, 214, 367-379.
-

-
- Kimm, M. A. & Prpic, N. M. (2006). Formation of the arthropod labrum by fusion of paired and rotated limb-bud-like primordia. *Zoomorphology*, 125, 147-155.
- Kirby, P., Beck, R., & Clarke, K. U. (1984). The stomatogastric nervous system of the house cricket *Acheta domesticus* L. II. Iontophoretic study of neuron anatomy. *Journal of Morphology*, 180, 105-124.
- Kloppenborg, P. (1995). Anatomy of the antennal motoneurons in the brain of the honeybee (*Apis mellifera*). *Journal of Comparative Neurology*, 363, 333-343.
- Kloppenborg, P., Camazine, S. M., Sun, X. J., Randolph, P., & Hildebrand, J. G. (1997). Organization of the antennal motor system in the sphinx moth *Manduca sexta*. *Cell and Tissue Research*, 287, 425-433.
- Kornberg, T., Siden, I., Ofarrell, P., & Simon, M. (1985). The *engrailed* locus of *Drosophila* - In situ localization of transcripts reveals compartment-specific expression. *Cell*, 40, 45-53.
- Kukalova-Peck, J. (1987). New Carboniferous Diplura, Monura, and Thysanura, the hexapod ground plan, and the role of thoracic side lobes in the origin of wings (Insecta). *Canadian Journal of Zoology*, 65, 2327-2345.
- Kukalova-Peck, J. (1991). Fossil history and the evolution of hexapod structures. In I.D.Naumann & CSIRO (Eds.), *The Insects of Australia* (pp. 141-179). Melbourne University Press, Melbourne.
- Kukalova-Peck, J. (1992). The "Uniramia" do not exist: The ground plan in the Pterygota as revealed by Permian Diaphanoptera from Russia (Insecta: Paleodictyopteroidea). *Canadian Journal of Zoology*, 70, 236-255.
- Kukalova-Peck, J. (1998). Arthropods phylogeny and basal morphological structures. In R.A.Forty & R. H. Thomas (Eds.), *Arthropods relationships* (pp. 249-268). Chapman and Hall, London.
- Kutsch, W. & Heckmann, R. (1995). Homologous structures, exemplified by motoneurons of Mandibulata. In O. Breidbach & W. Kutsch (Eds.), *The Nervous System of Invertebrates: an Evolutionary and Comparative Approach* (pp. 221-248). Birkhäuser Verlag Basal Switzerland.
- Kutsch, W. & Heckmann, R. (1995). Motor supply of the dorsal longitudinal muscles, I: homonomy and ontogeny of the motoneurons in locusts (Insecta, Caelifera). *Zoomorphology*, 115, 179-195.
- Lecuit, T. & Cohen, S. M. (1997). Proximal-distal axis formation in the *Drosophila* leg. *Nature*, 388, 139-145.
- Leuzinger, H. R., Wiesmann, R., & Lehmann, F. E. (1926). *Zur Kenntnis der Anatomie und Entwicklungsgeschichte der Stabheuschrecke Carusius morosus* Br. Gustav Fischer, Jena.
- Liu, Y., Maas, A., & Waloszek, D. (2010). Early embryonic development of the head region of *Gryllus assimilis* Fabricius, 1775 (Orthoptera, Insecta). *Arthropod Structure & Development*, 39, 382-395.
-

-
- Manton, S. M. (1960). Concerning Head Development in the Arthropods. *Biological Reviews of the Cambridge Philosophical Society*, 35, 265-282.
- Marder, E. (1999). Neural signalling: Does colocalization imply cotransmission? *Current Biology*, 9, 809-811.
- Matsuda, R. (1965). *Morphology and evolution of the insect head*. Memoirs of The American Entomological Institute. 334 pp.
- Matthews, R. W. & Matthews, J. R. (2010). The History and Scope of Insect Behavior. In *Insect Behavior* (2nd ed., pp. 1-41). Springer, Heidelberg.
- Maxmen, A., Browne, W. E., Martindale, M. Q., & Giribet, G. (2005). Neuroanatomy of sea spiders implies an appendicular origin of the protocerebral segment. *Nature*, 437, 1144-1148.
- Mayer, G. & Koch, M. (2005). Ultrastructure and fate of the nephridial anlagen in the antennal segment of *Epiperipatus biolleyi* (Onychophora, Peripatidae) - evidence for the onychophoran antennae being modified legs. *Arthropod Structure & Development*, 34, 471-480.
- Meier, T. & Reichert, H. (1991). Serially homologous development of the peripheral nervous system in the mouthparts of the grasshopper. *Journal of Comparative Neurology*, 305, 201-214.
- Mittmann, B. & Scholtz, G. (2003). Development of the nervous system in the "head" of *Limulus polyphemus* (Chelicerata : Xiphosura): morphological evidence for a correspondence between the segments of the chelicerae and of the (first) antennae of Mandibulata. *Development Genes and Evolution*, 213, 9-17.
- Moore, J. (2006). *An Introduction to the Invertebrates*. (1st ed.) Cambridge University Press, Cambridge.
- Morris, S. C. (1979). Burgess shale (Middle Cambrian) fauna. *Annual Review of Ecology and Systematics*, 10, 327-349.
- Morris, S. C. (1989). Burgess shale faunas and the cambrian explosion. *Science*, 246, 339-346.
- Morris, S. C. (1993). The fossil record and the early evolution of the metazoa. *Nature*, 361, 219-225.
- Morris, S. C. (2000). The Cambrian "explosion": Slow-fuse or megatonnage? *Proceedings of the National Academy of Sciences of the United States of America*, 97, 4426-4429.
- Muller, C. H. G., Rieger, V., Perez, Y., Hansson, N., & Harzsch, S. (2008). Neurophylogeny of chaetognatha: Can neuroanatomical characters shed light on the phylogenetic position of arrow worms? *Journal of Morphology*, 269, 1460-1461.
- Nishino, H. (2003). Local innervation patterns of the metathoracic flexor and extensor tibiae motor neurons in the cricket *Gryllus bimaculatus*. *Zoological Science*, 20, 697-707.
-

-
- Page, D. T. (2004). A mode of arthropod brain evolution suggested by *Drosophila* commissure development. *Evolution & Development*, 6, 25-31.
- Panganiban, G., Nagy, L., & Carroll, S. B. (1994). The role of the *distal less* gene in the development and evolution of insect limbs. *Current Biology*, 4, 671-675.
- Panganiban, G., Sebring, A., Nagy, L., & Carroll, S. (1995). The development of crustacean limbs and the evolution of arthropods. *Science*, 270, 1363-1366.
- Pearson, K. G. & Fournier, C. R. (1975). Nonspiking interneurons in walking system of cockroach. *Journal of Neurophysiology*, 38, 33-52.
- Pflüger, H. J. & Watson, A. H. D. (1988). Structure and distribution of dorsal unpaired median (DUM) neurons in the abdominal nerve cord of male and female locusts. *Journal of Comparative Neurology*, 268, 329-345.
- Phillips, C. E. (1980). An arthropod muscle innervated by nine excitatory motor neurons. *Journal of Experimental Biology*, 88, 249-258.
- Popadic, A., Panganiban, G., Rusch, D., Shear, W. A., & Kaufman, T. C. (1998). Molecular evidence for the gnathobasic derivation of arthropod mandibles and for the appendicular origin of the labrum and other structures. *Development Genes and Evolution*, 208, 142-150.
- Posnien, N., Bashasab, F., & Bucher, G. (2009). The insect upper lip (labrum) is a nonsegmental appendage-like structure. *Evolution & Development*, 11, 480-488.
- Posnien, N., Schinko, J. B., Kittelmann, S., & Bucher, G. (2010). Genetics, development and composition of the insect head - A beetle's view. *Arthropod Structure & Development*, 39, 399-410.
- Prpic, N. M., Janssen, R., Wigand, B., Klingler, M., & Damen, W. G. (2003). Gene expression in spider appendages reveals reversal of *exd/hth* spatial specificity, altered leg gap gene dynamics, and suggests divergent distal morphogen signaling. *Developmental Biology*, 264, 119-140.
- Prpic, N. M. & Tautz, D. (2003). The expression of the proximodistal axis patterning genes *Distal-less* and *dachshund* in the appendages of *Glomeris marginata* (Myriapoda: Diplopoda) suggests a special role of these genes in patterning the head appendages. *Developmental Biology*, 260, 97-112.
- Prpic, N. M., Wigand, B., Damen, W. G., & Klingler, M. (2001). Expression of *dachshund* in wild-type and *Distal-less* mutant *Tribolium* corroborates serial homologies in insect appendages. *Development Genes and Evolution*, 211, 467-477.
- Rast, G. F. & Bräunig, P. (1997). Pilocarpine-induced motor rhythms in the isolated locust suboesophageal ganglion. *Journal of Experimental Biology*, 200, 2197-2207.
- Rast, G. F. & Bräunig, P. (2001a). Feeding related motor patterns of the locust suboesophageal ganglion induced by pilocarpine and IBMX. *Journal of Insect Physiology*, 47, 43-53.
- Rast, G. F. & Bräunig, P. (2001b). Insect mouthpart motor patterns: Central circuits modified for highly derived appendages? *Neuroscience*, 108, 167-176.
-

-
- Rempel, J. G. (1975). The evolution of the insect head: The endless dispute. *Quaestiones Entomologicae*, 11, 7-25.
- Rempel, J. G. & Church, N. S. (1969). Embryology of *Lytta Viridana* Le Conte (Coleoptera - Meloidae) .V. blastoderm, germ layers, and body segments. *Canadian Journal of Zoology*, 47, 1157-1171.
- Rempel, J. G. & Church, N. S. (1971). Embryology of *Lytta-Viridana* Le Conte (Coleoptera - Meloidae) .7. 88 to 132 H - appendages, cephalic apodemes, and head segmentation. *Canadian Journal of Zoology*, 49, 1571-1581.
- Rieckhof, G. E., Casares, F., Ryoo, H. D., AbuShaar, M., & Mann, R. S. (1997). Nuclear translocation of *extradenticle* requires *homothorax*, which encodes an extradenticle-related homeodomain protein. *Cell*, 91, 171-183.
- Ritzmann, R. E., Fournier, C. R., & Pollack, A. J. (1983). Morphological and physiological identification of motor neurons innervating flight musculature in the cockroach, *Periplaneta americana*. *Journal of Experimental Zoology*, 225, 347-356.
- Rogers, B. T. & Kaufman, T. C. (1996). Structure of the insect head as revealed by the *EN* protein pattern in developing embryos. *Development*, 122, 3419-3432.
- Rogers, B. T. & Kaufman, T. C. (1997). Structure of the insect head in ontogeny and phylogeny: A view from *Drosophila*. *International Review of Cytology - A Survey of Cell Biology*, Vol 174, 174, 1-84.
- Rogers, B. T., Peterson, M. D., & Kaufman, T. C. (2002). The development and evolution of insect mouthparts as revealed by the expression patterns of gnathocephalic genes. *Evolution & Development*, 4, 96-110.
- Ronco, M., Uda, T., Mito, T., Minelli, A., Noji, S., & Klingler, M. (2008). Antenna and all gnathal appendages are similarly transformed by *homothorax* knock-down in the cricket *Gryllus bimaculatus*. *Developmental Biology*, 313, 80-92.
- Roonwal, M. L. (1937). Studies on the embryology of african migratory locust, *Locusta migratoria migratorioides* Reiche and Frm. (Orthoptera, Acrididae). II. Organogeny. *Philosophical Transactions of the Royal Society of London Series B-Biological Sciences*, 227, 175-244.
- Roonwal, M. L. (1938). Some recent advances in insect embryology with a complete bibliography of the subject. *Journal of the Royal Asiatic Society of Bengal*, 4, 17-105.
- Sakai, M. & Yamaguchi, T. (1983). Differential staining of insect neurons with Nickel and Cobalt. *Journal of Insect Physiology*, 29, 393-397.
- Sasaki, K. & Burrows, M. (1998). Innervation pattern of a pool of nine excitatory motor neurons in the flexor tibiae muscle of a locust hind leg. *Journal of Experimental Biology*, 201, 1885-1893.
- Schachtner, J. & Bräunig, P. (1993). The activity pattern of identified neurosecretory cells during feeding behavior in the locust. *Journal of Experimental Biology*, 185, 287-303.
-

-
- Schachtner, J. & Bräunig, P. (1995). Activity pattern of subesophageal ganglion cells innervating the salivary glands of the locust *Locusta migratoria*. *Journal of Comparative Physiology A-Sensory Neural and Behavioral Physiology*, 176, 491-501.
- Schmäh, M. & Wolf, H. (2003). Inhibitory motor neurones supply body wall muscles in the locust abdomen. *Journal of Experimental Biology*, 206, 445-455.
- Schmidt-Ott, U., Gonzalezgaitan, M., Jackle, H., & Technau, G. M. (1994). Number, identity, and sequence of the *Drosophila* head segments as revealed by neural elements and their deletion patterns in mutants. *Proceedings of the National Academy of Sciences of the United States of America*, 91, 8363-8367.
- Schmidt-Ott, U., Sander, K., & Technau, G. M. (1994). Expression of *engrailed* in embryos of a beetle and 5 dipteran species with special reference to the terminal regions. *Roux's Archives of Developmental Biology*, 203, 298-303.
- Schmidt-Ott, U. & Technau, G. M. (1992). Expression of *en* and *wg* in the embryonic head and brain of *Drosophila* indicates a refolded band of 7 segment remnants. *Development*, 116, 111-&.
- Schneuwly, S., Klemenz, R., & Gehring, W. J. (1987). Redesigning the body plan of *Drosophila* by ectopic expression of the homeotic gene *Antennapedia*. *Nature*, 325, 816-818.
- Scholtz, G. (1995). Head segmentation in Crustacea - An immunocytochemical study. *Zoology*, 98, 104-114.
- Scholtz, G. (2001). Evolution of developmental patterns in arthropods - the analysis of gene expression and its bearing on morphology and phylogenetics. *Zoology*, 103, 99-111.
- Scholtz, G. (2002). The Articulata hypothesis - or what is a segment? *Organisms Diversity & Evolution*, 2, 197-215.
- Scholtz, G. (2005). Homology and ontogeny: pattern and process in comparative developmental biology. *Theory.Biosci.*
- Scholtz, G. & Edgecombe, G. D. (2005). Heads, Hox and the phylogenetic position of trilobites. In S.Koenemann & R. A. Jenner (Eds.), *Crustacea and Arthropod relationships* (pp. 139-165).
- Scholtz, G. & Edgecombe, G. D. (2006). The evolution of arthropod heads: reconciling morphological, developmental and palaeontological evidence. *Development Genes and Evolution*, 216, 395-415.
- Scholtz, G., Mittmann, B., & Gerberding, M. (1998). The pattern of *Distal-less* expression in the mouthparts of crustaceans, myriapods and insects: new evidence for a gnathobasic mandible and the common origin of Mandibulata. *International Journal of Developmental Biology*, 42, 801-810.
- Schoppmeier, M. & Damen, W. G. (2001). Double-stranded RNA interference in the spider *Cupiennius salei*: the role of *Distal-less* is evolutionarily conserved in arthropod appendage formation. *Development Genes and Evolution*, 211, 76-82.
-

- Seath, I. (1977). Sensory feedback in control of mouthpart movements in desert locust *schistocerca gregaria*. *Physiological Entomology*, 2, 147-156.
- Siegler, M. V. S., Phong, M. P., & Pousman, C. A. (1991). Motor neurons supplying hindwing muscles of a grasshopper: Topography and distribution into anatomical groups. *Journal of Comparative Neurology*, 311, 342-355.
- Siewing, R. (1963). Zur problem der Arthropodenkopfsegmentierung. *Zoologischer Anzeiger*, 170, 429-468.
- Siewing, R. (1969). *Lehrbuch der Vergleichenden Entwicklungsgeschichte der Tiere*. Parey, Hamburg.
- Singh, S. (1981). The myth of intercalary segment in insect head. *Journal of Morphology*, 168, 17-42.
- Skorupski, P. & Hustert, R. (1991). Reflex pathways responsive to depression of the locust coxotrochanteral joint. *Journal of Experimental Biology*, 158, 599-605.
- Snodgrass, R. E. (1928). *Morphology and evolution of the insect head and its appendages*. Smithsonian Miscellaneous collections.
- Snodgrass, R. E. (1935). *Principles of Insect Morphology*. McGraw-hill Book Company, Inc.
- Snodgrass, R. E. (1960). Facts and theories concerning the insect head. *Smithsonian miscellaneous Collections*, 142, 1-61.
- Steffens, G. R. & Kutsch, W. (1995). Homonomies within the ventral muscle system and the associated motoneurons in the locust, *Schistocerca gregaria* (Insecta, Caelifera). *Zoomorphology*, 115, 133-150.
- Stevenson, P. A. & Meuser, S. (1997). Octopaminergic innervation and modulation of a locust flight steering muscle. *Journal of Experimental Biology*, 200, 633-642.
- Strausfeld, N. J. (1998). Crustacean - Insect relationships: The use of brain characters to derive phylogeny amongst segmented invertebrates. *Brain Behavior and Evolution*, 52, 186-206.
- Strausfeld, N. J. (2009). Brain organization and the origin of insects: an assessment. *Proceedings of the Royal Society B-Biological Sciences*, 276, 1929-1937.
- Strausfeld, N. J., Strausfeld, C. M., Loesel, R., Rowell, D., & Stowe, S. (2006). Arthropod phylogeny: onychophoran brain organization suggests an archaic relationship with a chelicerate stem lineage. *Proceedings of the Royal Society B-Biological Sciences*, 273, 1857-1866.
- Stretton, A. O. & Kravitz, E. A. (1968). Neuronal geometry: Determination with a technique of intracellular dye injection. *Science*, 162, 132-134.
- Struhl, G. (1981). A homeotic mutation transforming leg to antenna in *Drosophila*. *Nature*, 292, 635-638.

-
- Struhl, G. (1982). Genes controlling segmental specification in the *Drosophila* thorax. *Proceedings of the National Academy of Sciences of the United States of America*, 79, 7380-7384.
- Swales, L. S., Cournil, I., & Evans, P. D. (1992). The innervation of the closer muscle of the mesothoracic spiracle of the locust. *Tissue & Cell*, 24, 547-558.
- Tautz, D. (2004). Segmentation. *Developmental Cell*, 7, 301-312.
- Telford, M. J. & Thomas, R. H. (1998). Expression of homeobox genes shows chelicerate arthropods retain their deutocerebral segment. *Proceedings of the National Academy of Sciences of the United States of America*, 95, 10671-10675.
- Theophilidis, G. (1983). A comparative study of the anatomy and innervation of the metathoracic extensor tibia muscle in three orthopteran species. *Comparative Biochemistry and Physiology A-Physiology*, 75, 285-292.
- Theophilidis, G. & Burns, M. D. (1983). The innervation of the mesothoracic flexor tibiae muscle of the locust. *Journal of Experimental Biology*, 105, 373-388.
- Thomas, R. H. & Telford, M. J. (1999). Appendage development in embryos of the oribatid mite *Archezogozetes longisetosus* (Acari, Oribatei, Trhypochthoniidae). *Acta Zoologica*, 80, 193-200.
- Tiegs, O. W. (1941). The embryology and affinities of Symphyla, based on a study of *Hanseniella agilis*. *Quarterly Journal Of Microscopical Science*, 82, 1-125.
- Tiegs, O. W. (1947). The development and affinities of the Pauropoda, based on a study of *Pauropus silvaticus*. *Quarterly Journal Of Microscopical Science*, 88, 165-267;-275-336.
- Tyrer, N. M., Turner, J. D., & Altman, J. S. (1984). Identifiable neurons in the locust central nervous system that react with antibodies to serotonin. *Journal of Comparative Neurology*, 227, 313-330.
- Ullmann, S. L. (1964). The origin and structure of the mesoderm and the formation of coelomic sacs in *Tenebrio Molitor* L. (Insecta, Coleoptera). *Philosophical Transactions of the Royal Society of London Series B-Biological Sciences*, 248, 245-&.
- Urbach, R. & Technau, G. M. (2003). Early steps in building the insect brain: neuroblast formation and segmental patterning in the developing brain of different insect species. *Arthropod Structure & Development*, 32, 103-123.
- Urbach, R., Technau, G. M., & Breidbach, O. (2003). Spatial and temporal pattern of neuroblasts, proliferation, and Engrailed expression during early brain development in *Tenebrio molitor* L. (Coleoptera). *Arthropod Structure & Development*, 32, 125-140.
- Van den heuvel, M., Nusse, R., Johnston, P., & Lawrence, P. A. (1989). Distribution of the *wingless* gene product in *Drosophila* embryos - A protein involved in cell-cell communication. *Cell*, 59, 739-749.

- Wagele, J. W. & Misof, B. (2001). On quality of evidence in phylogeny reconstruction: a reply to Zrzavy's defence of the 'Ecdysozoa' hypothesis. *Journal of Zoological Systematics and Evolutionary Research*, 39, 165-176.
- Waloszek, D., Chen, J. Y., Maas, A., & Wang, X. Q. (2005). Early cambrian arthropods - new insights into arthropod head and structural evolution. *Arthropod Structure & Development*, 34, 189-205.
- Watson, A. H. D., Burrows, M., & Hale, J. P. (1985). The morphology and ultrastructure of common inhibitory motor neurons in the thorax of the locust. *Journal of Comparative Neurology*, 239, 341-359.
- Weber, H. (1952). Morphologie, Histologie und Entwicklungsgeschichte der Articulaten. II. Die Kopfsegmentierung und die Morphologie des Kopfes überhaupt. *Fortschritte der Zoologie*, 9, 18-231.
- Wilson, J. A. (1979a). Structure and function of serially homologous leg motor neurons in the locust .I. Anatomy. *Journal of Neurobiology*, 10, 41-65.
- Wilson, J. A. (1979b). Structure and function of serially homologous leg motor neurons in the locust .II. Physiology. *Journal of Neurobiology*, 10, 153-167.
- Wolf, H. (1990). Activity patterns of inhibitory motoneurons and their impact on leg movement in tethered walking locusts. *Journal of Experimental Biology*, 152, 281-304.
- Zacharias, D., Williams, J. L. D., Meier, T., & Reichert, H. (1993). Neurogenesis in the insect brain: Cellular identification and molecular characterization of brain neuroblasts in the grasshopper embryo. *Development*, 118, 941-955.

Acknowledgements

I deem it an utmost pleasure to be able to express the profound gratitude to reverend supervisor, **Prof. Dr. Peter Bräunig**, who guided me in an excellent and most professional manner throughout my research, and navigate me in the world of science. I really feel extremely proud to have worked under his dynamic guidance, consultory behaviour, constructive criticism, sympathetic attitude and keen interest throughout the course of these investigations and the write up of the manuscript.

I owe further thanks to **Priv.-Doz. Dr. rer. nat. Rudolf Loesel** for his readiness to review my work. He also deserves special gratitude for his skilful suggestions, and for providing the reference letter in continuing my financial aids.

A few lines are too short to make a complete account of my deep appreciation and hearties gratitude to my colleagues in the Institute for Biology-II particularly **Dr. Katrin Göbbels, Dr. Carsten Heuer, Simone Faller, Volker Buck, and Elisabeth Lipke** for their valuable suggestions, guidance, and help. I am really thankful to Simone Faller and Dr. Carsten for helping me to learn graphics editing software. I sincerely thank Dr. Katrin for her fruitful discussions as well as helpful advices. I have ever very inspiring and learned a lot of from her.

A great thank to **Andrzej Steckiewicz** for excellent technical assistance in making chemical solutions, and mostly for his willing to listen me, albeit I could not speak good German.

My friends- a gift of heaven, have their substitutes? No, never. I fervently extend my thanks from unfathomable depths of my heart to Mr. Amir Ishaque, without him, it was difficult to win a doctoral title. He has not only inspired me to work hard but also helped me in every moment. My sincere gratitude is to Mr. and Mrs. Riaz for their moral support. Wonderful company of M. Usman Anwar, Bilal Janjua, Dr. Ramzan khan, Dr. Ali Ahmad Naz, Dr. M. Sajid Hussain and M. Ilyas will ever zeal me to come back to unforgettable moments of life. My heartiest thank to Shaista Ilyas not only for proofreading the manuscript but also for her colourful moral support. My acknowledgement will not be completed, if I didn't show my sincerity to Zaheer Ahmad and Atif Musadiq, who have not only enriched the small niche of my friends during the last phase of my work but also inculcated right type of fortitude in me to scale hardest peaks and transform every stumbling block into a stepping stone.

I am greatly indebted to my sweetest and loveliest sisters: Sumera Alvi, Sajida Alvi and Baseerat Awan for their "unmole" love, mellifluous affections and consistent & priceless prayers. May they enjoy ever-lasting twitter?

I transcend my power of narration to express how I feel obliged to my dear parents. They always boosted my morale to fly too high to accomplish my goal and took me out of all predicaments, whenever I was into them.

Finally, thanks to Higher Education Commission (HEC) of Pakistan and German Academic Exchange Service (DAAD) for providing financial assistance to accomplish this project in Germany.

Curriculum Vitae

Personal data

Name: Abid Mahmood Alvi
Date of Birth: 09 June, 1981
Place of Birth: Layyah, Pakistan
Nationality: Pakistani

Education

2007-2011 PhD at institute for Biology-II, Unit of Developmental Biology and Morphology of Animals, RWTH Aachen University, Germany

2005-2006 Research fellow at National Institute for Biotechnology and Genetic Engineering (NIBGE), Faisalabad, Pakistan

2003-2004 M.Sc. (Hons.) Agri. Entomology, University of Agriculture, Faisalabad, Pakistan

1999-2002 B.Sc. (Hons.) Agri. Entomology, University of Agriculture, Faisalabad, Pakistan

1997-1998 Higher Secondary School Certificate GC, Layyah, Pakistan

1986-1996 High School Certificate, GMHS, Chowk Azam, Layyah, Pakistan